

IMPROVEMENT OF HEAT TRANSFER IN TUBE HEAT  
EXCHANGER VIA PASSIVE FLOW GENERATOR

FARAH ARINA BINTI IBRAHIM

FACULTY OF ENGINEERING  
UNIVERSITI MALAYA  
KUALA LUMPUR

2023

**IMPROVEMENT OF HEAT TRANSFER IN TUBE  
HEAT EXCHANGER VIA PASSIVE FLOW  
GENERATOR**

**FARAH ARINA BINTI IBRAHIM**

**DISSERTATION SUBMITTED IN FULFILMENT OF  
THE REQUIREMENTS FOR THE DEGREE OF MASTER  
OF ENGINEERING SCIENCE**

**FACULTY OF ENGINEERING  
UNIVERSITI MALAYA  
KUALA LUMPUR**

**2023**

**UNIVERSITI MALAYA**  
**ORIGINAL LITERARY WORK DECLARATION**

Name of Candidate: Farah Arina Binti Ibrahim

Matric No: 17198476/1

Name of Degree: Master of Engineering Science

Title of Project Paper/Research Report/Dissertation/Thesis (“this Work”):

Improvement Of Heat Transfer In Tube Heat Exchanger Via Passive Flow Generator

Field of Study: Thermodynamics and Fluid Mechanics

I do solemnly and sincerely declare that:

- (1) I am the sole author/writer of this Work;
- (2) This Work is original;
- (3) Any use of any work in which copyright exists was done by way of fair dealing and for permitted purposes and any excerpt or extract from, or reference to or reproduction of any copyright work has been disclosed expressly and sufficiently and the title of the Work and its authorship have been acknowledged in this Work;
- (4) I do not have any actual knowledge nor do I ought reasonably to know that the making of this work constitutes an infringement of any copyright work;
- (5) I hereby assign all and every rights in the copyright to this Work to the Universiti Malaya (“UM”), who henceforth shall be owner of the copyright in this Work and that any reproduction or use in any form or by any means whatsoever is prohibited without the written consent of UM having been first had and obtained;
- (6) I am fully aware that if in the course of making this Work I have infringed any copyright whether intentionally or otherwise, I may be subject to legal action or any other action as may be determined by UM.

Candidate’s Signature

Date: 25.10.2023

Subscribed and solemnly declared before,

Witness’s Signature

Date: 25.10.2023

Name:

Designation:

# **IMPROVEMENT OF HEAT TRANSFER IN TUBE HEAT EXCHANGER VIA PASSIVE FLOW GENERATOR**

## **ABSTRACT**

Internally treated tube heat exchanger surfaces are one of the passive heat transfer enhancements that have attracted the attention of the industry due to their high performance and low-cost requirements. In this study, the effect of pipe internal groove surface and wire coil insertion on heat transfer, velocity profile, and thermal enhancement efficiency was numerically analyzed and simulated at two bulk temperatures of 25 °C and 30 °C. Three variations of 1000 mm copper tubes were analyzed numerically: smooth surface; groove diameters of 1 mm and 0.5 mm; and wire coil inserts of 1 mm and 0.5 mm. The pitch length was held constant at 8 mm. However, to support these, an experiment for 1 mm wire coil insertion was conducted and shows significant results on the enhancement of heat transfer. In simulation, the Nusselt number of a wire coil insert tube with a diameter of 0.5 mm increased by 114 % at a Reynolds number of 8000 and by 31 % at a Reynolds number of 4000. Compared to a smooth tube, a 1 mm circular groove increased the Nusselt number by 136 % and 19 % at Reynolds numbers of 20000 and 24000, respectively. Furthermore, 1 mm of circular groove tube increased the heat transfer coefficient from 12,000 to 24,000 by 45 % to 192 %. In the experiment analysis of a 1 mm wire coil insert tube, the friction factor decreased while the Nusselt number increased at bulk temperatures of 25 °C and 30 °C from 46 % to 197 %. The heat transfer coefficient increased between 2.94 and 2.97 times in comparison to the smooth tube. It is concluded that the diameter of the groove and wire coil play an important role in heat transfer improvement and convection on the boundary layer surface.

**Keywords:** Heat transfer enhancement, grooving, wire coil insertion and Computational Fluid Dynamics.

# **PENINGKATAN PEMINDAHAN HABA DALAM TUBE HEAT EXCHANGER MELALUI PENJANA ALIRAN PASIF**

## **ABSTRAK**

Permukaan penukar haba tiub yang dirawat secara dalaman adalah salah satu peningkatan pemindahan haba pasif yang telah menarik perhatian industri kerana keperluan prestasi tinggi dan kos rendah. Dalam kajian ini, kesan permukaan alur dalaman paip dan sisipan gegelung dawai pada pemindahan haba, profil halaju, dan kecekapan peningkatan haba telah dianalisis secara berangka dan disimulasikan pada dua suhu pukal 25 °C dan 30 °C. Tiga variasi tiub kuprum 1000 mm dianalisis secara berangka: permukaan licin; diameter alur 1 mm dan 0.5 mm; dan sisipan gegelung dawai 1 mm dan 0.5 mm. Panjang pic dipegang tetap pada 8 mm. Walau bagaimanapun, untuk menyokongnya, satu eksperimen untuk pemasangan gegelung dawai 1 mm telah dijalankan dan menunjukkan hasil yang ketara pada peningkatan pemindahan haba. Dalam simulasi, nombor Nusselt bagi tiub sisipan gegelung dawai dengan diameter 0.5 mm meningkat sebanyak 114 % pada nombor Reynolds 8000 dan sebanyak 31 % pada nombor Reynolds 4000. Berbanding dengan tiub licin, alur bulat 1 mm meningkatkan nombor Nusselt sebanyak 136 % dan 19 % pada nombor Reynolds 20000 dan 24000, masing-masing. Tambahan pula, 1 mm tiub alur bulat meningkatkan pekali pemindahan haba daripada 12,000 kepada 24,000 sebanyak 45 % kepada 192 %. Dalam analisis eksperimen bagi tiub sisipan gegelung dawai 1 mm, faktor geseran berkurangan manakala nombor Nusselt meningkat pada suhu pukal 25 °C dan 30 °C daripada 46% kepada 197%. Pekali pemindahan haba meningkat antara 2.94 dan 2.97 kali berbanding dengan tiub licin. Disimpulkan bahawa diameter alur dan gegelung dawai memainkan peranan penting dalam peningkatan pemindahan haba dan perolakan pada permukaan lapisan sempadan.

Kata kunci: Peningkatan pemindahan haba, alur, sisipan gegelung wayar dan Dinamik Bendalir Pengiraan.

## ACKNOWLEDGEMENTS

Alhamdulillah, the highest honour and thanks Allah the Almighty for using his might to bring this dissertation to a successful conclusion. May Allah also grant His blessings to the Prophet Muhammad SAW, his family, and his companions.

Without the constant support of my supervisors, Dr. Mohd Ridha Bin Muhamad and Dr. Mohd Nashrul Mohd Zubir from the Faculty of Engineering, Prof. Dr. Zailan Siri, and Prof. Mohd Bin Omar from the Faculty of Science, this project would not have been successful. A special thank you to my supervisors for all of their tremendous help and counsel during this project. I would like to express my appreciation to Mr. Mohamed Moustofa Abdel Halim, a fellow master's student, and Mr. Muaz Bin Ahmad Hasbullah, a final-year engineering student at the Universiti Malaya, for their help and valuable contributions to this research.

My sincere gratitude is intended for my dear parents, Ibrahim Bin Hj Serad and Norzakiah Md Som, for their unending support and prayers. Also, a special thank you to my husband, Muhammad Safwan Bin Mohd Mansor, and my sister, Aizahani Binti Ibrahim, who have helped and supported me greatly in finishing my study. Thank you so much to my other family members, close friends, and everyone else who has helped and supported me throughout my educational path. May Allah reward each of you with wonderful things. Finally, I hope that others who are interested in this research issue will find this study helpful.

## TABLE OF CONTENTS

Abstract .....	iii
Abstrak .....	iv
Acknowledgements .....	v
Table of Contents .....	vi
List of Figures .....	viii
List of Tables.....	xii
List of Symbols and Abbreviations.....	xiii
<b>CHAPTER 1: INTRODUCTION .....</b>	<b>14</b>
1.1 Research Background .....	14
1.2 Problem statement and objectives .....	16
<b>CHAPTER 2: LITERATURE REVIEWS .....</b>	<b>18</b>
2.1 Heat exchanger .....	18
2.2 Heat transfer.....	19
2.3 Passive heat transfer augmentation.....	20
2.3.1 Internal grooving .....	23
2.3.2 Internal surface profile characteristic on heat transfer performance .....	28
2.3.3 Coil wire insert .....	31
2.5 Computational Fluid Dynamics.....	38
2.6 Summary.....	40
<b>CHAPTER 3: METHODOLOGY .....</b>	<b>41</b>
3.1 Flow Chart .....	41
3.2 Computational Model .....	42

3.2.1	Design and Meshing .....	42
3.2.2	Computational Fluid Dynamics Simulation .....	47
3.3	Heat transfer on conduit experiment.....	48
3.3.1	Material specification .....	48
3.3.2	Experimental setup .....	50
3.3.3	Experiment procedure .....	54
<b>CHAPTER 4: RESULT AND DISCUSSION.....</b>		<b>56</b>
4.1	Numerical Analysis .....	56
4.1.1	Temperature distribution .....	56
4.1.2	Velocity profiles .....	60
4.1.3	Nusselt Number .....	65
4.1.4	Heat transfer coefficient .....	69
4.1.5	Friction factor .....	72
4.1.6	Comparison wire coil insertion and circular groove .....	75
4.2	Experimental result: Wire coil inserts .....	77
4.2.1	Result validation for smooth tube .....	77
4.2.2	Nusselt number .....	79
4.2.3	Friction factor .....	80
4.2.4	Comparison heat transfer performance for different bulk temperature....	83
<b>CHAPTER 5: CONCLUSION.....</b>		<b>85</b>
References .....		86
List of Publications and Papers Presented .....		96



## LIST OF FIGURES

Figure 2.1: Schematic diagram of internal surface – Magnetic Abrasive Finishing process setup (Shinmura & Yamaguchi, 1995).....	25
Figure 2.2: The schematic diagram of the processing principle of magnetic abrasive finishing with combined electrochemical finishing in 3D model and machining tool structure (Ridha et al., 2015).....	26
Figure 2.3: (a) Internal tube grooving magnetic tool design (b) Magnetic grooving machine (Muhamad et al., 2021).....	27
Figure 2.4: Geometric shapes of the grooved tube; a) circular, b) rectangular and c) trapezoidal grooves (Bilen et al., 2009) .....	29
Figure 2.5: Groove pattern of a) spiral tube and b) herringbone tube (Kaji et al., 2012).....	29
Figure 2.6: Effects on Nusselt number for varies geometry for (a) $eD = 0.1$ and (b) $eD = 0.2$ (Ramadhan et al., 2013) .....	30
Figure 2.7: Result of heat transfer rate for each pattern in evaporator (Kaji et al., 2012) .....	30
Figure 2.8: Conventional wire coil dimensions (Promvonge, 2008) .....	32
Figure 2.9: Examples of the configurations of various wire coils (Ray & Kumar Jhinge, 2014) .....	32
Figure 2.10: Performance of (a) friction factor and (b) Nusselt number with variation wire coils at different Reynolds number (Kasturi et al., 2017) .....	33
Figure 2.11: Thermal performance factor at Reynolds number (Mohite et al., 2018)....	34
Figure 2.12: Comparison between experimental and predicted Nusselt number (Biswas & Salam, 2013) .....	38
Figure 2.13: Contour lines of streamwise velocity at a) $Re = 500$ and b) $Re = 600$ (Muñoz Esparza & Sanmiguel Rojas, 2011) .....	39
Figure 2.14: Temperature contour for Reynolds number 250 meshing size 0.5 mm (Yadav et al., 2022).....	40
Figure 3.1: Flow chart of research study.....	41
Figure 3.2: Close up 2D design of the surface (a) circular groove and (b) wire coil insert .....	43

Figure 3.3: Grid Independence.....	44
Figure 3.4: Mesh of the medium for (a) smooth tube, (b) wire coil insert tube and (c) circular groove tube.....	46
Figure 3.5: Close up of mesh of (a) 1 mm circular groove tube, (b) 0.5 mm circular groove tube, (c) 1 mm wire coil insert tube and (d) 0.5 mm wire coil insert tube.....	47
Figure 3.6: Wire stainless steel coil .....	48
Figure 3.7: Close up wire coil insert in tube .....	49
Figure 3.8: Schematic diagrams of the heat conduit experiment.....	51
Figure 3.9: Overall view of the experiment setup.....	51
Figure 4.1: Temperature distribution of smooth tube at $Re = 24000$ at bulk temperature $30\text{ }^{\circ}\text{C}$ .....	57
Figure 4.2: Near wall temperature contour of circular groove tubes (a) 1 mm at $Re = 16000$ , (b) 1 mm at $Re = 24000$ , (c) 0.5 mm at $Re=16000$ and (c) 0.5 mm at $Re=24000$ for bulk temperature $30\text{ }^{\circ}\text{C}$ .....	57
Figure 4.3: Near wall temperature contour of circular groove tubes (a) 1 mm at $Re = 16000$ , (b) 1 mm at $Re = 24000$ , (c) 0.5 mm at $Re=16000$ and (c) 0.5 mm at $Re=24000$ for bulk temperature $25\text{ }^{\circ}\text{C}$ .....	58
Figure 4.4: Near wall temperature contour of wire coil inserts tubes (a) 1 mm at $Re = 16000$ , (b) 1 mm at $Re = 24000$ , (c) 0.5 mm at $Re=16000$ and (c) 0.5 mm at $Re=24000$ for bulk temperature $30\text{ }^{\circ}\text{C}$ .....	59
Figure 4.5: Near wall temperature contour of wire coil inserts tubes (a) 1 mm at $Re = 16000$ , (b) 1 mm at $Re = 24000$ , (c) 0.5 mm at $Re=16000$ and (c) 0.5 mm at $Re=24000$ at for bulk temperature $25\text{ }^{\circ}\text{C}$ .....	60
Figure 4.6: Velocity profiles of circular groove tube (a) 1 mm and (b) 0.5 mm at $Re=24000$ for bulk temperature $30\text{ }^{\circ}\text{C}$ .....	61
Figure 4.7: Velocity profiles of circular groove tube (a) 1 mm and (b) 0.5 mm at $Re=24000$ for bulk temperature $25\text{ }^{\circ}\text{C}$ .....	62
Figure 4.8: Velocity profiles of wire coil insert tube (a) 1 mm and (b) 0.5 mm at $Re=24000$ for bulk temperature $30\text{ }^{\circ}\text{C}$ .....	64
Figure 4.9: Velocity profiles of wire coil insert tube (a) 1 mm and (b) 0.5 mm at $Re=24000$ for bulk temperature $25\text{ }^{\circ}\text{C}$ .....	65

Figure 4.10: Nusselt number with Reynolds number for simulation and empirical results on smooth tube .....	66
Figure 4.11: Nusselt number with Reynolds number for (a) wire coil insert tube and (b) circular groove tube bulk temperature 30°C .....	67
Figure 4.12: Heat transfer coefficient with Reynolds number for (a) wire coil insert tube and (b) circular groove tube for bulk temperature 30 °C .....	70
Figure 4.13: Heat transfer coefficient with Reynolds number for (a) wire coil insert tube and (b) circular groove tube for bulk temperature 25 °C .....	71
Figure 4.14: Friction factor with Reynolds number for simulation and empirical results on smooth tube .....	72
Figure 4.15: Friction factor with Reynolds number for (a) wire coil insert tubes and (b) circular groove tubes at bulk temperature 30 °C.....	74
Figure 4.16: Friction factor with Reynolds number for (a) wire coil insert tubes and (b) circular groove tubes at bulk temperature 25 °C.....	75
Figure 4.17: Variation Nusselt number with Reynolds number for all tubes at bulk temperature 30 °C. ....	75
Figure 4.18: Variation Friction factor with Reynolds number for all tubes at bulk temperature 30 °C. ....	76
Figure 4.19: Variation Friction factor with Reynolds number for all tubes at bulk temperature 25 °C. ....	76
Figure 4.20: Friction factor with Reynolds number for experiment and empirical results on smooth tube .....	78
Figure 4.21: Nusselt number with Reynolds number for experiment and empirical results on smooth tube .....	78
Figure 4.22: Nusselt number with different Reynolds number of 1 mm wire coil insert tube and smooth tube at (a) bulk temperature 25 °C and (b) bulk temperature 30 °C....	79
Figure 4.23: Friction factor with different Reynolds number of 1 mm wire coil insert tube and smooth tube at (a) bulk temperature 25 °C and (b) bulk temperature 30 °C.....	81
Figure 4.24: Heat transfer coefficient with different Reynolds number of 1 mm wire coil insert tube and smooth tube at (a) bulk temperature 25 °C and (b) bulk temperature 30 °C .....	82

Figure 4.25: Nusselt number with Reynolds number for 1 mm wire coil insert experimental at bulk temperatures 25 °C and 30 °C..... 83

Figure 4.26: Friction factor with Reynolds number for 1 mm wire coil insert experimental at bulk temperatures 25 °C and 30 °C..... 84

Figure 4.27: Heat transfer coefficient with Reynolds number for 1 mm wire coil insert experimental at bulk temperatures 25 °C and 30 °C..... 84

Universiti Malaya

## LIST OF TABLES

Table 2.1: Reynolds number categories .....	35
Table 3.1 Percentage difference of Nusselt number correspond to element size for smooth tube.....	44
Table 3.2: Geometry designs specification and meshing properties for all tubes.....	45
Table 3.3 : Boundary conditions and solution setup .....	47
Table 3.4: Inlet velocity for each Reynolds number .....	48
Table 3.5: Materials and fluid properties .....	50
Table 3.6: Equipment for heat conduit experiment.....	52
Table 4.1: Comparison Nusselt number in corresponds to Reynolds number at bulk temperatures 25 °C and 30 °C for (a) wire coil insert tube and (b) circular groove tube.....	68
Table 4.2: Validation Friction factor correspond to Reynolds number for smooth tube .....	77

## LIST OF SYMBOLS AND ABBREVIATIONS

$v_m$	: Mean fluid velocity [m/s]
$\nu$	: Kinematic viscosity [m <sup>2</sup> /s]
$A_i$	: Actual inside surface area of the test section [m <sup>2</sup> ]
C, $C_p$	: Specific heat, [Jkg <sup>-1</sup> K <sup>-1</sup> ]
$C_f$	: Skin friction coefficient
$p$	: Pitch of groove/coil
$e$	: Diameter of cross section of wire coil
$d$	: Diameter of groove
$k$	: Thermal Conductivity [watt]
$m$	: Mass rate of flow, [kgs <sup>-1</sup> ]
Nu	: Nusselt Number, [-]
$f$	: Friction factor, [-]
Pr	: Prandtl Number, [-]
$h$	: Heat transfer rate, [W]
Re	: Reynolds Number, [-]
$T_{in}, T_{out}$	: Temperature of inlet and outlet in tube [K]
$\alpha$	: Heat transfer coefficient [W/(m <sup>2</sup> K)]
$\mu$	: Viscosity of the fluid [Pa.s]
$\rho$	: Density [g/cm <sup>3</sup> ]
CFD	: Computational Fluid Dynamics
2D	: Two dimensional
MAF	: Magnetic Abrasive Finishing

## CHAPTER 1: INTRODUCTION

### 1.1 Research Background

To alleviating the energy crisis and combat global warming, the public and industry are increasingly demanding energy-efficient and green solutions. In industries such as transportation, power plants, factories, heating and cooling systems, heat exchangers with a high level of efficiency are necessary to minimize the energy consumption. Heat exchangers are machines that transfer heat from one medium to another, either gas, liquid, or a combination of both two mediums (Kiran et al., 2014). On the basis of the thermodynamic framework, two working fluids exchange heat via thermal contact using tubes contained within a cylindrical shell with a wide temperature and pressure range. The ratio of heat transmission to pressure loss defines the efficiency of a heat exchanger. The rapid fluid flow in the heat exchanger will facilitate heat transfer via convection and result in fluid pressure losses. To improve the efficiency of heat exchangers, however, it is highly difficult to alter the properties of the heat transfer material and fluid; only the surface area of the tube and fluid velocity can be adjusted for the same configuration (Acharya et al., 2021).

Enhancing the capacity of heat exchangers to transport heat is one of the numerous methods used to address this issue. The enhancement of heat exchangers to provide dependable, cost-effective, and efficient performance is beneficial to both the environment and industry (Ghajar, 2020). As a result, numerous techniques were employed to enhance the heat transfer rate of the heat exchanger. Within the current technological context, one of the possible strategies is to gain control over the boundary layer domain, where heat and mass transfer are predominated. In addition, the rate of heat transfer can be increased by increasing the heat transfer area and generating swirling or secondary flows (Pandey, 2015). Therefore, three methods have been developed in order to increase the rate of heat transfer: passive, active, and compound. In this study, passive

enhancement will be employed completely. The passive method focuses on modifying the internal surface profile.

Internal surface profiling is a technique that is gaining popularity in modern industrial applications despite the fact that tool size limitations and restrictions on the inner surface profile have posed a persistent challenge to researchers. Internal grooving and insertion turbulators, such as twisted tapes and wire coils, have been highlighted in a number of prior studies as methods for accelerating heat transfer. Heat exchangers with internal grooves are utilized in a variety of industrial applications, including heating, ventilation, and air-cooled heat exchangers. Taking advantage of the growing trend in microscale innovations, Kadir et al. (2009) noted that grooved tubes increase the heat transfer area and permit the redevelopment of boundary layers, resulting in more effective heat transfer. Treated surfaces and coiled tubes promote pressure losses and increases in the heat transfer coefficient. These alternatives demonstrate that introducing turbulence into a fluid by destroying its thermal and viscous boundary layers can enhance the heat transfer of the fluid (Promvongse, 2008). The performance of fluid flow is significantly influenced by the selection of tube insert and insert shape, so not all insertion turbulators are applicable (Wang & Sunden, 2002).

In the past, experimental analysis served as the primary research method for predicting fluid flow behavior. Today, nevertheless, Computational Fluid Dynamics (CFD) is widely utilized in a variety of research fields. As a result of the development of digital technology in the present day, numerical methods for expressing complex mathematical problems can be bypassed by computers and an immediate solution can be obtained. Software-based numerical analysis is one of the most prevalent techniques for examining and evaluating the thermodynamic, fluid flow, and heat transfer properties of a system. Instead of calculating the answer, computers allow you to focus more on the formulation and interpretation of the problem (Gaudiani, 2008). Rather than relying solely on



computer simulations or experimental analysis, however, many modern research methods combine the two approaches. The analysis of heat transfer is made more reliable by comparing computational and experimental methods.

## **1.2 Problem statement and objectives**

Passive enhancement of heat transfer is the current trend to improve heat exchanger performance. The method attempts to modulate the solid-fluid interface layer to make it more conductive, resulting in enhanced heat transfer and fouling removal. However, the associated complication to overall system performance has limited its use within a thermal engineering perspective. The majority of the problems stem from pressure and pumping losses; fouling deposition as a result of increased surface area; colloidal instability; surface erosion as a result of bubble implosion; and attenuation of wave propagation. Therefore, the main purpose of this research is to investigate the flow and heat transfer performance in a closed conduit configuration with inner surface modification.

The internal groove tube and wire coil inserted tube are the primary subjects of this study. Experimentation and numerical analysis are used to investigate the fundamental properties of flow and heat transfer in the solid-liquid interface region of the subjects, in order to expand the working limits of heat exchangers beyond their typical limits. A numerical analysis is carried out to validate the experimental hypothesis. The acquired data is helpful to design of the next generation of heat exchangers, which incorporate compactness and energy efficiency. This would benefit a wide range of businesses and ultimately help the nation provide a substantial amount of renewable energy to consumers.

Thus, below are the objectives of this research:

1. To conduct numerical investigation on the effect of internal grooving and wire coil insertion on heat transfer performance of smooth pipe.
2. To compare the heat transfer performance between internal grooving and wire coil insertion.
3. To conduct experimental investigation on heat transfer performance using wire coil insert.

Universiti Malaya

## CHAPTER 2: LITERATURE REVIEWS

In this chapter, existing research that is noteworthy and relevant to this topic is reviewed. A literature review is required for a comprehensive understanding of a particular research project. E-journals, e-books, and product catalogues were used to locate relevant research papers for the present study. Existing research on this topic has examined the evolution of heat transfer theory, enhancements to heat transfer, and internal profile modifications. In addition, this section describes the computational fluid dynamics and empirical equations implemented in previous studies. The importance of this research problem was determined by a review of the relevant literature.

### 2.1 Heat exchanger

Heat exchanger tubes with higher capacity, reliability, economics, a simplistic fabrication design, and minimal maintenance needs are in high demand today (Al-Gburi et al., 2023; Aly et al., 2017). There are many different types of heat exchangers, including double-tube, shell-and-tube, tube-in-tube, and plate models. Shell and tube exchangers are widely employed in the engineering industry. According to Nitheesh Krishnan and Suresh Kumar (2016), shell and tube has a number of advantages, including the ability to vary pressures and pressure drops over a wide range and to accommodate thermal stress at a low cost. These are the fundamental parts of a heat exchanger: tubes, tube sheet, shell, tube side channels and nozzles, baffles, channel covers, and tube nozzles (Mukherjee, 1998). Dewan et al. (2004) mentioned that the most difficult aspect of designing a heat exchanger is making the apparatus compact while achieving a high heat transfer rate with minimal pumping power. Therefore, changes to the body or the operating fluid of the heat exchangers are examples of these procedures (Zimparov, 2002). There are three important processes of heat transfer in a compact heat exchanger: convection of heat between the fluid and the tube wall; heat transfer from the inner and outer tube surface; and heat

transfer from the tube to the surrounding fluid (Giram & Patil, 2013). This study relates more to the convection of heat between fluid and the tube wall. Nevertheless, all types of heat exchangers serve the same function in terms of heat transfer. The only distinction lies in the transmission's methods and operating principle.

## 2.2 Heat transfer

Heat is the energy transmitted from a high temperature environment to a low temperature. This process quantity is denoted by the letters  $q$  or  $Q$  with the SI unit Joules,  $J$ . The heat transfer process is driven by the temperature difference between two mediums, and the amount of heat transferred for a given temperature change is proportional to the temperature difference,  $\Delta T$  and the mass of the substance,  $m$  being heated as follows.

$$Q = mc\Delta T \quad (2.1)$$

Radiation, conduction, and convection are the three modes of heat transfer. In the mechanism of conduction, energy is transferred via physical contact. The conduction mechanism is subdivided into two processes: steady-state heat conduction and transient heat conduction. This mechanism exists in all phases without any form of motion. Thermodynamics dictates that the conduction of heat transfer begins in a transient state and then reaches a steady state until thermal equilibrium is achieved (Dincer & Erdemir, 2021). The thermal radiation process is the emission of heat by electromagnetic radiation, which is dependent on the temperature of the body and the type of surface (Lienhard IV & Lienhard V, 2001). In the radiation process, which does not require the use of a medium, heat is transmitted through waves. Convection, on the other hand, is the most challenging of the heat transmission mechanisms. Bergman et al. (2011) stated that the convection process consists of energy diffusion and fluid advection. It is also stated that it occurs when there is a temperature difference between the fluid in motion and the

boundary. Establishing control over the boundary layer domain, which is dominated by heat and mass transmission, is one of the technologically feasible options.

There are two types of convection processes: forced convection and natural convection. Due to instrument or thermal expansion, the difference in density between these two types exists (Young, 2012). Natural convection is a method of heat transfer in which the fluid motion is governed by natural forces and external factors have no effect. Due to heat transfer, the exterior temperature of a hot object decreases as the air temperature rises. According to researchers, forced convection is the most common mode of heat transfer in heat exchangers, which is enhanced by disruption and turbulence enhancers like fake grooved or fluted tubes (Ramadhan et al., 2013). Air conditioning and steam turbines are the most common examples of forced convection in the industrial world. Internal flow convection is convection heat transfer that happens in a flow through pipes or ducts. Prior to this, few studies on forced convection in internally modified tubes had been conducted. The experiment of forced convection heat transfer on various parameters of dimpled tubes revealed that smaller depths and diameters result in a higher rate of heat transfer compared to smooth tubes (Apet & Borse, 2015).

### **2.3 Passive heat transfer augmentation**

Thermodynamic fluids researchers have been particularly interested in enhancing heat transfer efficiency in heat exchangers (Bergles, 1999). One of the potential ways, from a technological standpoint, is to establish control over the boundary layer domain, which is dominated by heat and mass transmission. There are three categories of enhancement techniques: passive, active, and compound. In the past, researchers have used both passive and active strategies to control the boundary layer (Webb, 1994). Passive heat transfer augmentation entails physical modification of the surface in contact with the fluid without the use of external power and at a low cost, employing a variety of techniques such as

altering the surface profile, inserting flow swirling devices, and modifying fluid properties (Léal et al., 2013). This approach is utilized to increase the heat transfer coefficient by fostering turbulent flow. Active techniques require the use of external power, which can be expensive. The compound method combines multiple techniques to enhance heat enhancement (Kareem et al., 2015).

In engineering industries, the passive method is commonly used to improve thermal performance. In addition to being cost-effective and not requiring external direct power, this method promotes a higher heat transfer coefficient by modifying the underlying behavior geometrically (Pandey, 2015). Surface modification, which is a passive technique, has improved overall thermal performance and is widely used in modern heat exchangers because it is particularly effective at enhancing heat transfer. Global industrial revolutions have established surface profiling industries to an absolute standard. In the past decade, the demand for products with superior surface finishes has increased (Heng et al., 2017). Focusing on the surface profile modification strategy, the concept involves increasing the total surface area and generating artificial wake through flow obstruction and expansion, such as grooved tubes and turbulator insertions. This prompted firms engaged in the modification of surface profiling to investigate and develop alternative machining techniques capable of achieving the desired result.

Due to tool size limitations and the inner surface profile restriction, inner surface modification of tight conduits has remained a persistent challenge for researchers (Jha & Jain, 2006). Several options for enhancing the rate of heat transfer in tubes have been discovered in passive methods, including extended surfaces, treated surfaces and inserts. Allan Harry Richard and Agilan (2015) concluded that the extended surface (fins) made of copper has a higher thermal conductivity and produces a 94 percent efficiency. In heat exchangers, grooved and coated surfaces are examples of widely used treated surfaces techniques for boiling and condensation (Sonawane et al., 2016). Compared to smooth

tubes, tubes with internal grooves generate turbulence to facilitate fluid mixing and reduce the thickness of the boundary layer. The grooved tubes are frequently used in heat exchangers due to their ease of fabrication and superior heat transfer enhancement (Aroonrat et al., 2013). This would increase heat transfer by encouraging flow mixing and thinning in the sublayer zone of a viscous fluid. Insertion tubes, such as wire coils, twisted inserts, and dimples, are generally regarded as significant thermal enhancements. Matani and Dahake (2013) studied the thermal characteristics of a tube with twisted tape and wire coil and concluded that wire coil is more effective than twisted tape.

Conventional machining techniques such as lapping, grinding, honing, polishing, and brushing have been used to alter heat exchanger were able to improve the heat transfer performance. Nevertheless, these approaches are not enough to keep up with the increasing demand to produce compact and high-performance heat exchanger. Moreover, traditional processes frequently result in undesirable surface flaws, jeopardizing the surface finishing's overall quality. Extrusion is the typical method for achieving different conduit cross-sectional profiles. This method is used to manufacture wicker tubes (Promvongse, 2008). However, profiles produced by extrusion vary only in cross-sectional profile without axial variation. Although it is understood that the flow is directed axially along the tube, this configuration prevents the pipe from achieving its maximum heat transfer enhancement potential. Embossing, which is typically used to create herringbone tubes, is an additional unorthodox method for generating a modified inner surface (Miyara et al., 2003). In this process, a flat metal strip is embossed or stamped with a specific-shaped die, rolled into round tubes, and then inductively welded (Miyara et al., 2003). Researchers have focused on this type of pipe due to its advantageous ability to induce wake and disrupt the boundary layer via recirculation. Li et al. (2017) investigated the condensation of R410A refrigerant on a shell and tube heat exchanger with an exterior microgroove surface modification. He pointed out that micro fins function better at higher

fluid mass velocity, but smooth tubes perform better at lower velocity. He attributed the film thickening and reduced heat transfer performance to the surface tension effect, which dominates as the surface area increases.

Extrusion is the typical method for manufacturing conduits with various cross-sectional profiles. Micro-fabrication techniques, such as surface printing and embossing, have been implemented to create more structured surfaces with the goal of increasing the heat transfer surface and generating secondary recirculation flow (T.Ebisu et al., 1998). Regularly, the manufacturing phase is undervalued, and production constraints are not taken into account. This results in multiple iterations between the workshop and designer, resulting in a financial loss. As an enhancement technique, the grooving technique has recently been the focus of research. In terms of heat transmission and pressure reduction, the studied designs yielded promising outcomes. The various designs studied produced encouraging results in terms better of heat transmission, and reduction in pumping pressure penalty. In the production of axially grooved heat tubes, according to Omur et al. (2017), a block of metal is compressed and forced to flow through a die opening with a smaller cross-sectional area. In order to create such narrow grooves, it is necessary to apply high compressive forces, which will disrupt the extrusion and groove geometry (Omur et al., 2017). The grooving techniques that generate turbulent flow in a pipe have a number of benefits, including an increase in the rate of heat transfer, a decrease in the rate of energy consumption, and a reduction in the total cost.

### **2.3.1 Internal grooving**

Despite limitations on internal surface modification, non-conventional machining techniques, such as Magnetic Abrasive Finishing, can produce better finishing grooves with low cost and the ability to fabricate a wide variety of groove dimensions, especially for internal profile surfaces (Ridha et al., 2015). Using the concept of magnetic fields, a

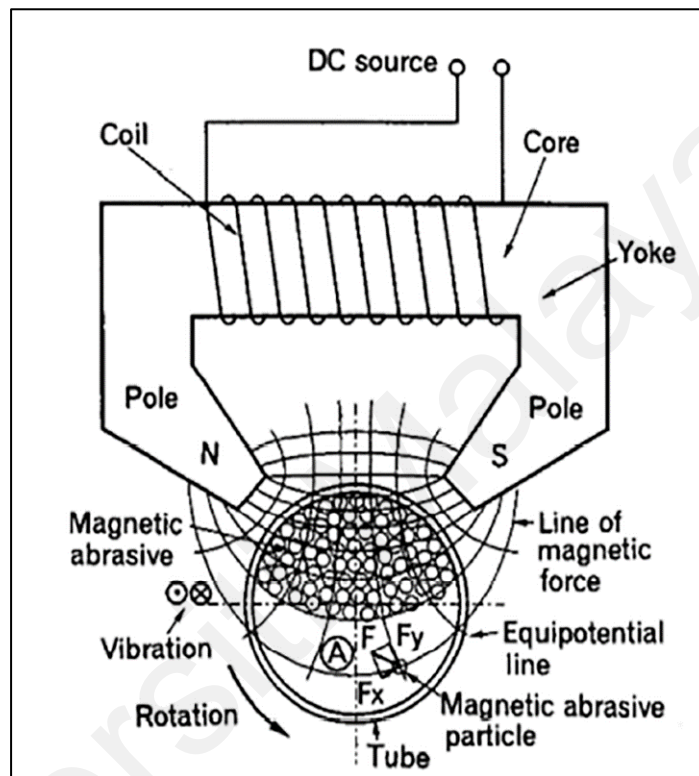


nontraditional technique for inner surface modification has thus been studied in recent years. Magnetic Abrasive Finishing (MAF) is an innovative method for producing different microgroove profiles utilizing magnetic abrasive. MAF is a non-traditional, ultra-finishing technique that is regarded as one of the most advanced manufacturing processes of the past decade. Due to its operational principle of employing very low force and loose abrasives, the procedures and techniques are more reliable than other methods. These experimental conditions safeguard the machining surfaces against detrimental effects. In a multitude of ways, MAF technology is vastly superior to the majority of machining techniques. Kumar et al. (2013) reported that MAF surface finishing is superior to conventional finishing techniques like lapping, honing, and abrasive flow finishing.

Using MAF, variable parameters such as abrasives, rotation speed, etc. can be used to generate a wide range of surface characteristics. Due to the comparative reduction of friction in the machining area, MAF is able to provide superior finishing properties. In addition, the MAF process expands areas of reach. Due to the fact that abrasives and magnetic fields play a role in finishing, MAF makes it possible to machine even minute areas. MAF processes are more efficient when their setup is independent of the object being finished. The abrasives serve as cutting instruments in the cutting process, which is governed by a magnetic field (Patil et al., 2012). MAF was created to overcome obstacles such as the high cost of finishing high-strength materials, high energy consumption, lower ecological safety, and the inadequacy and complexity of structures with complex shapes and small dimensions. Without regard to the length of the pipe, a vast array of groove types can be manufactured.

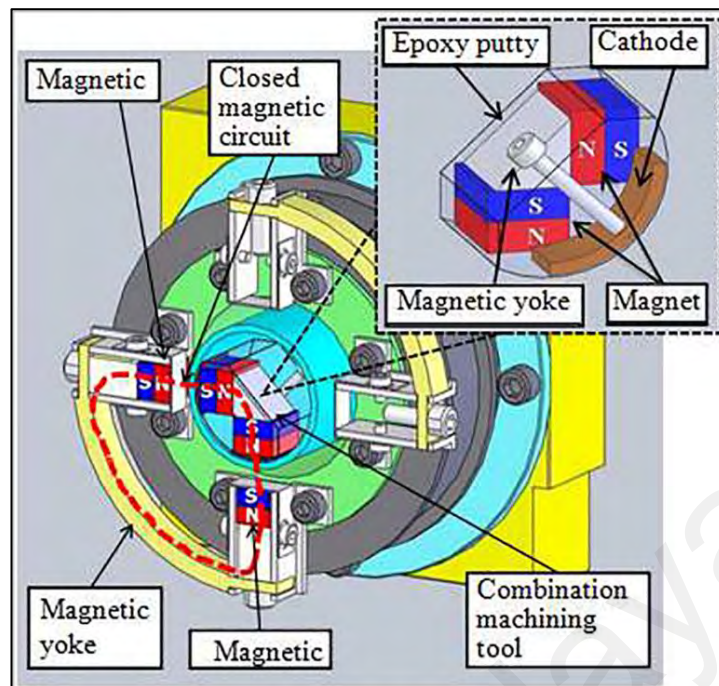
Researchers proposed a modification of external cylindrical object finishing to internal MAF in order to remove surface irregularities and impurities from the internal surface of cylindrical objects using MAF (Shinmura & Yamaguchi, 1995). The study depicts in

Figure 2.1 the proposed direct current magnetic abrasive system for use with a fixed pole system. The magnetic field generated by magnets surrounding the abrasives determines the cutting force of the abrasives. These abrasive particles are packed into the working gap, also known as the space between the workpiece and the magnet.



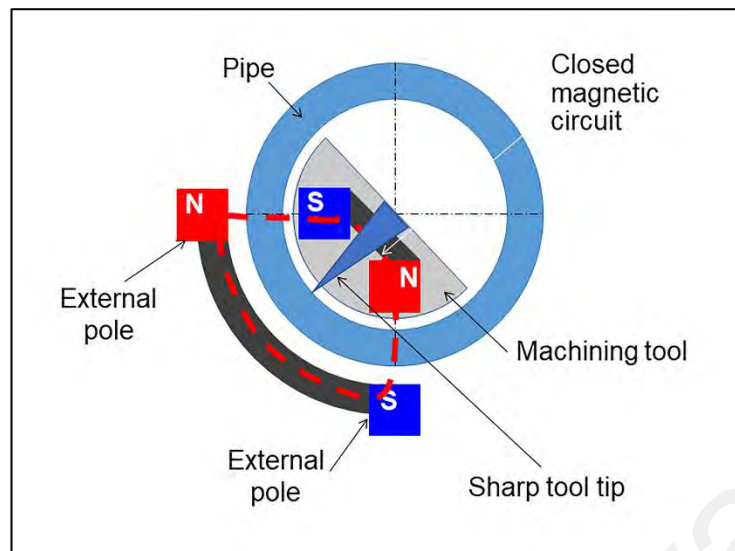
**Figure 2.1: Schematic diagram of internal surface – Magnetic Abrasive Finishing process setup (Shinmura & Yamaguchi, 1995)**

Ridha et al. (2015) have developed a device for achieving the desired surface finishing of aluminum tubes with greater control and uniformity of the surface profile. They include a set of permanent magnets on both the interior and exterior of the tube, with the magnet mounted on the jig outside the tube controlling the motion of the interior magnet via a close magnetic circuit configuration.

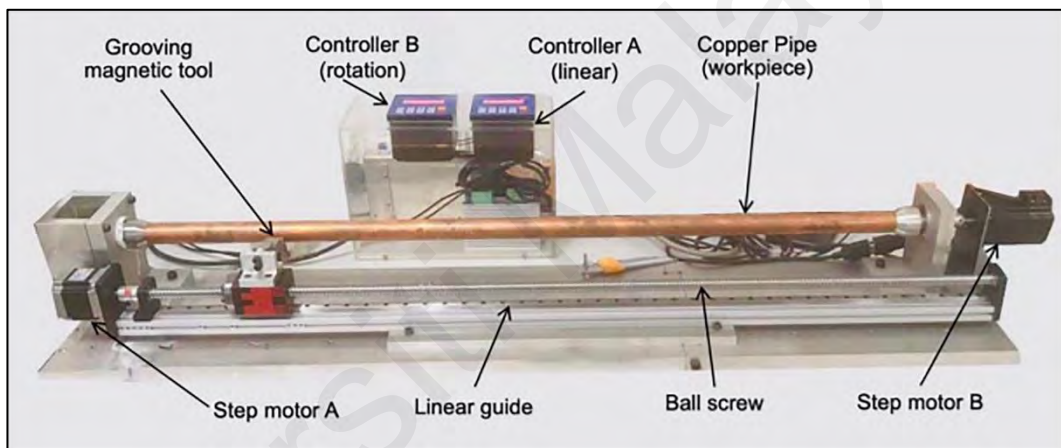


**Figure 2.2: The schematic diagram of the processing principle of magnetic abrasive finishing with combined electrochemical finishing in 3D model and machining tool structure (Ridha et al., 2015)**

Due to the ease of finishing nonferrous materials such as copper, aluminum, and brass, only nonferromagnetic surface pipe will be used (Heng et al., 2017). Kadhum et al. (2015) discovered that the nonferromagnetic surface (Aluminum) is extremely sensitive to magnetic abrasive powder concentration and working gap. Copper has the highest thermal conductivity when compared to brass and aluminum (Allan Harry Richard & Agilan, 2015; Sonawane et al., 2016), consequently, this study will employ this material. MAF machining is also preferred for internal surface finishing due to its superior surface finish. When performing a MAF operation, multiple parameters, which can be categorized as input and output process parameters, must be considered. Input parameters influence output parameters as a result of the MAF process. The magnetic abrasive type, abrasive particles, working gap, axial vibration, grinding oil, and workpiece material are input parameters (Kadhum et al., 2015; Kumar et al., 2013). As output parameters, surface roughness and removal weight are included.



(a)



(b)

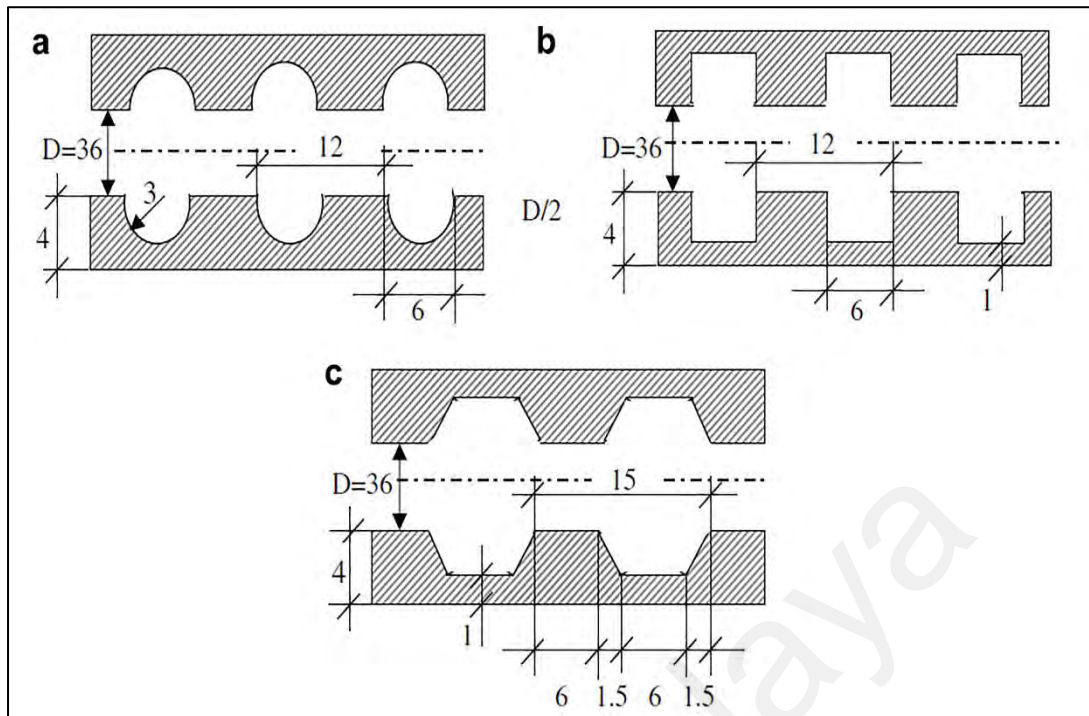
**Figure 2.3: (a) Internal tube grooving magnetic tool design (b) Magnetic grooving machine (Muhamad et al., 2021)**

In the study by (Muhamad et al., 2021) study, a new micro-grooving technique based on the MAF concept was developed. The study concluded that the process of micro-grooving is reliable and low cost, in addition to being able to fabricate superfinishing successfully. According to Figure 2.3(b), the external magnet is positioned on the linear guide rail, and the magnetic field produced between the internal and external magnets is capable of producing a groove along the entire length of the tube (Eid et al., 2021).

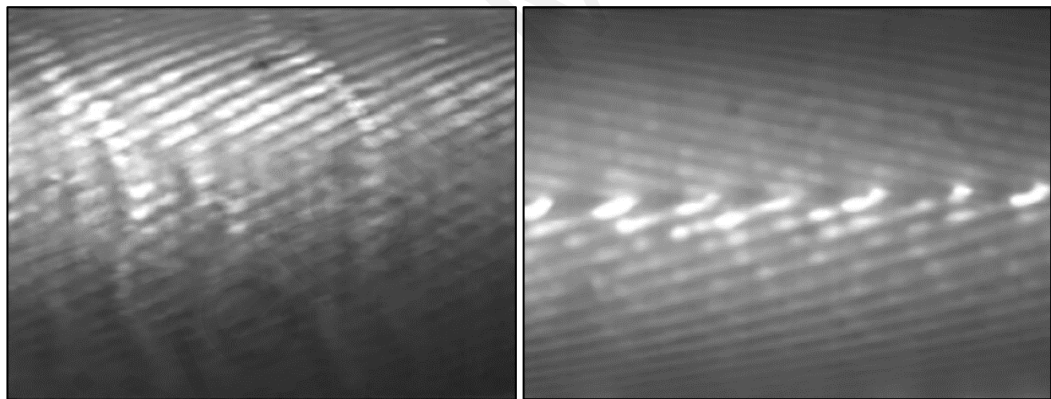
### **2.3.2 Internal surface profile characteristic on heat transfer performance**

According to T.Ebisu et al. (1998) the increase in heat transfer within inner grooved tubes is caused by the formation of a uniform film layer on the side wall of the tube, which increases the surface's wettability. Previous research has paved the way for additional investigation into the phenomena that occur in the active zone of a tube and produce such a significant increase in heat transmission. Under condensation heat exchange modes, an increase in the heat transfer coefficient of up to 300 percent was observed (Lambrechts et al., 2006). However, the welding required to connect the two ends of the flat plate raises concerns regarding the product's durability and efficacy, as it is well known that seamless pipes produced without welding are stronger than welded pipes. These grooved tubes induce turbulence or flow disturbance, which is required to reduce the thickness of the boundary layer when compared to smooth tubes. Because they transfer heat more efficiently, grooved tubes are preferred over smooth tubes.

Internal profiling is a technique that is rapidly gaining acceptance in industrial applications of the present day. Numerous studies are being conducted in this field to produce the best groove pattern capable of producing quality results due to its ability to alter the specific characteristics of fluid flow. Current internal grooving patterns on the market include herringbone, spirally grooved, and helical, among others. These applications of internal grooving are frequently associated with enhancing the heat transfer efficiency of a closed channel. The impact of groove geometry on the heat transfer of inner grooved tubes has been investigated by researchers. Bilen et al. (2009) and Kaji et al. (2012) studied a limited number of groove shapes, such as circular, trapezoidal, rectangular, spiral, and herringbone. Kaji et al. (2012) conducted research with three types of grooves as fixed variables: a smooth tube as a reference, spirally grooved grooves, and herringbone grooves.



**Figure 2.4: Geometric shapes of the grooved tube; a) circular, b) rectangular and c) trapezoidal grooves (Bilen et al., 2009)**

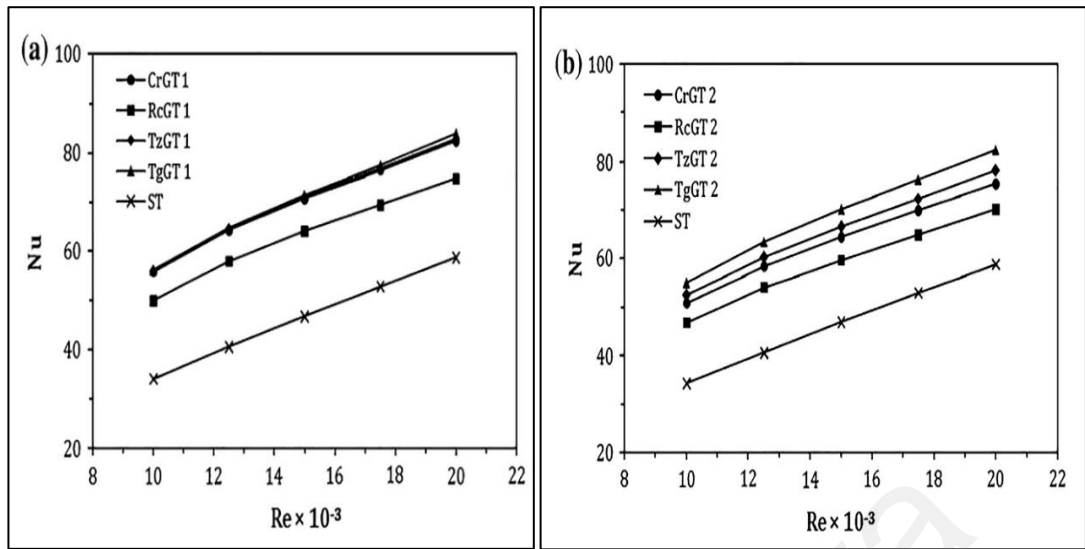


a)

b)

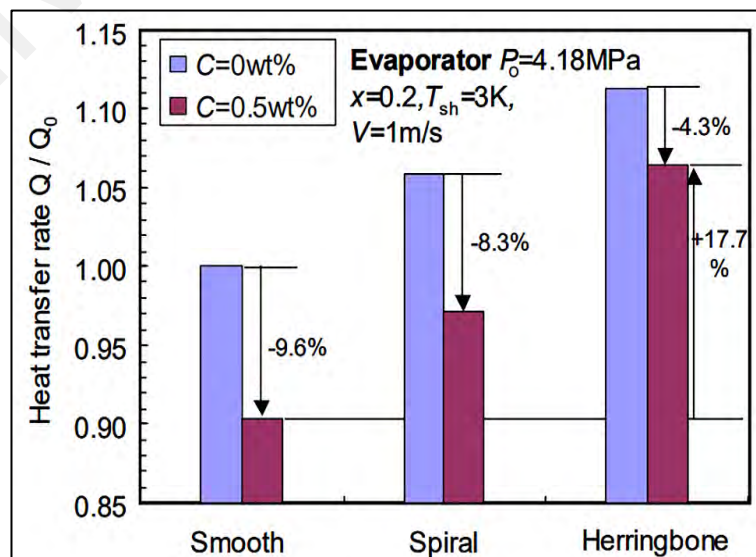
**Figure 2.5: Groove pattern of a) spiral tube and b) herringbone tube (Kaji et al., 2012)**

With a Reynolds number range of 10,000 to 38,000, circular grooves exhibited the greatest improvement in heat transfer at 63 % (Bilen et al., 2009). In terms of thermal performances circular and trapezoidal grooves recorded up to  $Re = 30\,000$ . It is concluded that optimum entropy generation is similar for all the studied grooves of  $Re = 17000$ .



**Figure 2.6: Effects on Nusselt number for varies geometry for (a)  $\frac{e}{D} = 0.1$  and (b)  $\frac{e}{D} = 0.2$  (Ramadhan et al., 2013)**

Ramadhan et al. (2013) found that the triangular groove produced the best results. The groove with the highest Nusselt number is the triangular groove TgGT, followed by the trapezoidal groove TzGT, the circular groove CrGT, and the rectangular groove RcGT. As shown in Figure 2.6, the Nusselt number is directly proportional to the Reynolds number. For greater comprehension, flow visualization is also conducted through transparent glass. Experiment results demonstrated that the herringbone pattern was the most efficient groove pattern, achieving the highest heat transfer coefficient.



**Figure 2.7: Result of heat transfer rate for each pattern in evaporator (Kaji et al., 2012)**

Researchers discovered that the geometry of the inner groove has a significant effect on the thermal analysis. To induce turbulence, the aforementioned concept has been extensively adopted to produce wicker and herringbone tubes with varying cross-sectional profiles (Miyara et al., 2003). In a series of studies, Miyara et al. (2003) addressed heat transfer phenomena utilizing herringbone tubes. He reasoned that the accumulation and dispersion of liquid at the converging and diverging sections of the fin grooves were the most crucial factors in promoting heat transfer. He went on to explain that a low liquid flow rate during condensation and evaporation results in the formation of a significantly thinner film, which corresponds to a higher heat transfer coefficient.

### **2.3.3 Coil wire insert**

Several researchers examined the impact of wire coil inserts on the enhancement of heat transfer. Previous research has uncovered numerous types of wire coil inserts. There are a number of benefits associated with the use of wire coil inserts, including an easy install-remove process, simple manufacturing, and low cost, as well as a reduction in fouling without altering the internal surface of the tube (Jafari Nasr et al., 2010; Liu & Sakr, 2013; Sonawane et al., 2016). According to Garcia et al. (2007), the wire coil modification is more reliable than twisted tape in promoting the transition from laminar to turbulent flow. In addition, a wire coil can increase the friction factor of laminar flow by up to 40% compared to a smooth tube (Garcia et al., 2007). Principal parameters for assessing thermal performance include pitch, diameter, and the ratio of pitch to diameter. According to Muñoz Esparza and Sanmiguel Rojas (2011), Chompookham et al. (2022) and Gunes et al. (2010), as the ratio of pitch to diameter increases, the friction factor decreases. However, a decrease in the pitch ratio results in a greater number of coils, leading to an increase in the Nusselt number (Azmi et al., 2021; Keklikcioglu & Ozceyhan, 2016; Syam Sundar et al., 2017).



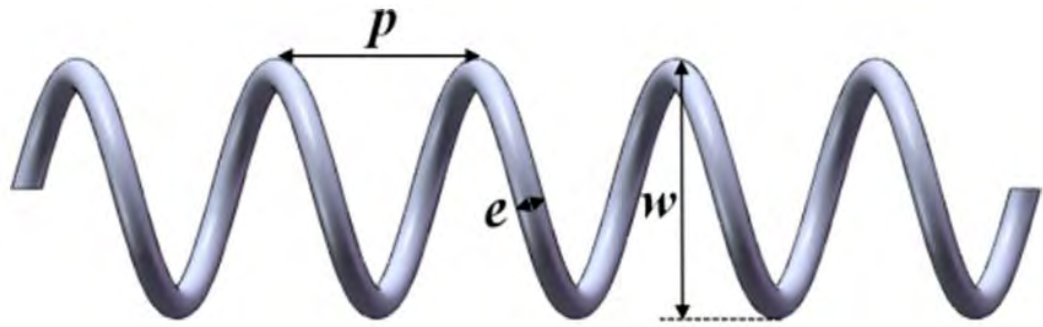


Figure 2.8: Conventional wire coil dimensions (Promvong, 2008)



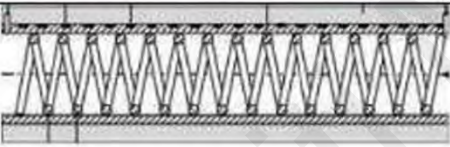



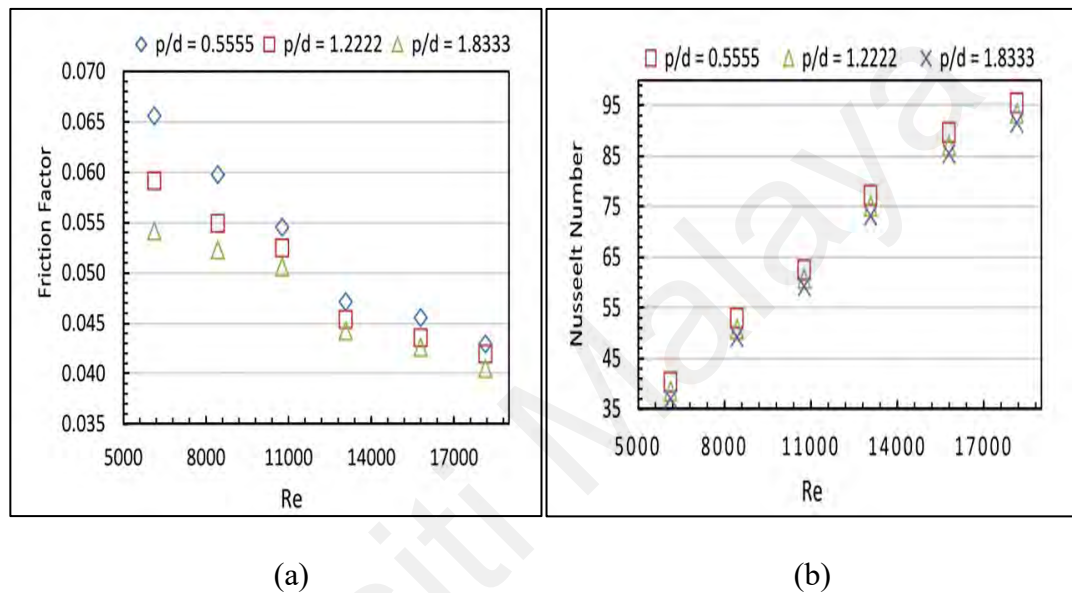
	<ul style="list-style-type: none"> <li>• Coiled square wires</li> </ul>
	<ul style="list-style-type: none"> <li>• Non-uniform wire coil combined with twisted tape</li> </ul>
	<ul style="list-style-type: none"> <li>• Coiled wire turbulators</li> </ul>
	<ul style="list-style-type: none"> <li>• Twisted tape and wire coil</li> </ul>
	<ul style="list-style-type: none"> <li>• Triangle cross sectioned coiled wire</li> </ul>
	<ul style="list-style-type: none"> <li>• Wire coil in pipe</li> </ul>

Figure 2.9: Examples of the configurations of various wire coils (Ray & Kumar Jhinge, 2014)

Chompookham et al. (2022) classified wire coils into 2 groups: conventional wire coils and modified wire coils such as in Figure 2.9. In addition, cross section shape, direction rotation and cross section orientation of wire coil provide an impact on the heat transfer

(Yu et al., 2020). Dang and Wang (2021) mentioned that twined coil insert tubes provide better thermal performance, such as increment about 12-38.2 for heat transfer rate and about 7.7-18.1 for friction factor, compared to smooth tubes. The longitudinal vortices are produced provide the better fluid mixing, thermal redevelopment and dynamic boundary layers at the tube wall (Feng et al., 2017; Keklikcioglu & Ozceyhan, 2018).

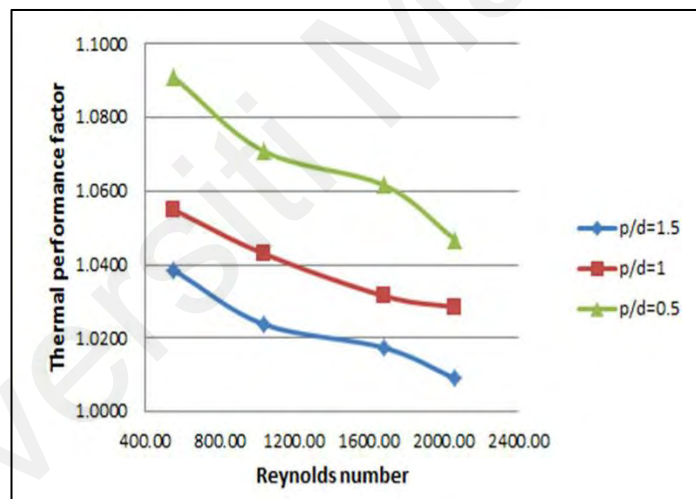


**Figure 2.10: Performance of (a) friction factor and (b) Nusselt number with variation wire coils at different Reynolds number (Kasturi et al., 2017)**

Thermal performance investigation of 10 mm, 22 mm, and 33 mm wire coil inserts tubes in Figure 2.10 revealed that (a) the friction factor increases up to 7.42 % (10 mm), 9.85 % (22 mm), and 15.6 % (33 mm); and (b) the Nusselt number increases up to 6.42 % (10 mm), 4.06 % (22 mm), and 1.21 % (33 mm) as compared to a smooth tube (Kasturi et al., 2017). In studies on the enhancement of heat transfer, the diameter and pitch of a wire coil are significant. Zidan et al. (2018) examined heat transfer and friction factor for various wire coil cross sections with Reynolds numbers between 11000 and 37500. By decreasing the pitch and increasing the diameter, thermal efficiency improved. This assertion is supported by research conducted by Göksu and Yilmaz (2021), who determined that diamond wire coil has the highest Nusselt number with a 98 % increase,

followed by triangular and circular wire coils, and smooth tube. Padmanabhan et al. (2021) reached the conclusion that wire coil inserts with varying pitch distances of 5 mm and 15 mm improved the Nusselt number by 63.91 and 31.39 percent, respectively. The smaller the pitch of a helical coil, the greater the heat transfer because of the increased turbulence and flow path (Zidan et al., 2018).

Parallel and counter flow are the two types of fluid flow. For all coiled wires, the convective heat transfer coefficient rises by 450 % for counter flow and 400 % for parallel flow (Zohir et al., 2015). Mohite et al. (2018) experimented with three distinct cross sections for wire coil inserts: circular, triangular, and square with 10 mm, 20 mm, and 30 mm pitch. In comparison to triangular and circular cross sections, the square cross section wire coil proved to be the most effective as represented in Figure 2.11.



**Figure 2.11: Thermal performance factor at Reynolds number (Mohite et al., 2018)**

Regardless of the diameter and pitch of the wire coil, the mass flow rates of hot and cold fluid also affect the rate of heat transfer and the effectiveness of heat transfer; wire coil inserts with 50 mm, 75 mm, and 100 mm helical pitches were tested at 55 °C and 65 °C (Sreenivisalu Reddy et al., 2017). Consequently, in this study, two distinct temperatures will be proposed for the experimental procedure.

## 2.4 Empirical equation

To determine parameters that cannot be determined theoretically due to the involvement of complex physics, empirical equations derived from experimentation are required. Several nondimensional numbers, such as the Reynolds number, Nusselt number, and Prandtl number, can be utilized to evaluate and analyze the thermal performance of a heat pipe. Convection may be a complex mode, but due to its many variables, it is possible to make improvements by adjusting these variables and determining their optimal values. In calculating the flow in a heat exchanger, the Reynolds number is a crucial factor to consider. The Reynolds number is a unitless number that identifies the condition of flow and is defined based on the inner tube diameter and flow velocity. There are three conditions for the Reynolds number;

**Table 2.1: Reynolds number categories**

Reynolds number	Flow condition
$< 2300$	Laminar
$2300 \leq Re \leq 4000$	Transitional
$> 4000$	Turbulent

Based on Bergman et al. (2011), the Reynolds number can be calculated using Equation (2.2) as following;

$$Re = \frac{\rho v_m D}{\mu} = \frac{v_m D}{\nu} \quad (2.2)$$

where  $\rho$  is the density of the fluid,  $v_m$  is the mean fluid velocity at the inlet of the test section,  $D$  is the inner diameter of the test tube,  $\mu$  is the dynamic viscosity of the fluid, and  $\nu = \frac{\mu}{\rho}$  is the kinematic viscosity of the fluid.

The definition of the Nusselt number, which is the ratio of convective to conductive heat transfer, is as follows in Equation (2.3) (Sanvicente et al., 2013);

$$Nu_D = \frac{h_o D}{k} \quad (2.3)$$

where  $h_o$  is the average heat transfer coefficient of the fluid flowing inside the test section, and  $k$  is the thermal conductivity of the fluid. Bergman et al. (2011) utilized this equation to compare tubes with and without inserts in their study. The greater the Nusselt number, the more efficient the convective rate of heat transfer. Typically, the Nusselt number is a function of the Reynolds number and the Prandtl number for turbulent flow.

A Prandtl is a boundary layer with a relative thickness to the thermal boundary layer. These two variables have an impact on the rate of heat transfer. Lesser Prandtl numbers indicate greater heat transmission. This is as a result of the fact that the greater the thermal boundary layer, the faster heat dissipates through the fluid. Prandtl is represented by the Equation (2.4):

$$Pr = \frac{\mu c_p}{k} \quad (2.4)$$

where  $\mu c_p$  is the molecular diffusivity of momentum and  $k$  is the thermal conductivity of the fluid. The thermal diffusivity predominates when the Prandtl number is less than 1, whereas the momentum diffusivity predominates when the number is greater than 1.

In heat transfer studies, the coefficient of heat transfer, friction factor, and efficiency all play an important role in numerical analysis. Using the following formula, the average heat transfer coefficient was determined:

$$h = \frac{Q}{A_i \times (T_s - T_f)} \quad (2.5)$$

where  $T_s$  is the mean temperature of inner surface of tube,  $T_f$  is the mean temperature of fluid,  $A_i$  is the surface area inside the tube and  $Q = VI$  is the energy supply.

The friction factor is related to the Reynolds number, and its value depends on whether the flow is laminar, turbulent, or transitional. The friction factor is a method for quantifying pipe flow frictional losses. When analyzing the heat transfer efficiency of a tube, it is crucial to evaluate this characteristic. In order to determine the friction factor,

$f$  for fully developed flow in a circular tube, the pressure drop across the test tube is measured. That is to say,

$$f = \frac{\Delta P}{\left(\frac{L}{D_i}\right)\left(\frac{\rho v^2}{2}\right)} \quad (2.6)$$

where  $\Delta P$  is the pressure drop between the inlet and outlet of the test tube measured by the differential pressure transmitter. The correlations proposed by Blasius (1913), which are defined by the following Equation (2.8), can also be utilized to calculate the friction factor for smooth tube:

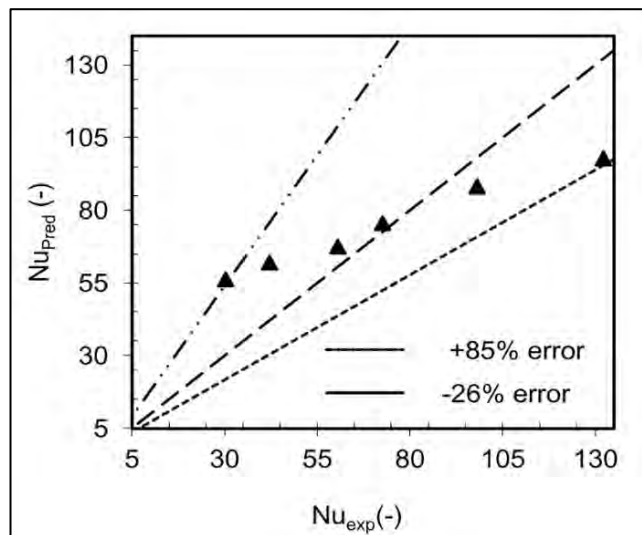
$$f = 4 C_f = 0.0316 Re^{-1/4} \quad (2.7)$$

where  $C_f$  is the skin friction coefficient.

In order to calculate its performance factor, the heat transfer efficiency equation must be used as presented in Equation (2.8) (Yusof et al., 2022),

$$\text{Effectiveness} = \frac{hA\Delta T}{hA\Delta T_s} = \frac{Nu}{Nu_s} \quad (2.8)$$

where  $Nu$  is the Nusselt number of the treated surface tube,  $Nu_s$  is the Nusselt number of smooth tube. Validation data is important in order to compare between experimental and established empirical correlations which are formed using dimensionless numbers. Mostly previous will use Gnielinski, Dittus and Boelter; and Petukhov equations. The empirical correlations with experiment data and the errors of Nusselt numbers are presented as in Figure 2.12.



**Figure 2.12: Comparison between experimental and predicted Nusselt number (Biswas & Salam, 2013)**

## 2.5 Computational Fluid Dynamics

Recently, Computational Fluid Dynamics (CFD) has gained in popularity as a method for designing, analyzing, and optimizing new processes that involved fluid interactions. The industry has increasingly utilized CFD to simulate processes as it has become more accurate, efficient, and cost-effective over time. ANSYS, OpenFOAM, MatLab, and COMSOL are common software that have been extensively applied. CFD have proven to be accurate in predicting fluid flow, pressure drop, friction factor, and heat transfer rate for complex industrial geometries; as a result, it is now the preferred tool for thermal-fluid engineering design and analysis (Aubin et al., 2004). Numerous researchers have used CFD to examine a vast array of concepts, designs, dimensions, and materials. In CFD, it is necessary to take the steps outlined by Vennila et al. (2017): fluid domain extraction, surface meshing, volume meshing, solving, post-processing, and report generation. The simulation results include power, circulation, heat transfer coefficient, friction factor, thermal-hydraulic performance, and changes in pressure. In order to obtain thermal performance, Hasgul and Cakmak (2022) and Chaudhari et al. (2021) noted that the CFD method determine thermal performance using Equation (2.9) to (2.11).

Conservation of mass or Continuity equation:

$$\frac{\partial(\rho u_i)}{\partial x_i} = 0 \quad (2.9)$$

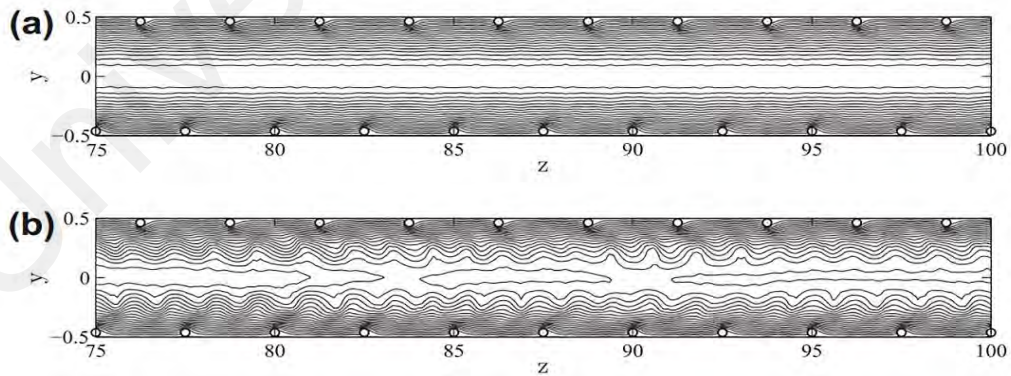
Conservation of momentum equation:

$$\frac{\partial(\rho u_i)}{\partial t} + \frac{\partial(\rho u_i u_j)}{\partial x_j} = \frac{\partial P}{\partial x_j} + \frac{\partial}{\partial x_j} \left( \mu \left( \frac{\partial(u_i)}{\partial x_j} + \frac{\partial(u_j)}{\partial x_i} \right) - \frac{2}{3} \mu \frac{\partial(u_i)}{\partial x_k} \delta_{ij} \right) \quad (2.10)$$

Energy equation:

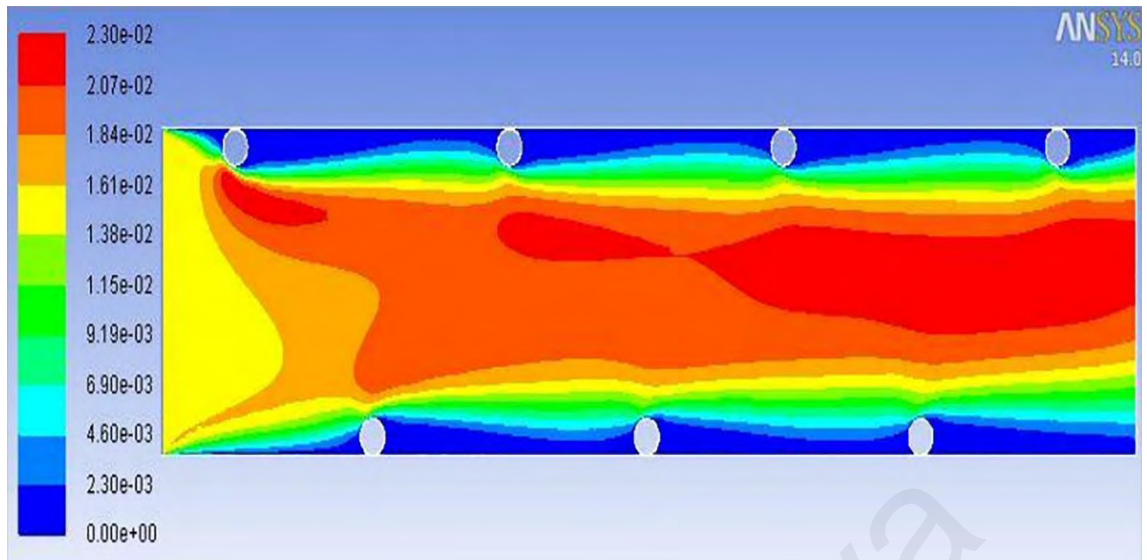
$$\frac{\partial}{\partial x} \left( \rho \mu_i C_p T - k \frac{\partial T}{\partial x_j} \right) = u_j \frac{\partial P}{\partial x_j} + \left[ \mu \left( \frac{\partial(u_i)}{\partial x_j} + \frac{\partial(u_j)}{\partial x_i} \right) - \frac{2}{3} \mu \frac{\partial(u_i)}{\partial x_k} \delta_{ij} \right] \quad (2.11)$$

In addition, CFD is advantageous because it provides detailed contours, plots, graphs, and values that reflect fluid flow and heat transfer, which would be challenging to observe using an experimental setup. In their study, Ramadhan et al. (2013) employed CFD to examine a variety of geometries. Muñoz Esparza and Sanmiguel Rojas (2011) presented the contour lines of streamwise velocity in the longitudinal  $yz$  plane as Figure 2.13 to aid comprehension of the effect of the instabilities of pressure drop increment. The temperature distribution was obtained with ANSYS FLUENT, as shown in Figure 2.14.



**Figure 2.13: Contour lines of streamwise velocity at a)  $Re = 500$  and b)  $Re = 600$  (Muñoz Esparza & Sanmiguel Rojas, 2011)**





**Figure 2.14: Temperature contour for Reynolds number 250 meshing size 0.5 mm (Yadav et al., 2022)**

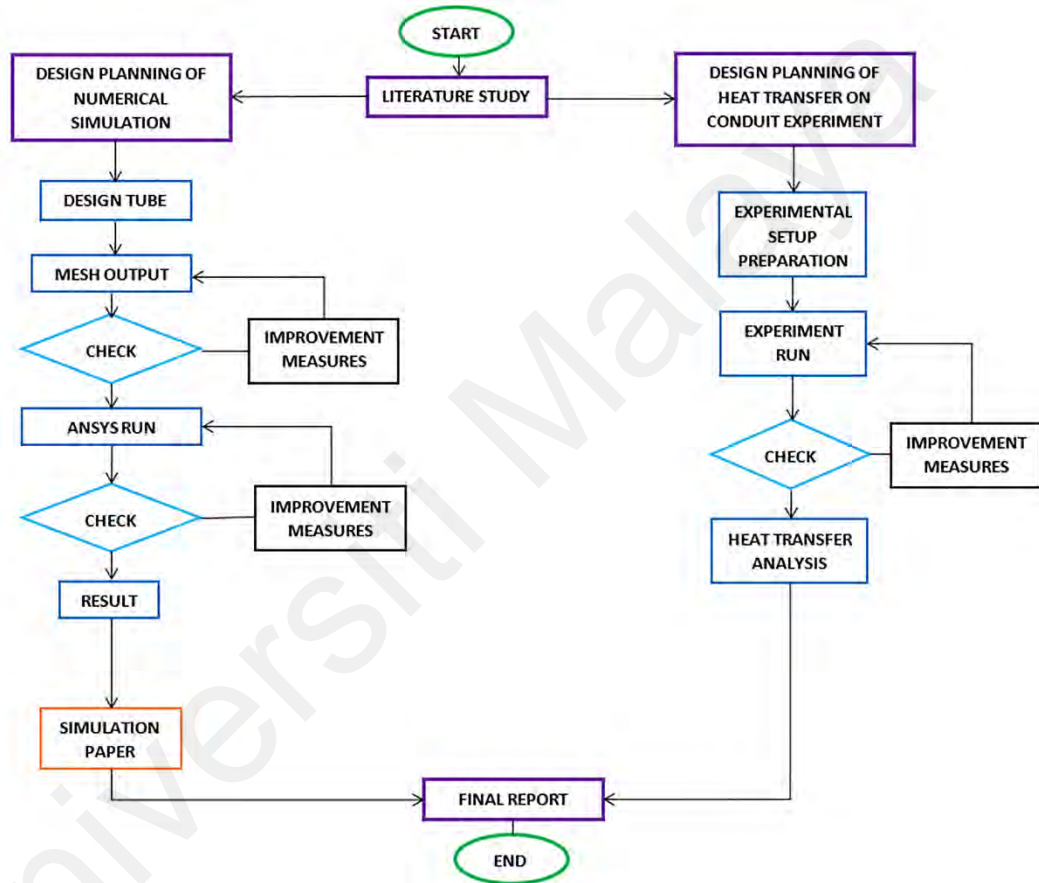
## 2.6 Summary

From a review of the relevant literature, there are few gaps in knowledge and information regarding the effects of heat transfer performance in groove and wire coil tubes. Therefore, the present research is conducted to further investigate the various configurations and thermal performance of internal groove tube and wire coil insert tube. This is to consolidate the current understanding of heat transfer enhancement via surface profile modification. Moreover, numerical methods and experimentation are employed.

## CHAPTER 3: METHODOLOGY

This section elaborates on the research flowchart for numerical analysis for groove and wire coil insert tubes, as well as the heat transfer on conduit experiment for a wire coil insert tube.

### 3.1 Flow Chart



**Figure 3.1: Flow chart of research study**

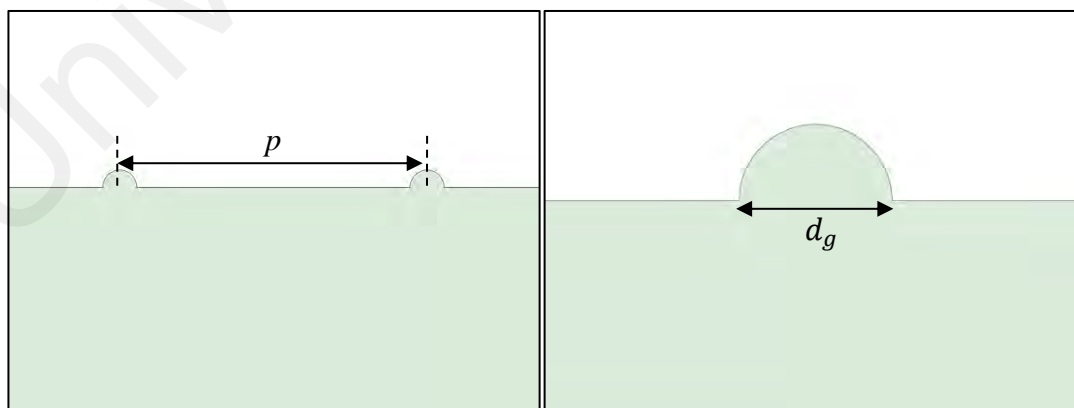
Figure 3.1 presents the flowchart of this research in detail. Beginning with a literature review on passive heat transfer augmentation analysis for surface internal profiling, such as grooves and wire coil inserts, the investigation then moves on to the experimental phase. On the basis of previous research, various approaches and methods for tackling this area can be considered for this further improvement. After specifying the parameters of the numerical analysis, the simulation is performed. The primary objective of this study is to compare the heat transfer performance of grooved and coil-inserted tubes.

Additionally, the research will demonstrate the effect of coil insertion on two distinct surface tube and bulk temperatures. The comparison between numerical analysis and experimental data will be elaborated more in the next chapter.

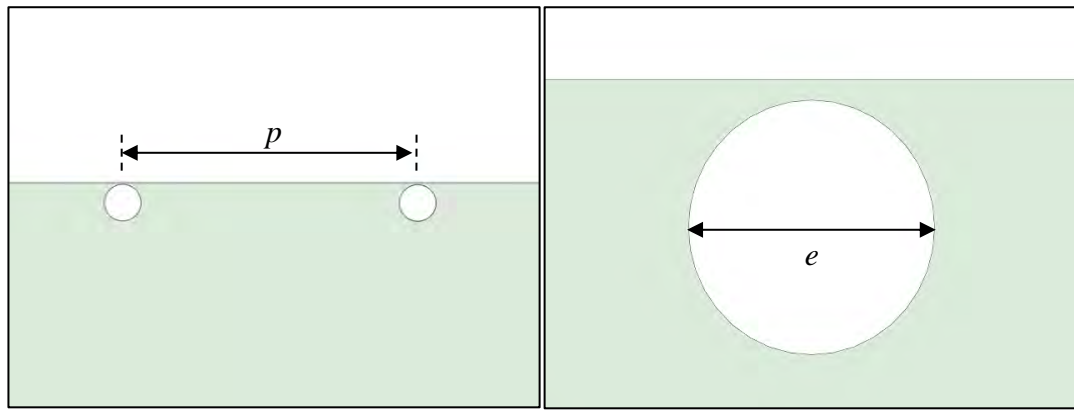
## 3.2 Computational Model

### 3.2.1 Design and Meshing

This study will simulate five distinct surface versions of the copper tube, each with a length of 1000 mm and a diameter of 25 mm. All designs are 2D which sketched using the SpaceClaim software, a component of the Ansys<sup>TM</sup> V20 software. A groove and a wire coil insert are depicted in detail in Figure 3.2. There are two designs based on this fact: groove tube and wire coil insert tube. This study will investigate two distinct lengths of the diameter of the groove,  $d_g$ , and the diameter of the cross section of the wire coil,  $e$ , specifically 0.5 mm and 1 mm. The groove pitch and wire coil pitch,  $p$  of all treated tubes, however, remain constant at 8 mm. Due to the uncertainty of the cross-sectional dimensions of the wire coil, there is a 0.04 mm gap between the coil and tube surface is made in Figure 3.2(b).



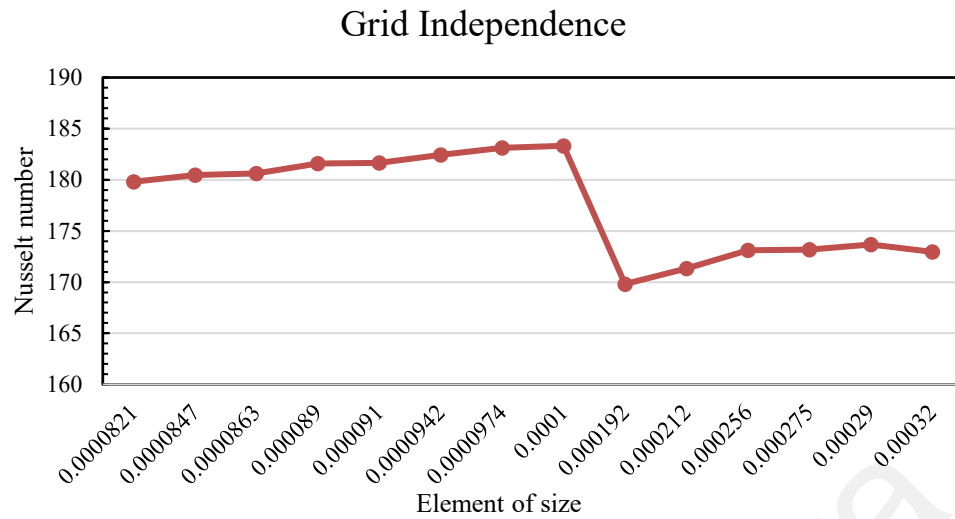
(a)



(b)

**Figure 3.2: Close up 2D design of the surface (a) circular groove and (b) wire coil insert**

Grid-independent tests are conducted to verify the appropriate element size of the meshing to be employed in this experiment. According to Haidong and Zhiqiang (John) (2012), the selection of an optimal grid design plays a critical role in computational fluid dynamics (CFD). The grid independence test is a method used to determine the most optimal grid configuration that yields the least number of grids while maintaining consistency in numerical analysis outcomes (Lee et al., 2020; Tu et al., 2019). According to the data presented in Figure 3.3, there is a consistent increase in the Nusselt number when the element size ranges from 0.0000821m to 0.0001m. However, beyond an element size of 0.000192m, the Nusselt number begins to exhibit fluctuations. In Table 3.1, the percentage difference is calculated between the research data and the empirical value of Petukhov (Ali et al., 2015). Since the difference is within 5% of the empirical value, it can be inferred that selecting 0.0001m is a favourable option for the purpose of this simulation.



**Figure 3.3: Grid Independence**

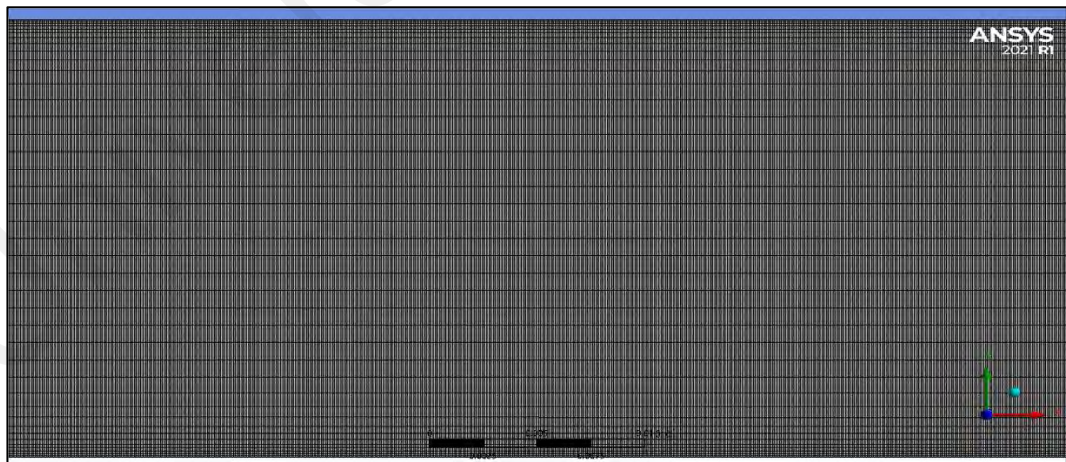
**Table 3.1 Percentage difference of Nusselt number correspond to element size for smooth tube**

Element size (m)	Difference (%)
0.0000821	1.026
0.0000847	0.664
0.0000863	0.579
0.000089	0.042
0.000091	0.018
0.0000942	0.416
0.0000974	0.794
0.0001	0.904

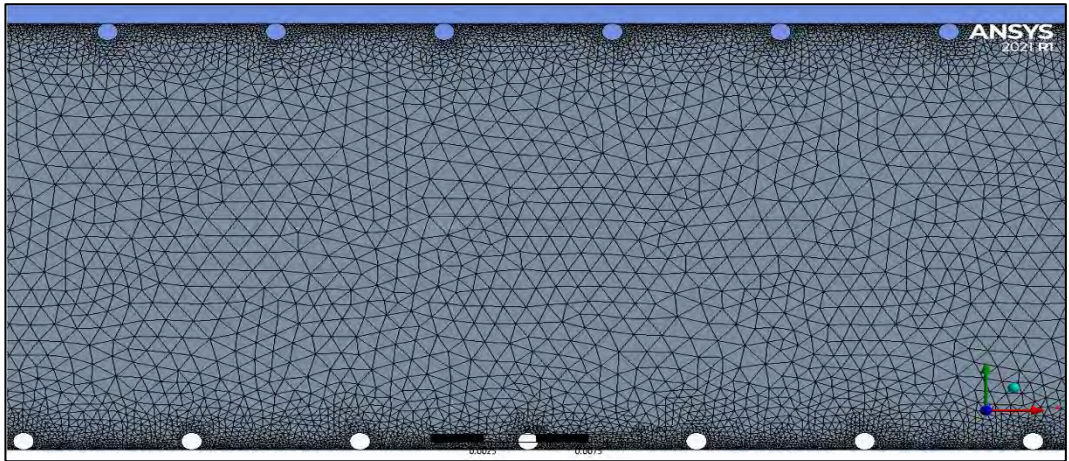
**Table 3.2: Geometry designs specification and meshing properties for all tubes**

<b>Tubes</b>	<b>Diameter (mm)</b>	<b>Nodes</b>	<b>Element No.</b>
Smooth	25	335410	160332
Circular Grooved	1	349564	166746
	0.5	341898	163161
Wire coil insert	1	314330	287560
	0.5	344344	161448

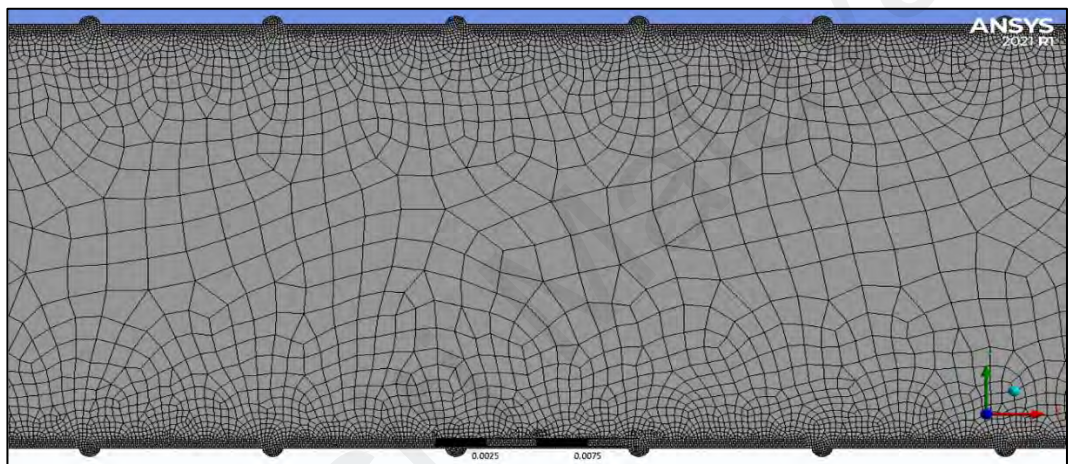
Flow and thermal conditions are considered when coordinating the components within the smooth tube. The wall effect can be accurately predicted by a high-quality mesh with boundary layers in the wall region. Face meshing and edge sizing with element size of 0.0001m are incorporated into the copper tube wall in order to achieve an excellent transverse and structured meshing. As shown in Figures 3.3 and 3.4, tubes with distinct groove and wire coil insert patterns were meshed using the same technique.



(a)

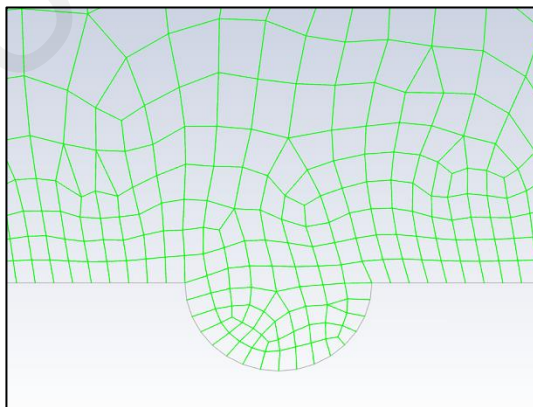


(b)

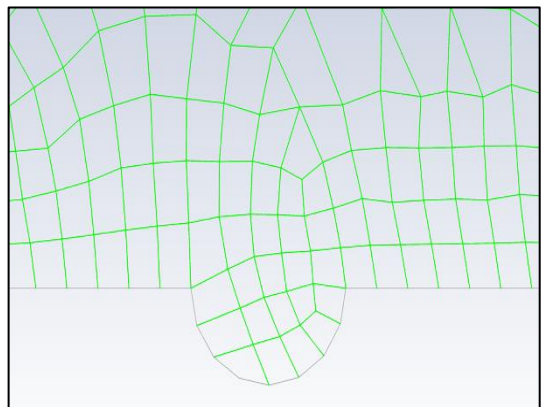


(c)

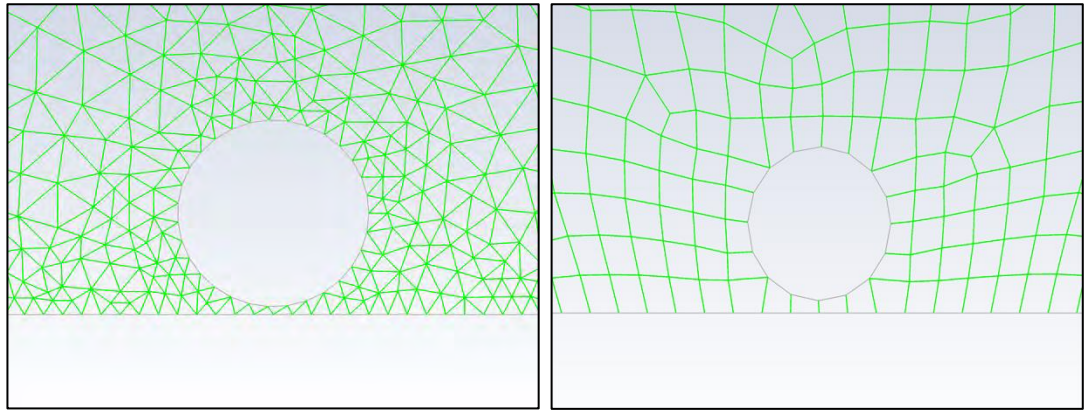
**Figure 3.4: Mesh of the medium for (a) smooth tube, (b) wire coil insert tube and (c) circular groove tube**



(a)



(b)



(c)

(d)

**Figure 3.5: Close up of mesh of (a) 1 mm circular groove tube, (b) 0.5 mm circular groove tube, (c) 1 mm wire coil insert tube and (d) 0.5 mm wire coil insert tube**

### 3.2.2 Computational Fluid Dynamics Simulation

Setting up model and boundary conditions is the first step in CFD simulation. In this study, the realizable of enhanced wall treatment and k-epsilon model are chosen for their thermal effects. Based on Table 3.2, detailed consideration is also given to boundary conditions such as the inlet, outlet, and wall. The entry velocity of the fluid is crucial for the inlet. Table 3.3 calculates the velocity at the inlet according to the desired Reynolds number.

**Table 3.3 : Boundary conditions and solution setup**

Inlet and outlet temperature	298.15 K, 303.15 K,
Heat flux	5092 W/m <sup>2</sup>
Pressure-Velocity Coupling Scheme	SIMPLE
Initialization Methods	Hybrid



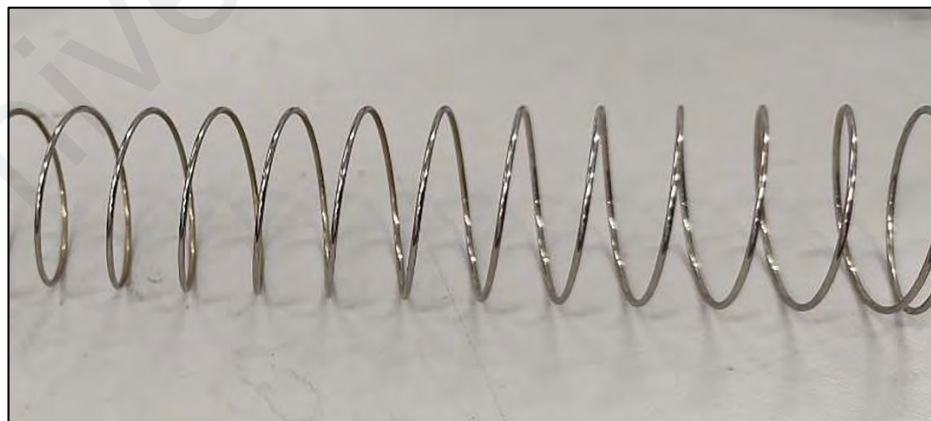
**Table 3.4: Inlet velocity for each Reynolds number**

No.	Reynolds number	Velocity at inlet [m/s]
1	4,000	0.16096
2	8,000	0.32193
3	12,000	0.48289
4	16,000	0.64385
5	20,000	0.80481
6	24,000	0.96578

### **3.3 Heat transfer on conduit experiment**

#### **3.3.1 Material specification**

The material specifications for this experiment are crucial, as they will produce excellent results. As the experiment in this study will involve fluid, it is impossible to eliminate the possibility of corrosion in the heated copper tube caused by the wire. As a result, stainless steel wire is chosen for the coil's construction. Moreover, the material of the wire does not play a significant role in the research, as the theory focuses on flow mixing induced by the coil.



**Figure 3.6: Wire stainless steel coil**



**Figure 3.7: Close up wire coil insert in tube**

The wire coil insert used in this experiment is made by bending a stainless-steel wire with a 1 mm diameter into a coil with a dimensionless wire diameter  $\frac{e}{d}$  of 0.04 and a dimensionless pitch  $\frac{p}{d}$  of 0.32. The coil of stainless steel is a helically-shaped coil that must be deformed into spring coils. The 8 mm pitch helically wound coil has been determined in this study. It has been demonstrated that the addition of a coil to a tube can improve heat transfer performance. A very limited amount of research has been conducted on the effect of changing the temperature of a heat tube on its performance as a heat transfer medium.

Consequently, it was also decided to conduct experiment with two different bulk temperatures of 25 °C and 30 °C; and compare the heat transfer performance of two systems:

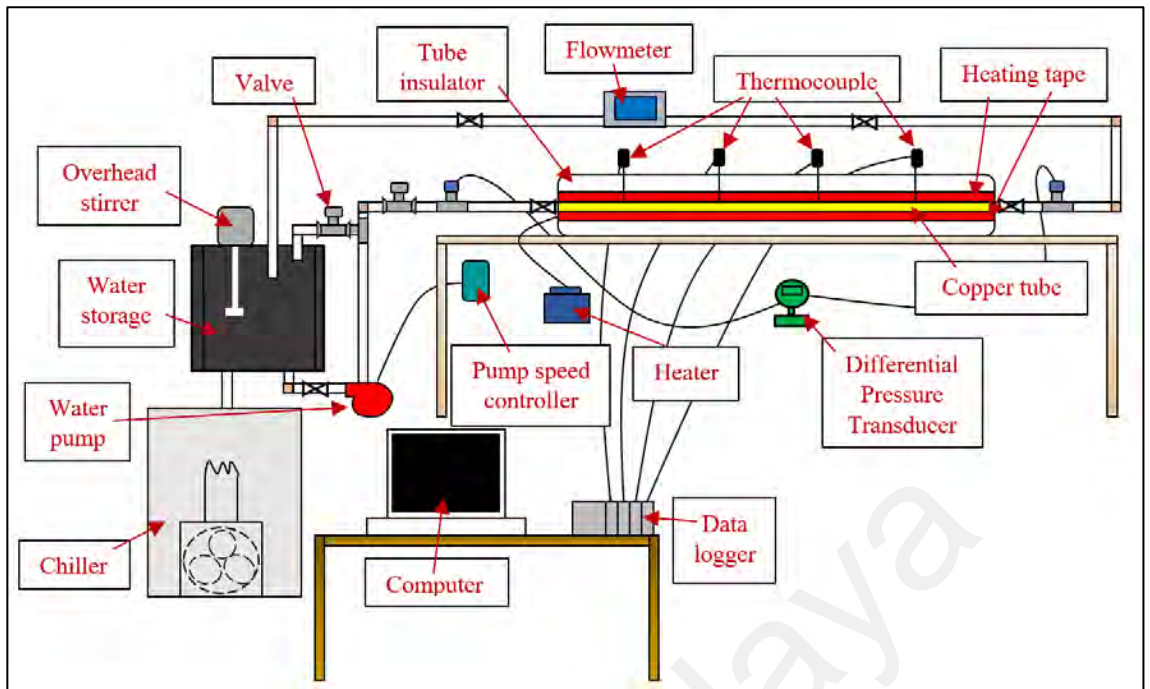
- i. Smooth tube
- ii. Tube flow with 1mm helically coiled stainless steel

**Table 3.5:**Materials and fluid properties

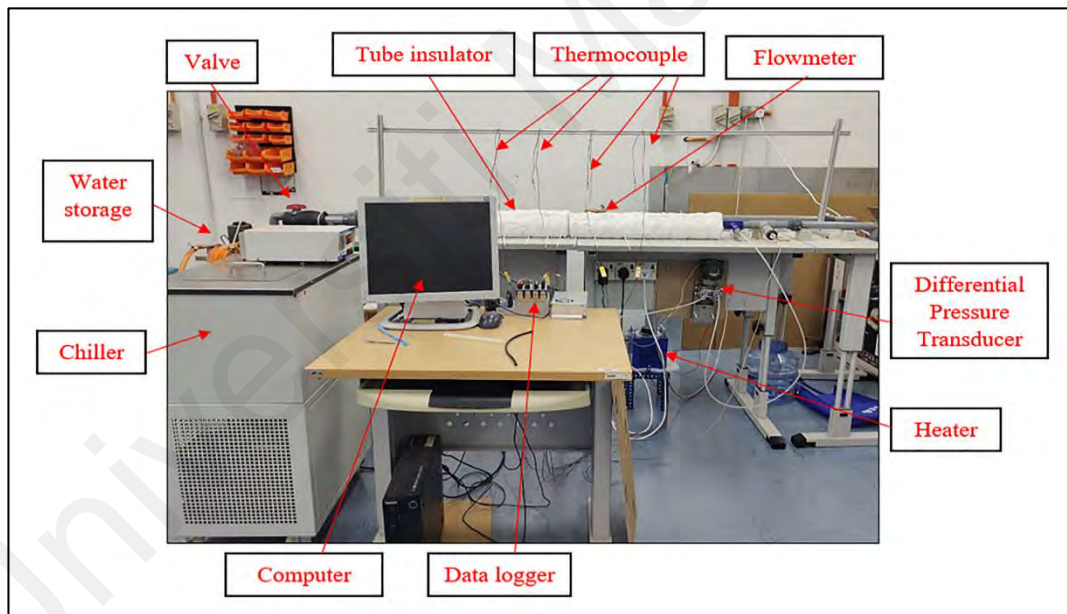
<b>Coil</b>	Material	Stainless steel 304
	Density	$8000 \text{ kg/m}^3$
	Diameter of cross section, $e$	1 mm
	Pitch length, $p$	8 mm
<b>Pipe</b>	Material	Copper
	Internal diameter	0.25 mm
	Outer diameter	0.27 mm
	Area	$0.00049087 \text{ m}^2$
	Length	1000 mm
<b>Fluid</b>	Material	Distilled water
	Density	$997 \text{ kg/m}^3$
	Thermal Conductivity, $k$	$0.6071 \text{ W/m} - \text{K}$
	Viscosity	$0.001003 \text{ kg/m} - \text{s}$
	Specific Heat, $C_p$	$4182 \text{ J/kg} - \text{K}$
	Prandtl number	6.99091

### 3.3.2 Experimental setup

To investigate the effect of wire diameter coil of stainless-steel wire in copper tube heat exchanger, a setup resembling a heat transfer workaround is constructed. An experimental set up was established based on tube heat exchanger heat transfer process. Figure A is a diagram of a miniature heat exchanger comprising a copper tube section for heat transfer, a chiller, a storage tank, a flowmeter, a pump, and a data acquisition system.



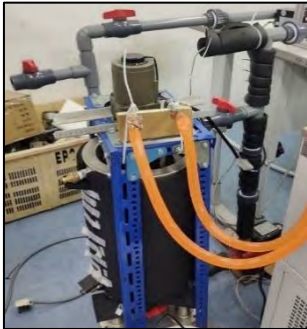
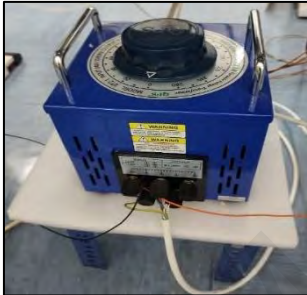


**Figure 3.8: Schematic diagrams of the heat conduit experiment**






**Figure 3.9: Overall view of the experiment setup**

The function of each apparatus and piece of equipment utilized in this experiment is described and listed in detail. To obtain accurate data that conforms to the theory of heat transfer, and thus place our experiment within an acceptable range, the equipment and apparatus used must be precise and appropriate.

**Table 3.6: Equipment for heat conduit experiment**

Equipment name	Figure	Function
Chiller		To adjust the temperature of a fluid to the specified temperature.
Variable voltage transformer		To provide different range of voltage.
Flowmeter		To measure the flow rate of the fluid in range for higher than 600 L/h.
Pump speed controller		To control the speed of pump required temperature and the flow of the pump.

Data logger		Read analogue data from a sensor (thermocouple) and process it with a computer to obtain the required measurement data.
Differential pressure transducer		To determine the difference in pressure between the inlet and outlet of a copper tube.
Tube insulator		Calcium silicate is used to insulate the copper tube against heat loss.

In this experiment design, the parameters and data to be measured are:

- a) Inlet and out temperature of fluid
- b) Temperature of heat tube at 4 points
- c) Pressure differential between the inlet and output
- d) Fluid flowrate
- e) Heater voltage and current

All of these variables are necessary for calculating the Reynolds number, the Nusselt number, the actual heat flux, the temperature of the bulk fluid, and the inner surface temperature. From these numbers, the experimental heat transfer coefficient between the

conventional smooth tube with wire coil inserts at bulk temperatures of 30 °C and 25 °C may be determined.

### 3.3.3 Experiment procedure

In this experiment, a 1 mm-diameter wire coil tube is subjected to two experimental runs at bulk temperatures of 25 °C and 30 °C. There are three distinct phases to the experimental technique. In the first portion of the copper tube, where heat will induce the copper tube, a number of sensors will be embedded for data reading. The copper tube is encased in cotton fiber to limit heat loss to the surrounding environment and maintain minimum variance in future results. Four k-type thermocouples are placed equidistantly from each other beginning at a distance of 0.196 m, and they are coupled to an NI DAQ device for obtaining temperature data at a specific spot. Each thermocouple was calibrated to 0.1 °C accuracy between 20 °C and 50 °C range. Using LabView software installed on the computer, the initial temperature of thermocouples is determined and recorded into National Instruments™ (NI) data logging system. The air conditioner and heating are activated separately. Observation of the temperature difference between the input and output for purposes of zero error and offset.

The second part is responsible for transferring fluid into the exchanger's base, for which a pump is necessary. PVC pipe is used to transmit the entire heat exchanger flow. There is one device and three types of sensors and transducers along the piping system. The pump receives water from the storage tank before the flow begins. The fluid will be pumped through the first resistance temperature detector (RTD) following the pump. Fluid then continues to flow to a second initial sensor referred to as the differential pressure sensor before proceeding to the copper heat tube section. Both devices are operated to compute the temperature difference and pressure at the inlet and outlet. Simultaneously, the heater knob is adjusted between 140 V and 160 V, and a multimeter

is used to tune the heater power supply to the range of 533-537 W by observing the voltage and current in real time. The fluid flow rate data is obtained after letting the pump run for approximately 10 minutes. During fluid flow back into the storage tank, the flowmeter sensor will measure the fluid's rate of flow. Once the input temperature reaches a stable state, the bulk temperature reading is recorded. The method is repeated with the flowrate incrementing by 284 L/h, 568 L/h, 853 L/h, 1138 L/h, 1422 L/h and 1706 L/h. The heater is then switched off first, followed by the chiller and the pump.

Universiti Malaya



## CHAPTER 4: RESULT AND DISCUSSION

The outcomes of simulation and experiment were discussed in this section. The temperature contour, rate of heat transfer, velocity profile, Nusselt number, and heat transfer coefficient at varied inlet velocities for the smooth, circularly grooved, and coil-inserted tubes were derived from the Ansys<sup>TM</sup> software numerical analysis. In addition, the experimental results for the tube with a coil inserted were presented in order to validate the numerical analysis.

### 4.1 Numerical Analysis

CFD-based numerical analysis produced the temperature contour, heat transfer rate, velocity profile, and Nusselt number at changing inlet velocities for tubes with smooth and four different interior geometries at two bulk temperatures; 25 °C and 30 °C.

#### 4.1.1 Temperature distribution

The temperature contour depicts the fluctuating temperature change of the fluid throughout the simulation. Figure 4.1 illustrates the temperature contours of the smooth tube, whereas Figure 4.2 and Figure 4.3 illustrate the temperature contours of the grooved tubes; and Figure 4.4 and Figure 4.5 depict the temperature distribution of wire coil tubes.

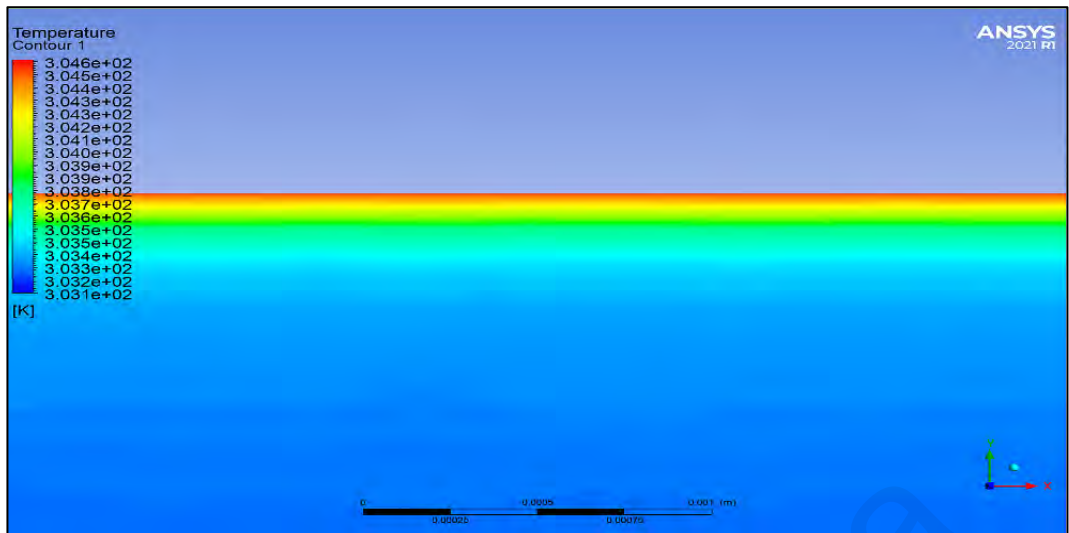


Figure 4.1: Temperature distribution of smooth tube at  $Re = 24000$  at bulk temperature  $30\text{ }^{\circ}\text{C}$

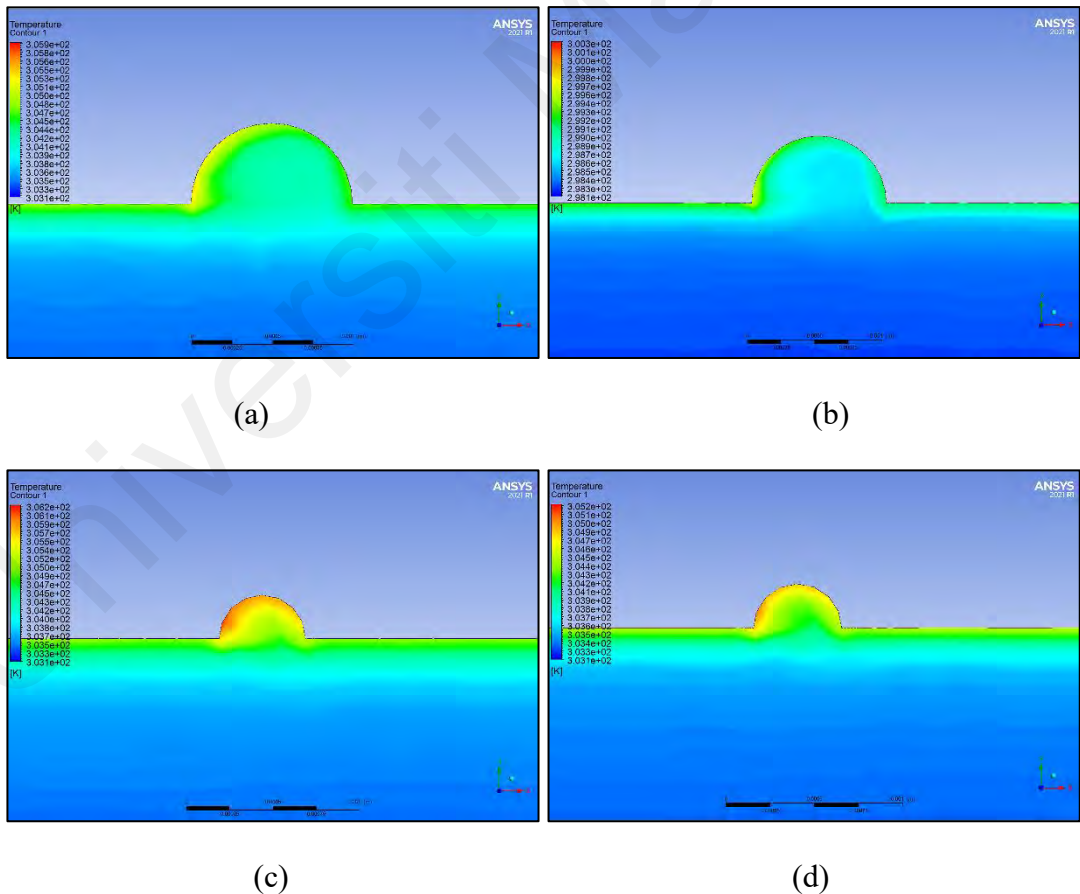
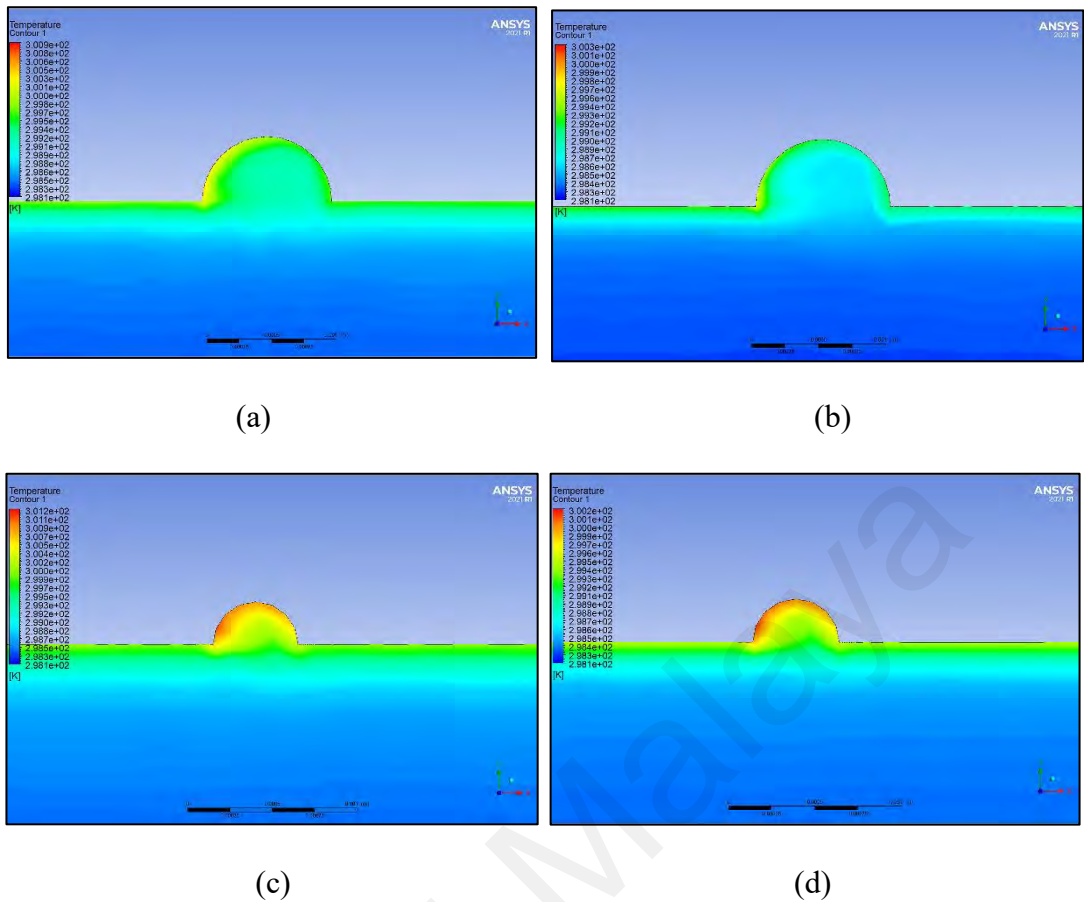
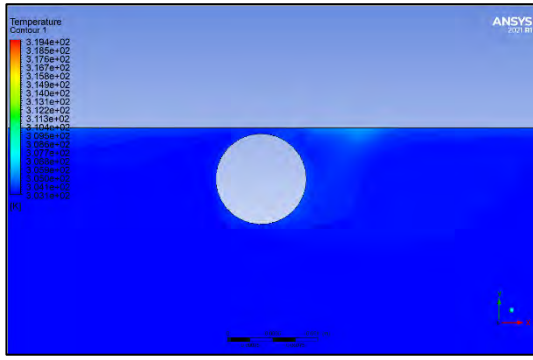


Figure 4.2: Near wall temperature contour of circular groove tubes (a) 1 mm at  $Re = 16000$ , (b) 1 mm at  $Re = 24000$ , (c) 0.5 mm at  $Re=16000$  and (c) 0.5 mm at  $Re=24000$  for bulk temperature  $30\text{ }^{\circ}\text{C}$

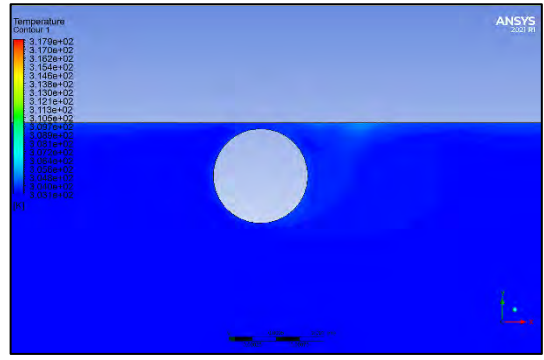


**Figure 4.3: Near wall temperature contour of circular groove tubes (a) 1 mm at  $Re = 16000$ , (b) 1 mm at  $Re = 24000$ , (c) 0.5 mm at  $Re=16000$  and (c) 0.5 mm at  $Re=24000$  for bulk temperature  $25\text{ }^{\circ}\text{C}$**

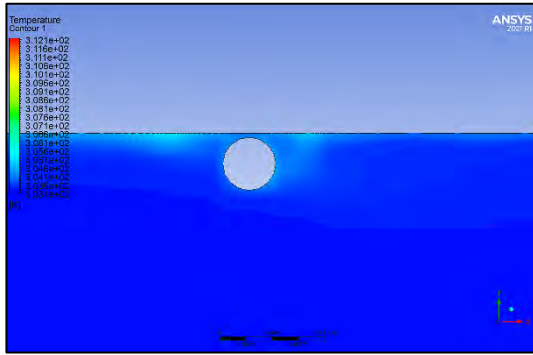
Observations indicate that the flow has a direct influence on temperature. On the basis of the temperature distribution, the heat dissipation of larger groove results in decrease the temperature compared to the smaller groove as the fluid enters the grooves and swirls, at one corner relative to the fluid's angle of entry. It is widely accepted that the shape of the groove has a substantial impact on the heat dissipation process. A rounder form with a smoother surface will likely have better flow and disperse heat more evenly throughout the grooves. As seen in Figure 4.2 and Figure 4.3, the circular groove profiles disperse heat to a greater extent than those with a lower Reynolds number.



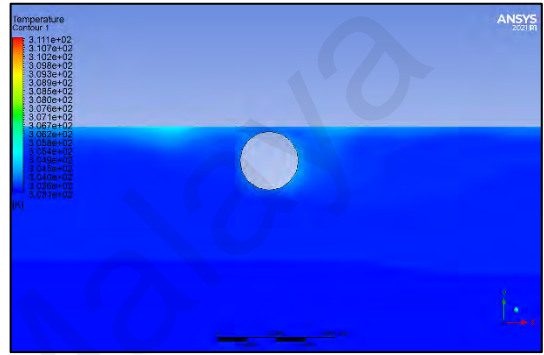
(a)



(b)

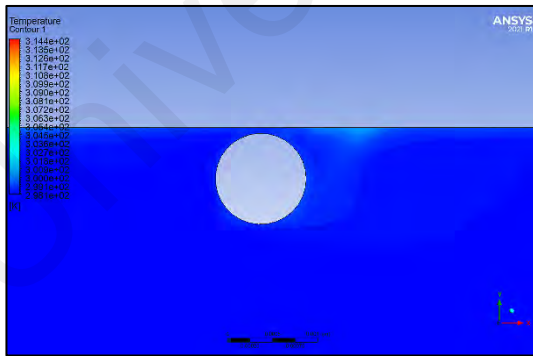


(c)

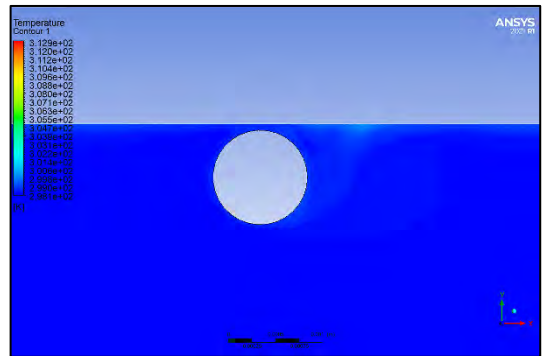


(d)

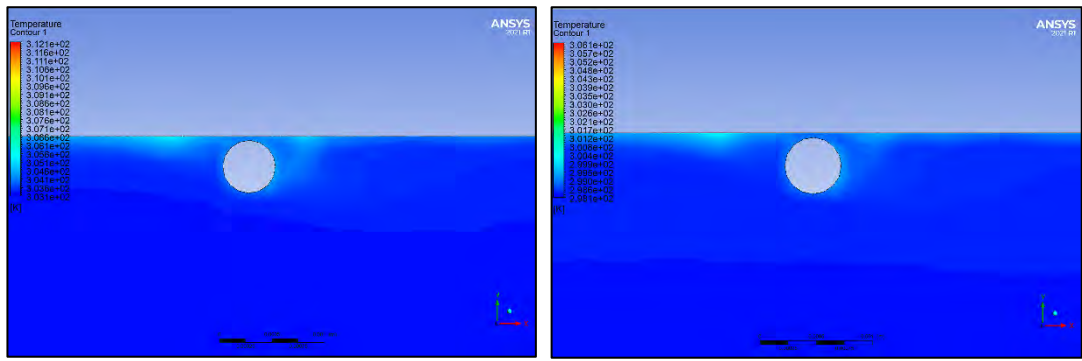
**Figure 4.4: Near wall temperature contour of wire coil inserts tubes (a) 1 mm at  $Re = 16000$ , (b) 1 mm at  $Re = 24000$ , (c) 0.5 mm at  $Re=16000$  and (d) 0.5 mm at  $Re=24000$  for bulk temperature  $30\text{ }^\circ\text{C}$**



(a)



(b)

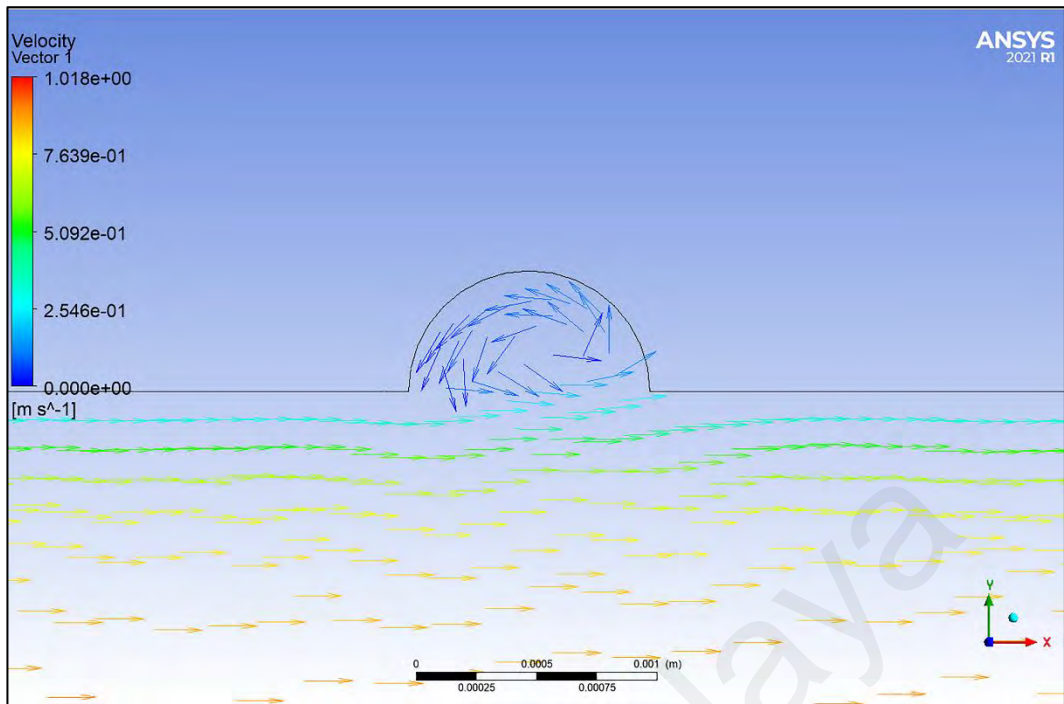


**Figure 4.5: Near wall temperature contour of wire coil inserts tubes (a) 1 mm at  $Re = 16000$ , (b) 1 mm at  $Re = 24000$ , (c) 0.5 mm at  $Re=16000$  and (c) 0.5 mm at  $Re=24000$  at for bulk temperature  $25\text{ }^{\circ}\text{C}$**

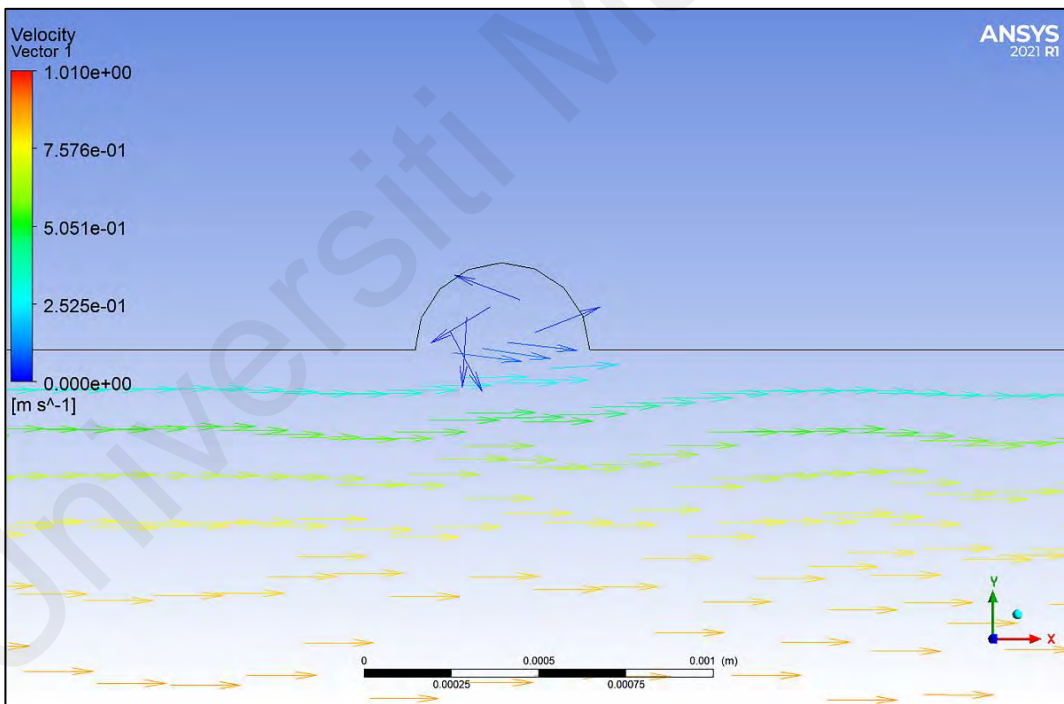
As seen in Figure 4.4 and Figure 4.5, the wire coil inserts profiles disperse heat more than those with a lower Reynolds number. The fluid flow swirls around the coil causes the temperature to decrease. The diameter of cross section coil has a substantial impact on the heat dissipation process.

#### 4.1.2 Velocity profiles

As seen in Figure 4.6 and Figure 4.7, the velocity vector of the circularly groove tubes, which reflects the rate of fluid location change within the tube, illustrates the effects of adding grooves to the geometry, which alters the flow pattern. The impact of adding grooves to the geometry of the tube, which has altered the flow pattern as depicted in the figures. The convection behaviour of a segment of a groove indicates an increase in the rate of heat transfer. The influence of such flow conditions varies with groove width, and the strength and persistence of this recirculation will have a direct effect on heat transport close to the wall surface.

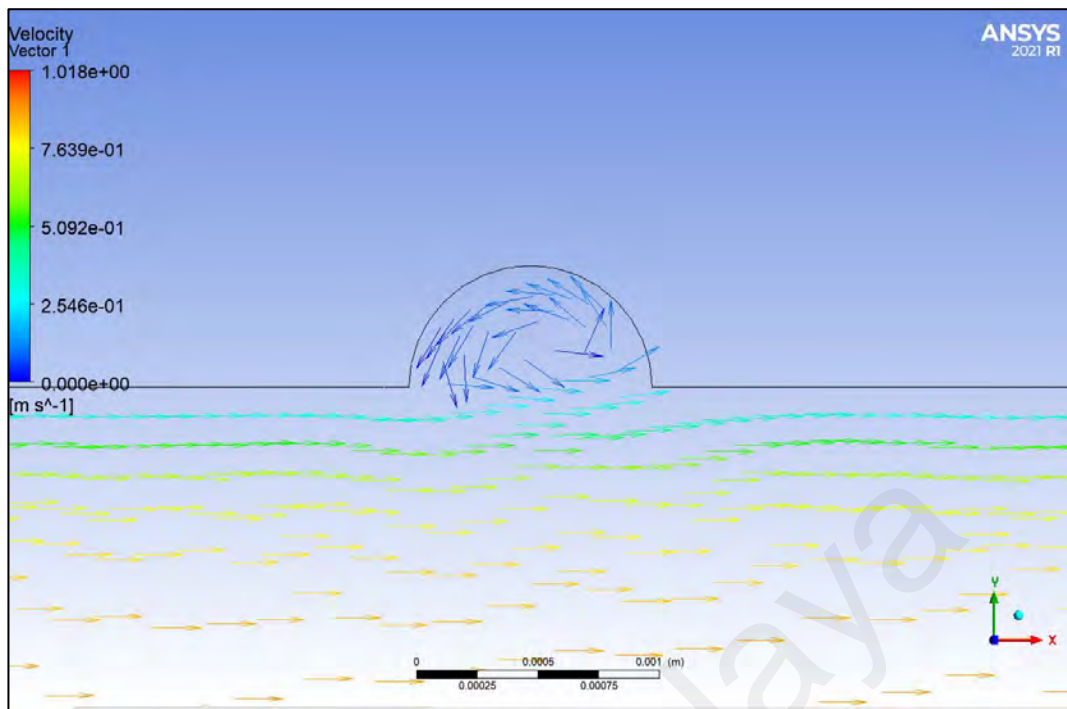


(a)

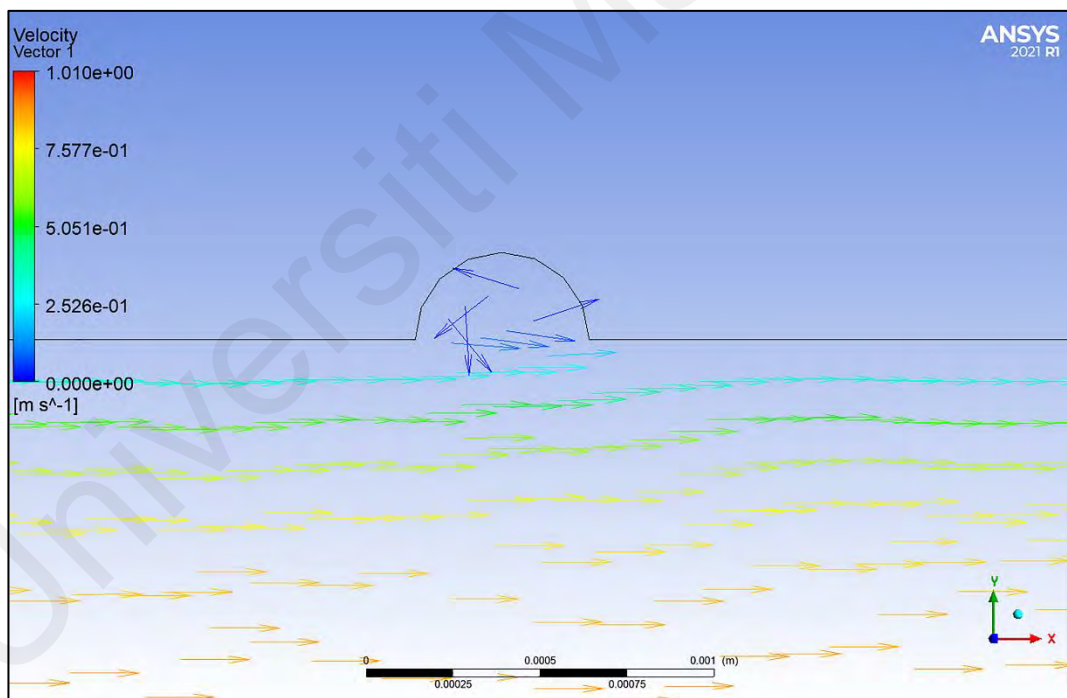


(b)

**Figure 4.6: Velocity profiles of circular groove tube (a) 1 mm and (b) 0.5 mm at  $Re=24000$  for bulk temperature  $30\text{ }^{\circ}\text{C}$**



(a)

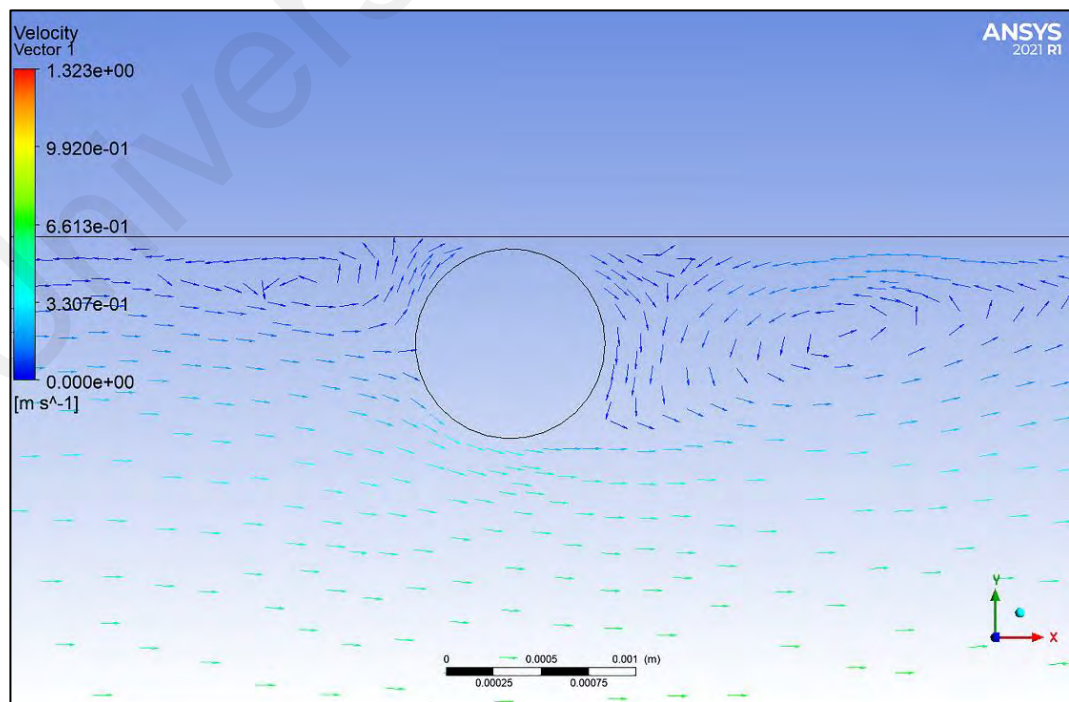


(b)

**Figure 4.7: Velocity profiles of circular groove tube (a) 1 mm and (b) 0.5 mm at  $Re=24000$  for bulk temperature  $25\text{ }^{\circ}\text{C}$**

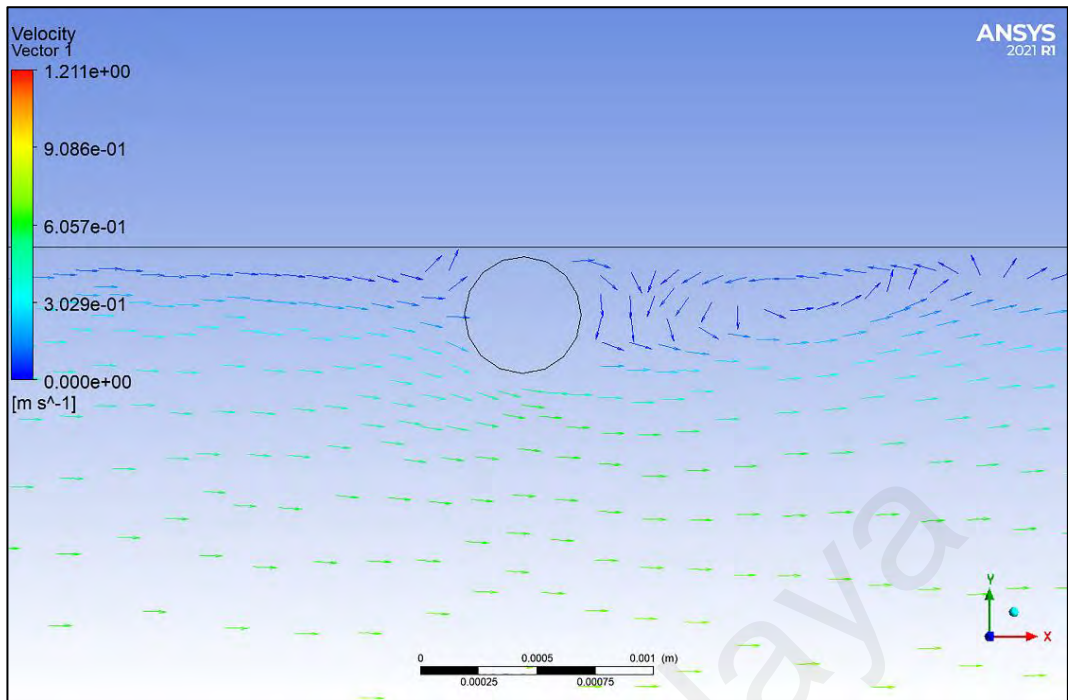
The convection behaviour of the groove section indicates an increase in heat transfer rate. At the void section of the microgroove, it is shown that a circulation or swirling motion is generated. This explains the increase in the rate of heat transfer for micro-grooved tubes, which is associated with improved convection behaviour, particularly on the groove ribs. In addition, the results demonstrate that recirculation becomes more pronounced as the depth-to-pitch ratio increases from 0.5 mm to 1 mm. The effect of such flow conditions varies with the width of the groove, and the intensity and persistence of this recirculation will have a direct effect on heat transport close to the wall surface. Increased heat transfer rate is indicated by the convection behaviour of the groove section.

Figure 4.8 and Figure 4.9 depict the velocity vector for wire coil insert tubes. On the basis of velocity profiles, the flow region oscillates more with 1 mm diameter wire coil inserts than with 0.5 mm diameter wire coil inserts because the ratio between the diameter of the wire coil and the diameter of the tube is greater for the 1 mm diameter wire coil inserts.



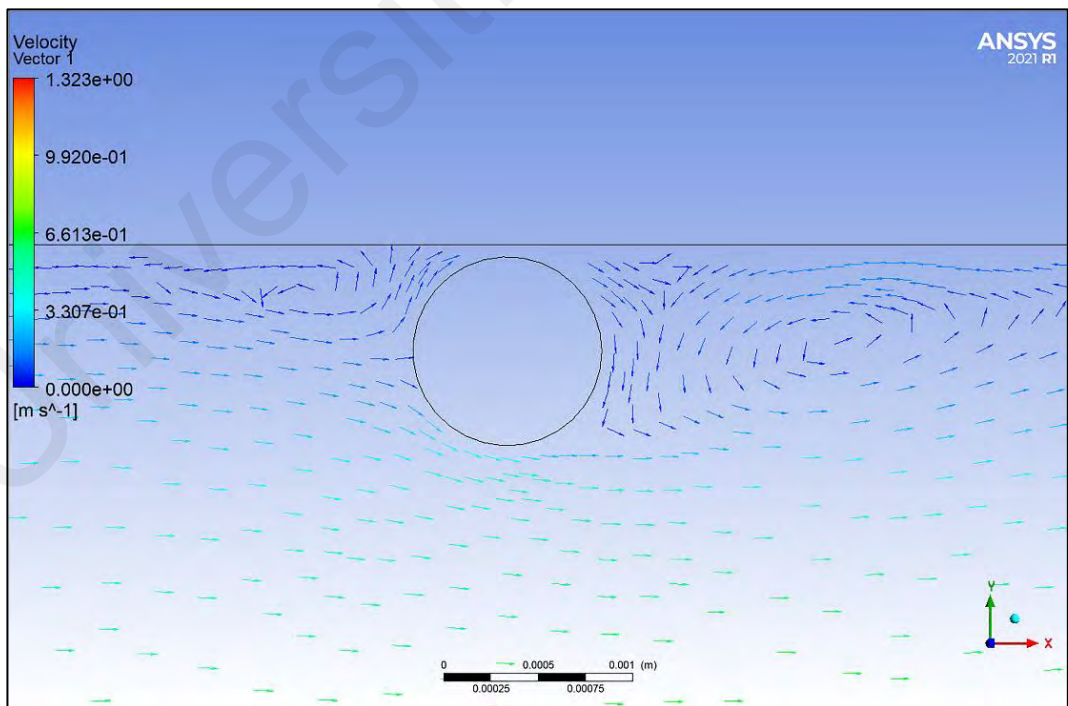
(a)



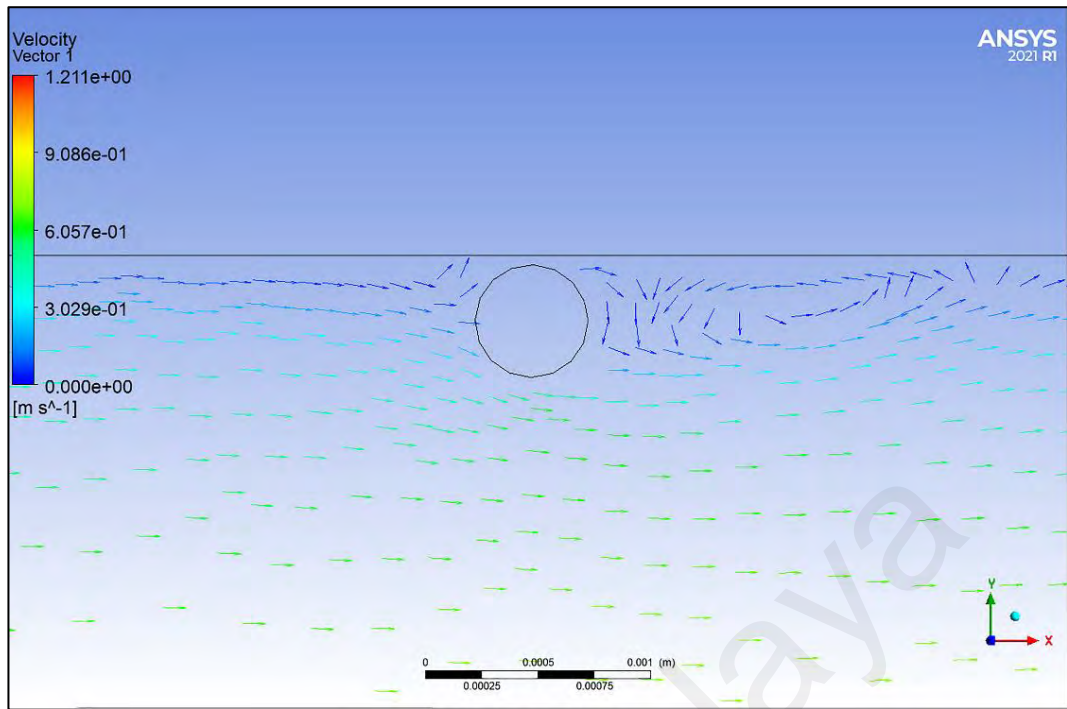


(b)

**Figure 4.8: Velocity profiles of wire coil insert tube (a) 1 mm and (b) 0.5 mm at  $Re=24000$  for bulk temperature  $30\text{ }^{\circ}\text{C}$**



(a)



(b)

**Figure 4.9: Velocity profiles of wire coil insert tube (a) 1 mm and (b) 0.5 mm at Re=24000 for bulk temperature 25 °C**

#### 4.1.3 Nusselt Number

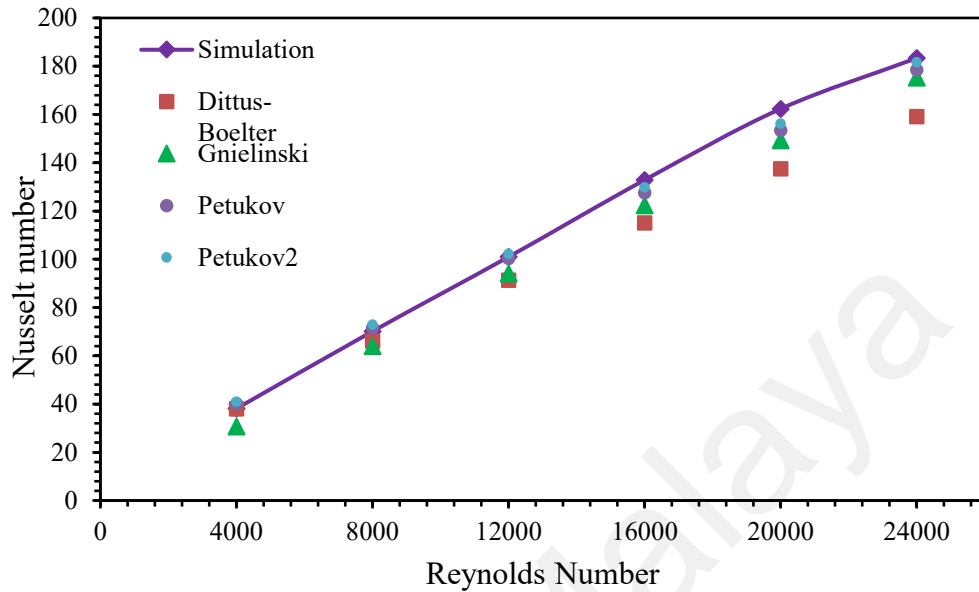
Validation of data is essential for demonstrating the dependability of the research findings. For the Nusselt number, Dittus-Boelter, Gnielinski, Petukhov, and Petukhov2 can serve as a point of reference for smooth tubes. These four equations have been utilized in numerous studies.

$$\text{Dittus and Boelter:} \quad Nu = 0.023 \times Pr^{0.4} \times Re^{\frac{4}{5}} \quad (4.1)$$

$$\text{Gnielinski:} \quad Nu = \frac{\left(\frac{f}{8}\right) \times (Re - 1000) \times Pr}{1.07 + \left(12.7 \times \left(\frac{f}{8}\right)^{0.5} \times \left(Pr^{\frac{2}{3}} - 1\right)\right)} \quad (4.2)$$

$$\text{Petukov:} \quad Nu = \frac{\left(\frac{f}{8}\right) \times Re \times Pr}{1.07 + \left(12.7 \times \left(\frac{f}{8}\right)^{0.5} \times \left(Pr^{\frac{2}{3}} - 1\right)\right)} \quad (4.3)$$

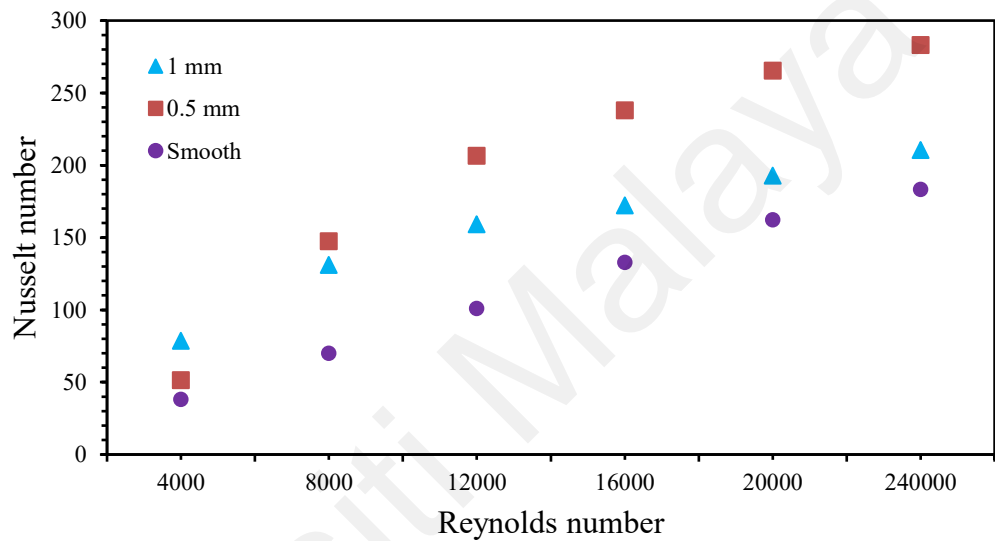
Petukov2: 
$$Nu = \frac{\left(\frac{f}{8}\right) \times Re \times Pr}{1.07 + \left(12.7 \times \left(\frac{f}{8}\right)^{0.5} \times \left(Pr^{\frac{2}{3}} - 1\right)\right)} \left(\frac{0.0008001}{0.0006817}\right)^{0.11} \quad (4.4)$$



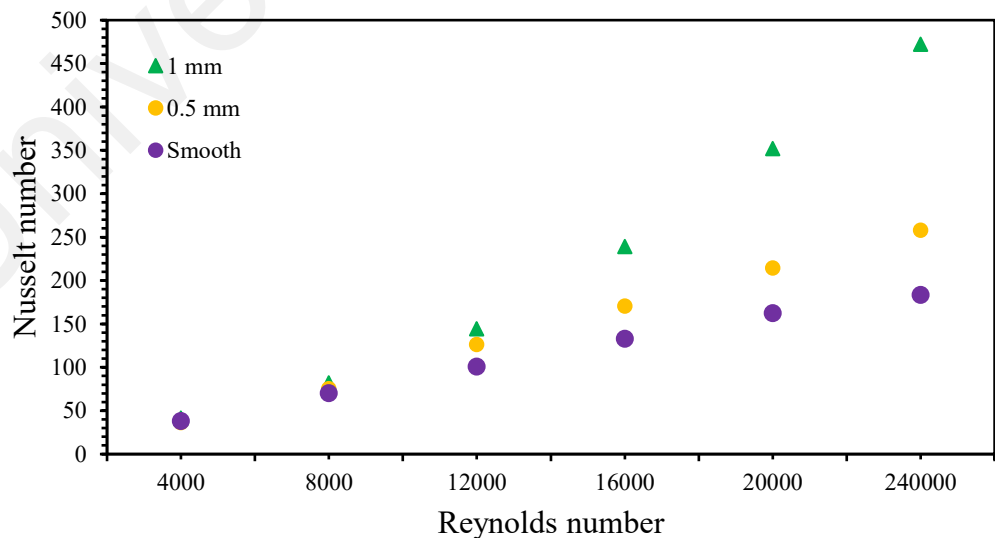
**Figure 4.10: Nusselt number with Reynolds number for simulation and empirical results on smooth tube**

Figure 4.10 depicts the linear relationship between the Nusselt number and the Reynolds number. This data validated the simulation setup by comparing the Nusselt number result of the smooth tube simulation to the empirical results of Equation (4.1). (4.4). It demonstrates that the simulation result for the Nusselt number of a smooth tube most closely corresponds to the empirical results of Petukov2. The error point range is adequate for validating the simulation setup of this study so that it can be utilized to investigate other treated tubes. Figure 4.11 illustrates the Nusselt number at increasing Reynolds number for wire coil insert and circular grooved profiles at bulk temperature 30 °C. By comparing the results of the two different tube designs to those of the smooth tube, the effects of varying treated surface specification on heat transfer performance are easier to compare and comprehend. The Nusselt number is calculated at point 0.901 m for all tubes. The trend in the graph indicates that an inlet flow with a high velocity is required for the Nusselt number to surpass that of the smooth tubes. The 0.5 mm wire coil insert

tube (Figure 4.11 (a)) and the 1mm circular grooved tube (Figure 4.11(b)) are advantageous configurations for both treated surface tubes. According to Figure 4.11(a), the wire coil insert tube with a 1 mm diameter begins at a greater value than the other tubes, but the 0.5 mm tube surpasses it until  $Re=24000$ . 0.5 mm demonstrates the greatest increase of Nusselt number over smooth tube at Reynolds number of 8000 (114 %) and the least increase at Reynold's number of 4000 (31 %).



(a)



(b)

**Figure 4.11: Nusselt number with Reynolds number for (a) wire coil insert tube and (b) circular groove tube bulk temperature 30°C**

In Figure 4.11(b), the Nusselt number is plotted as the Reynolds number increases for 1 mm and 0.5 mm circular groove tubes. 1 mm circular groove demonstrates an increase of 136 % and 192 % in the Nusselt number at Reynolds number of 20000 and 24000 in comparison to a smooth tube. Among the three tested variations, this is the best candidate for providing superior thermal management. While for 0.5 mm, the highest increment of Nusselt number 59 % at Re=24000.

**Table 4.1: Comparison Nusselt number in corresponds to Reynolds number at bulk temperatures 25 °C and 30 °C for (a) wire coil insert tube and (b) circular groove tube**

Reynolds number	1 mm		0.5 mm	
	25 °C	30 °C	25 °C	30 °C
4000	79.5864	79.5864	51.5436	51.5436
8000	127.642	127.666	147.52	147.52
12000	150.662	150.686	206.545	206.532
16000	164.981	164.972	237.924	237.916
20000	183.281	183.281	265.362	265.362
24000	206.062	206.086	283.135	283.135

(a)

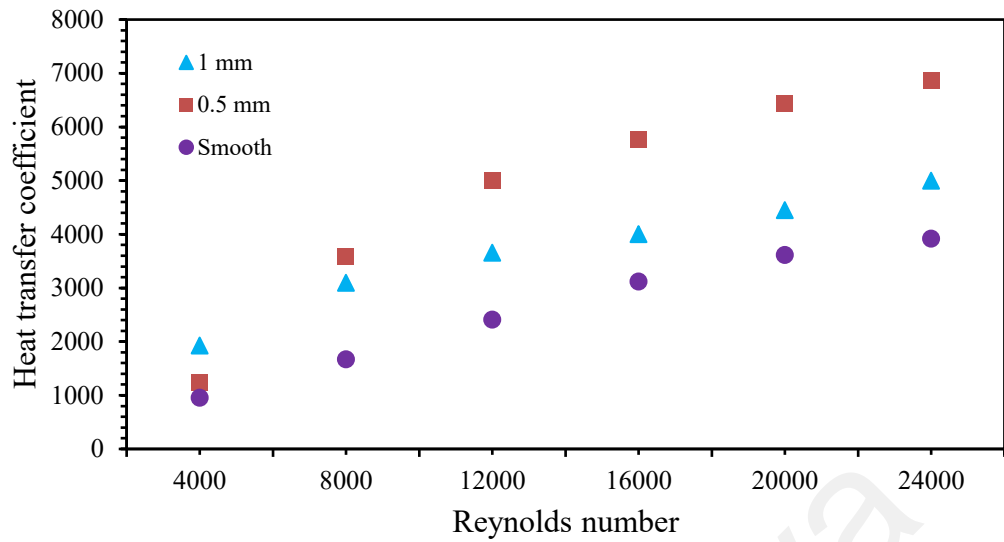
Reynolds number	1 mm		0.5 mm	
	25 °C	30 °C	25 °C	30 °C
4000	41.620	41.628	36.4549	36.4549
8000	82.017	82.017	75.372	75.374
12000	144.414	144.414	126.262	126.263
16000	239.108	239.108	170.470	170.470
20000	351.922	351.926	214.402	214.405
24000	472.171	472.171	257.941	257.941

(b)

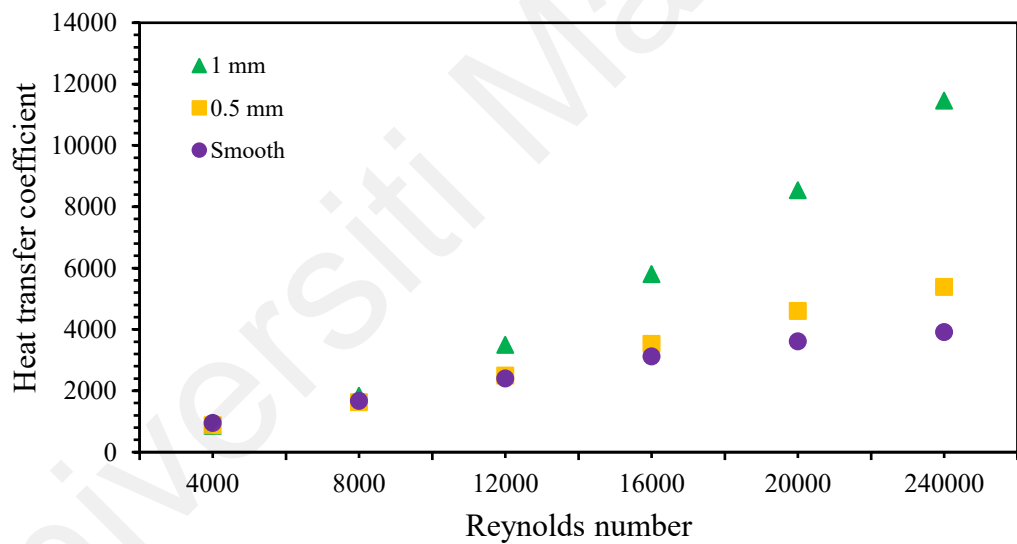
Table 4.1 demonstrates that small differences in bulk temperature do not result in significant changes in the Nusselt number. Due to the similar turbulence profile that manifests on the tube section, this is the case.

#### **4.1.4 Heat transfer coefficient**

The coefficient of heat transfer is determined by dividing the heat flux by the temperature difference. The data was obtained by calculating the difference in temperature between a surface temperature point and the average temperature of a vertical cross section. In addition, Figure 4.12 and Figure 4.13 provide insight into the different levels of heat transfer coefficient for treated surface configurations as the Reynolds number increases. The coefficient of heat transfer is determined by dividing the heat flux by the temperature difference. The data was obtained by calculating the difference in temperature between a temperature point and the average temperature of a vertical cross section. In accordance with Figures 4.12(a) and 4.13(a), the 0.5 mm wire coil insert tube demonstrates the greatest improvement in heat transfer coefficient at Reynolds numbers 8000 and 12000 for both bulk temperatures 30 °C and 25 °C temperatures. At bulk temperature 25 °C, 0.5 mm results in the greatest increase of 114 % and 108 %, while at bulk temperature 30 °C, the increase is 114 % and 107 %. At bulk temperature 30 °C, the 1 mm wire coil insert tube shows the greatest improvement at 123 % and 104 % for Reynolds numbers 4000 and 8000, respectively.

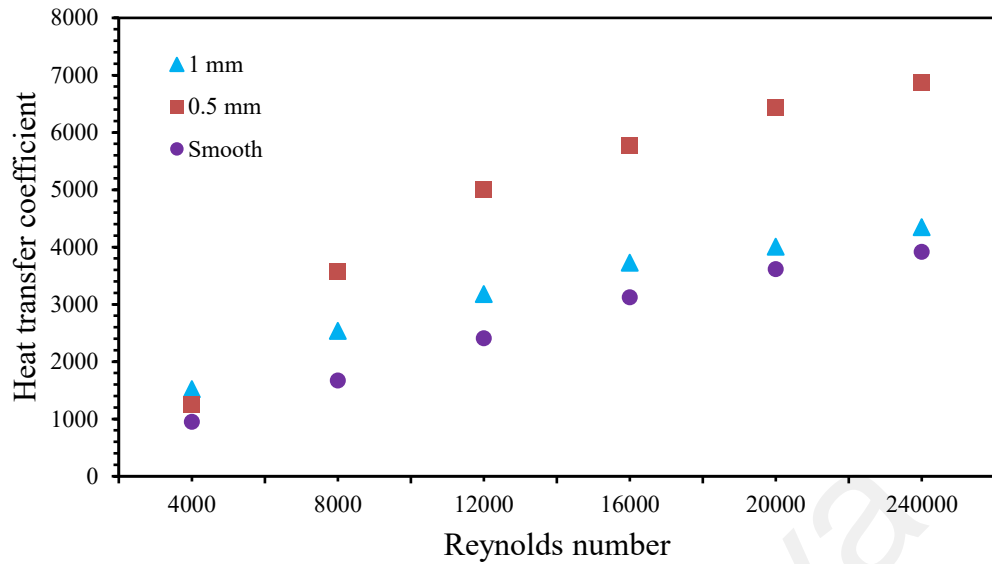


(a)

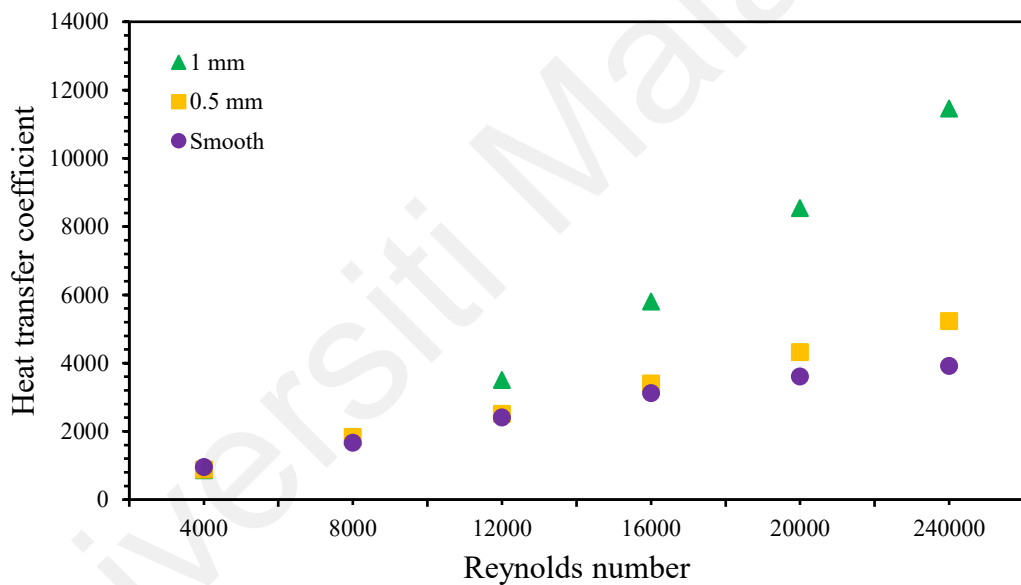


(b)

**Figure 4.12: Heat transfer coefficient with Reynolds number for (a) wire coil insert tube and (b) circular groove tube for bulk temperature 30 °C**



(a)



(b)

**Figure 4.13: Heat transfer coefficient with Reynolds number for (a) wire coil insert tube and (b) circular groove tube for bulk temperature 25 °C**

Due to the high turbulence dissipation and convection, the coefficient of heat transfer rises as groove diameter and Reynolds number increase. The increase in surface area also contributes to the interface required for convections to propagate. In addition, the heat transfer coefficient increases toward the end of the micro-groove tubes, which can be attributed to the disruption of the boundary layer in that section as a result of increased



fluid transverse mixing. Referring to Figures 4.12(b) and 4.13(b), 1 mm of circular groove tube increases the heat transfer coefficient from Reynolds number 12,000 to 24,000 by 45 % to 192 %. In contrast, along the same Reynolds number range, the heat transfer coefficient of 0.5 mm circular groove tube increases by a small percentage, from 13 % to 37 %.

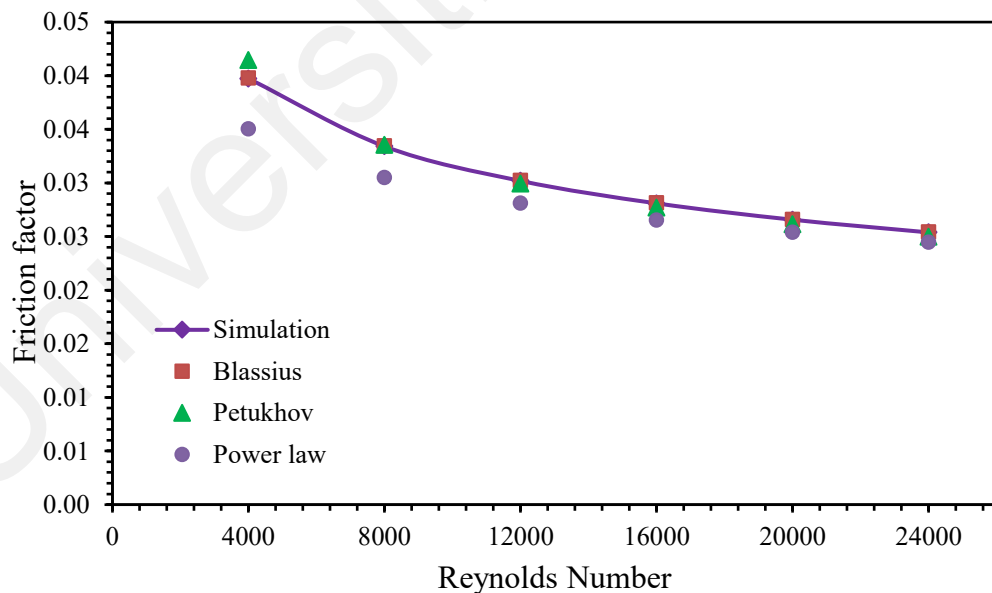
#### 4.1.5 Friction factor

For friction factor,  $f$ , validation data can be referred to Blasius, Petukhov, and Power law equations:

$$\text{Blasius:} \quad f = 4 \times 0.0791 \times Re^{-\frac{1}{4}} \quad (4.5)$$

$$\text{Power Law:} \quad f = 0.184 \times Re^{-\frac{1}{5}} \quad (4.6)$$

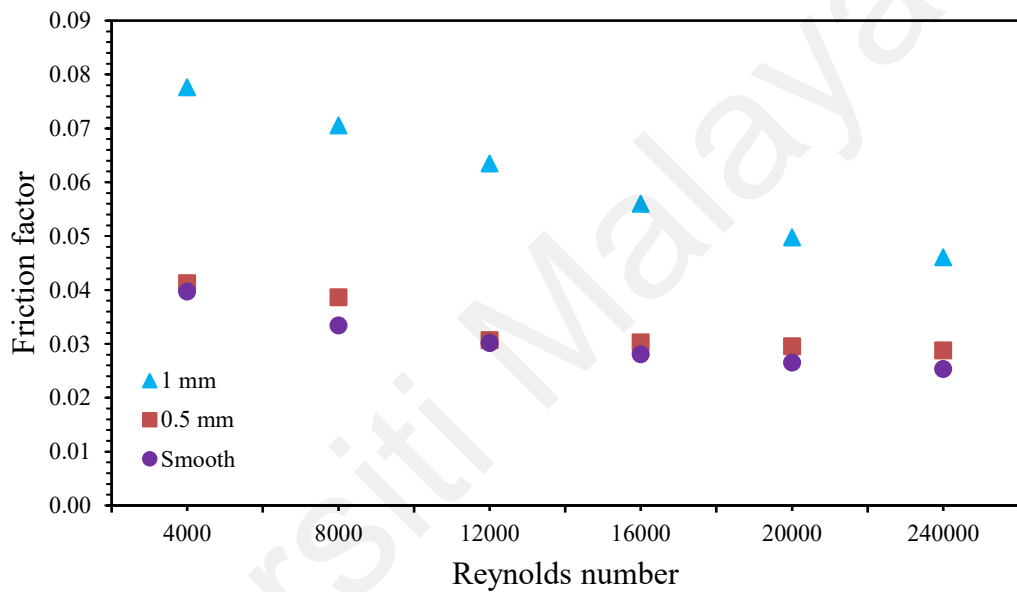
$$\text{Petukhov:} \quad f = \left( (0.791 \times \ln(Re)) - 1.64 \right)^{-2} \quad (4.7)$$



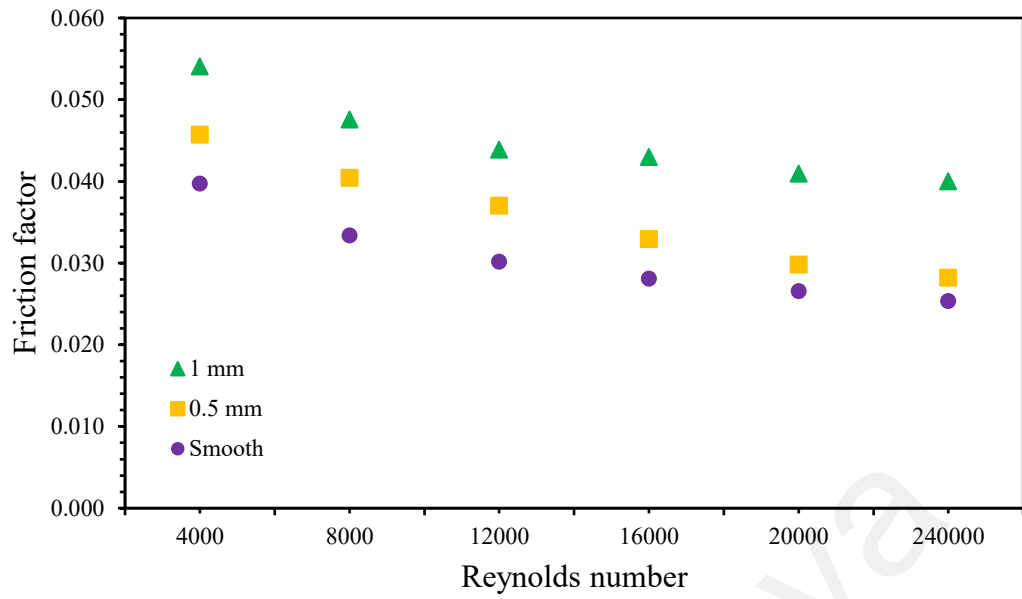
**Figure 4.14: Friction factor with Reynolds number for simulation and empirical results on smooth tube**

Based on Figure 4.14, the validation of friction factor on smooth tube with comparison to Equations (4.5) to (4.7) showed all points are close together. The value deviates by no more than 6 %, with the highest difference percentage being 5.3 %, indicating that the

simulation data is correct. So, this simulation setup has been proven to work and can be used in our simulations to test how well the other treated tubes work. The friction factor versus the Reynolds number is depicted in Figure 4.15 and Figure 4.16 for all designs. From the coefficient of friction, the friction factor is calculated. Observing all figures reveal that the friction factor decreases with increasing Reynolds number. Wire coil insert tubes with a 1 mm diameter have the highest friction factor compared to tubes with treated surfaces and tubes with a smooth surface.

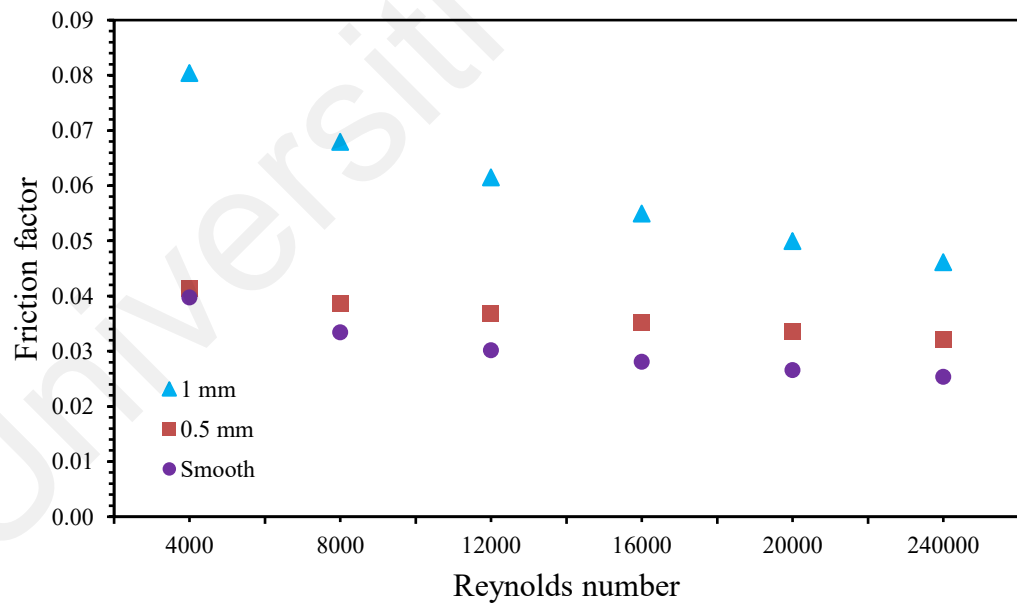


(a)

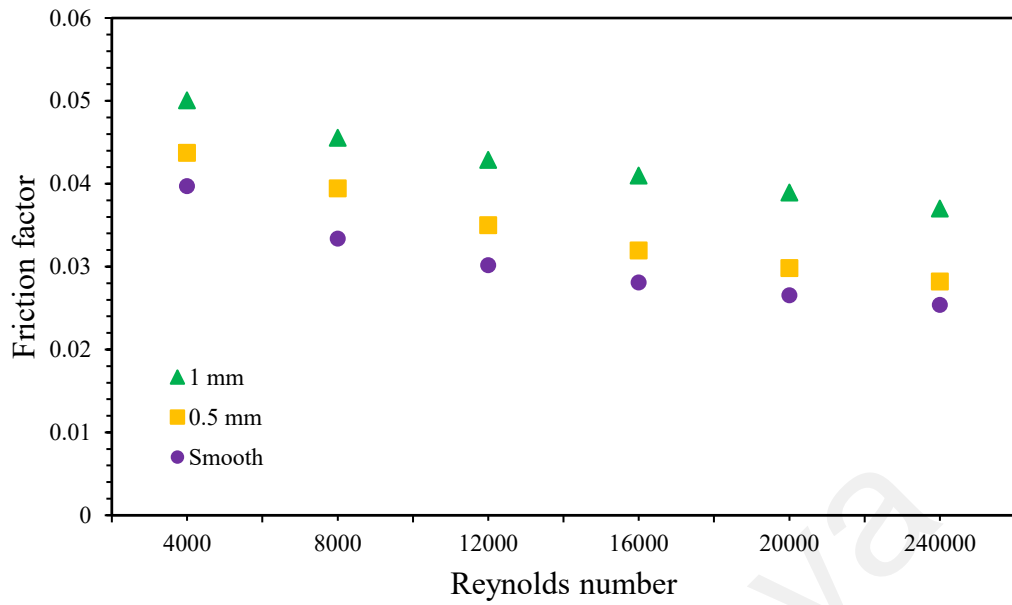


(b)

**Figure 4.15: Friction factor with Reynolds number for (a) wire coil insert tubes and (b) circular groove tubes at bulk temperature 30 °C.**



(a)

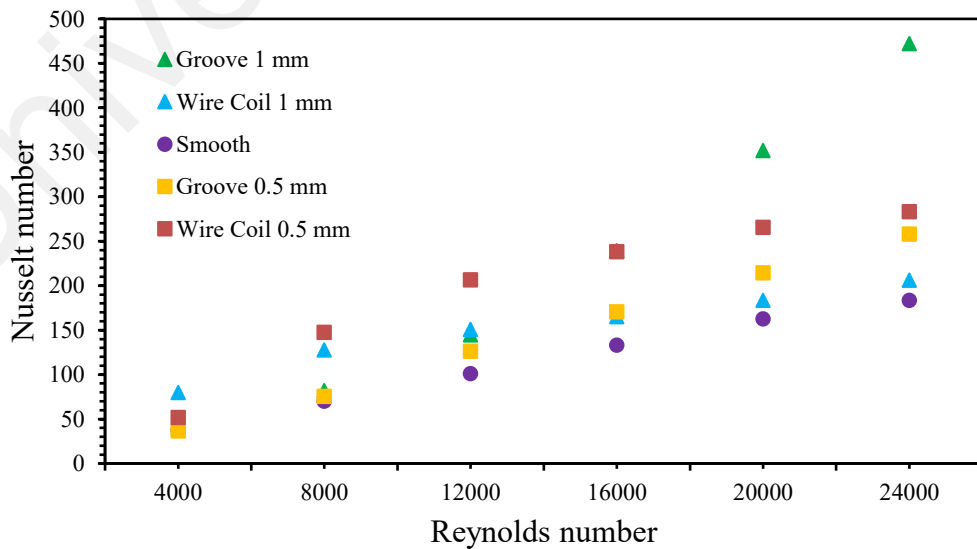


(b)

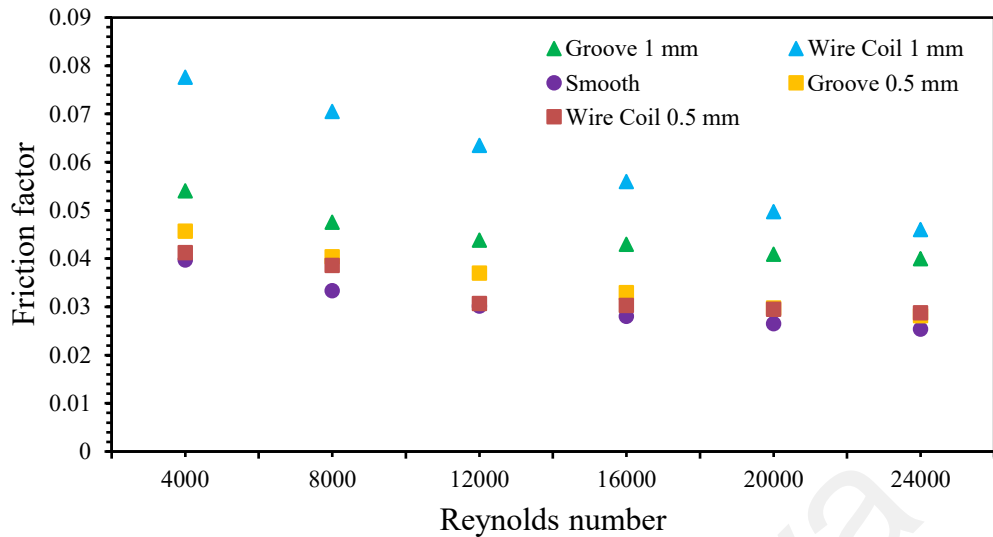
**Figure 4.16: Friction factor with Reynolds number for (a) wire coil insert tubes and (b) circular groove tubes at bulk temperature 25 °C.**

#### 4.1.6 Comparison wire coil insertion and circular groove

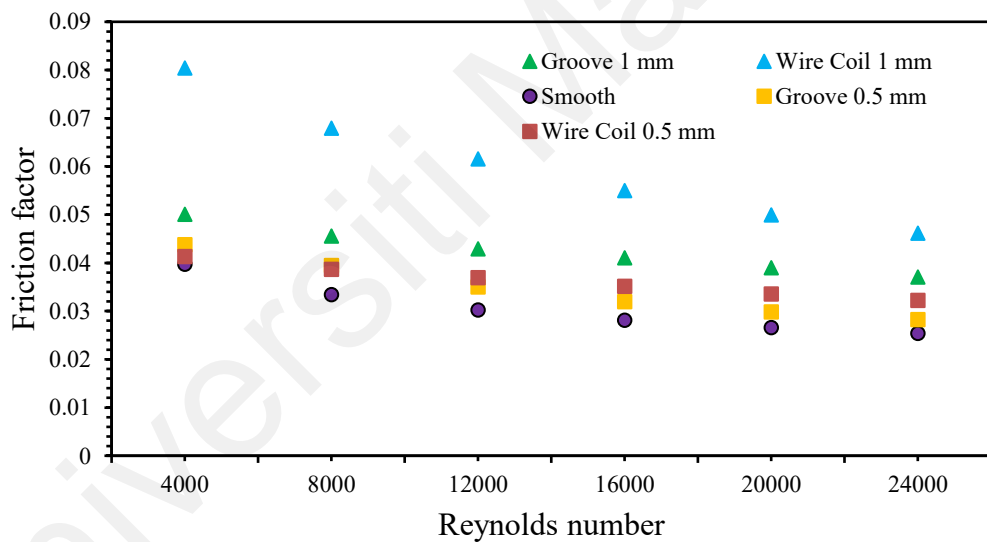
In this section, the comparison data between wire coil insertion and circular groove tubes reviewed.



**Figure 4.17: Variation Nusselt number with Reynolds number for all tubes at bulk temperature 30 °C.**



**Figure 4.18: Variation Friction factor with Reynolds number for all tubes at bulk temperature 30 °C.**



**Figure 4.19: Variation Friction factor with Reynolds number for all tubes at bulk temperature 25 °C.**

The circular groove tube provided a significant increase in Nusselt number, as shown in Figure 4.17. The increment of 1 mm circular groove is superior to the other tubes. While based on Figure 4.18 and Figure 4.19, all tubes displayed decreasing trends of friction factor, with the 1 mm wire coil insert tube having the highest value relative to the others. Consequently, this justification leads to experimental investigation using wire coil insertion.

## 4.2 Experimental result: Wire coil inserts

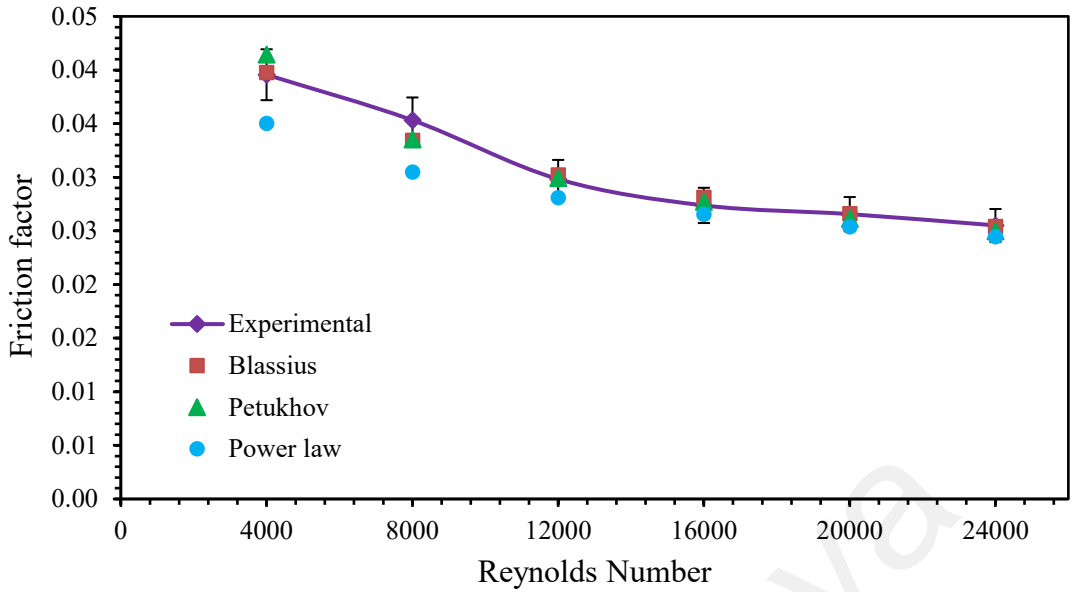
### 4.2.1 Result validation for smooth tube

An uncertainty analysis was performed on the calculated Nusselt number and friction factor data based on error propagation principle underlined by Kline and McClintock (1953) as well as Taylor and Thompson (1998). The results give the highest uncertainty of approximately 6% and 10% for Nusselt number and friction factor respectively, both fall within the acceptable range stipulated by the empirical values. The results indicated that the experimental setup can be adopted to study the effect of internal surface modification on tube heat exchanger for improving the heat transfer performance.

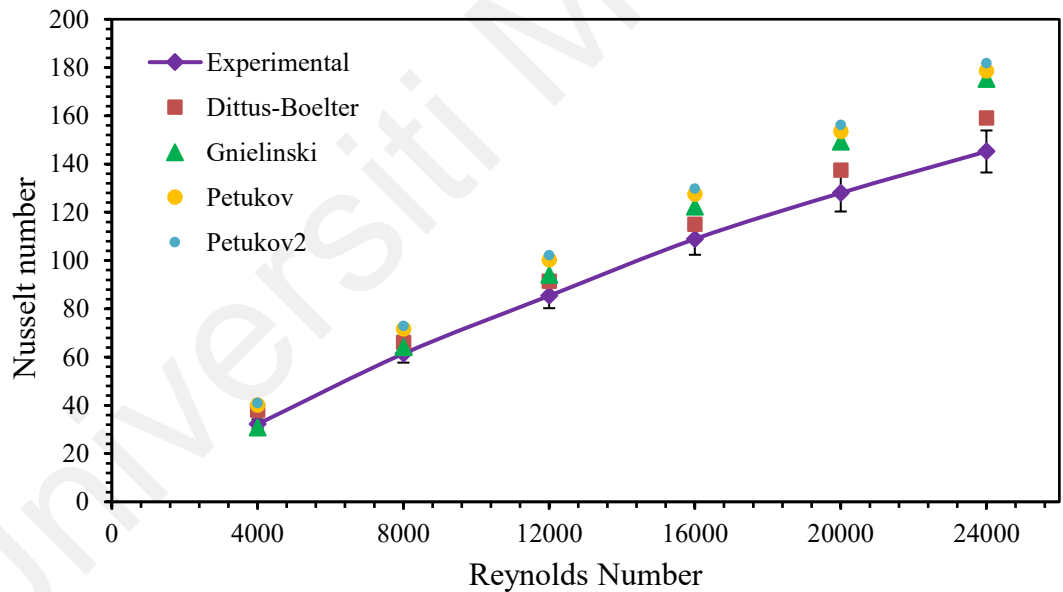
**Table 4.2: Validation Friction factor correspond to Reynolds number for smooth tube**

Reynolds number	Friction factor				
	Experimental	Blasius	Petukhov	Power law	Difference (%)
4000.00	0.0396	0.0398	0.0414	0.0350	0.568
8000.00	0.0353	0.0335	0.0335	0.0305	5.285
12000.00	0.0298	0.0302	0.0299	0.0281	1.351
16000.00	0.0274	0.0281	0.0277	0.0265	2.769
20000.00	0.0266	0.0266	0.0262	0.0254	0.166
24000.00	0.0255	0.0254	0.0250	0.0245	0.352

In this research, the Blasius is used as the reference point to the experimental value for friction factor in order to validate the experimental analysis. Based on the Table 4.2 and Figure 4.20, the difference range of friction factor resulted from 0.166 % until 5.285 % which verify the experimental data is reliable.



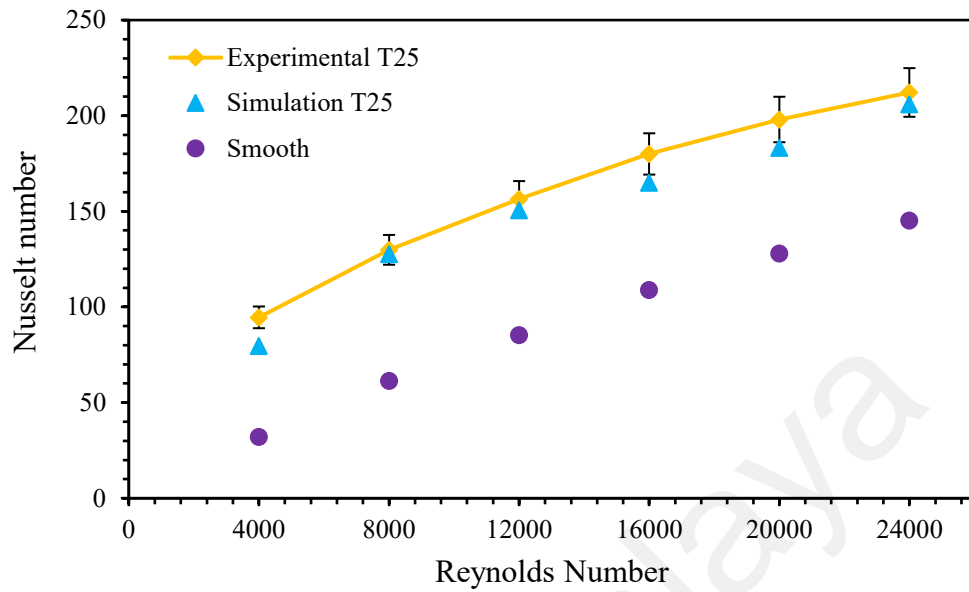
**Figure 4.20: Friction factor with Reynolds number for experiment and empirical results on smooth tube**



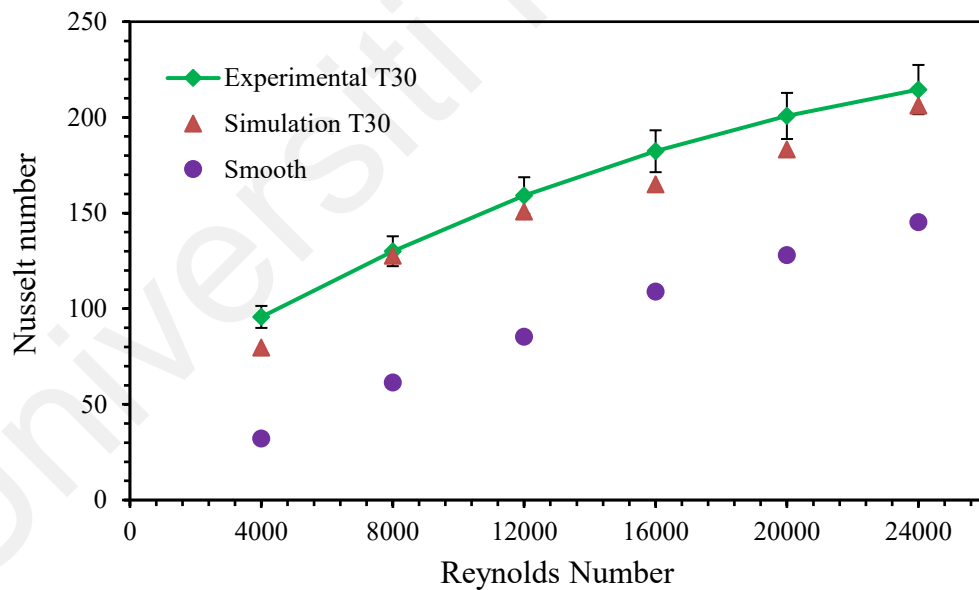
**Figure 4.21: Nusselt number with Reynolds number for experiment and empirical results on smooth tube**

Based on Figure 4.21, the Nusselt number of smooth tube increased with Reynolds number. The error point is within acceptable range for validating the experimental setup to be effective and reliable for conducting the investigation on other tubes.

#### 4.2.2 Nusselt number



(a)



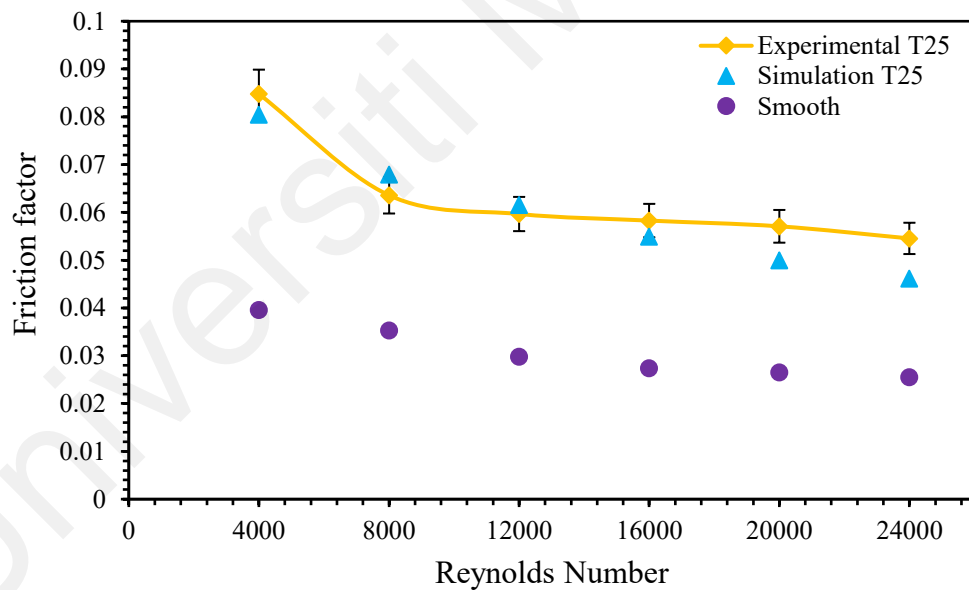
(b)

**Figure 4.22: Nusselt number with different Reynolds number of 1 mm wire coil insert tube and smooth tube at (a) bulk temperature 25 °C and (b) bulk temperature 30 °C**

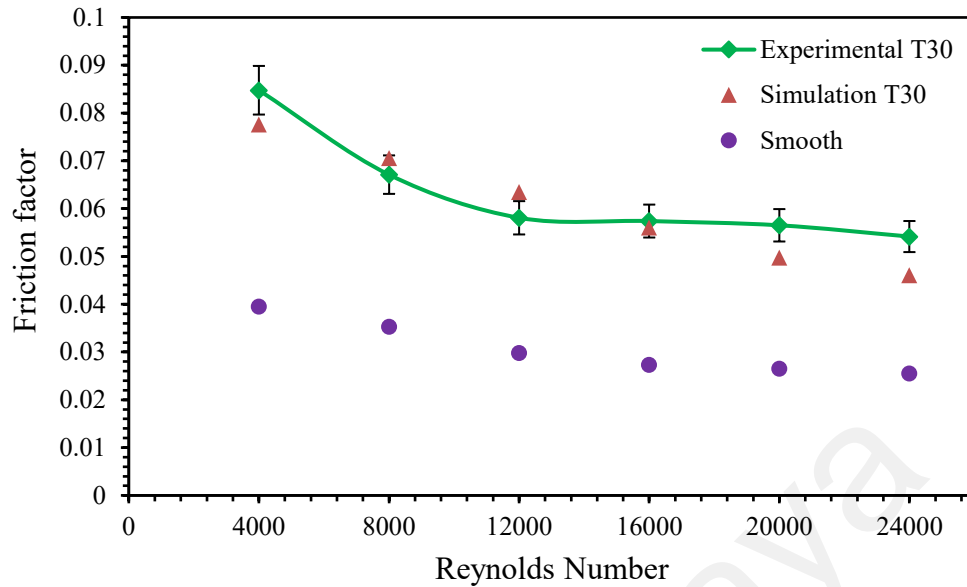


Based on the experimental data, Figure 4.22 depicts the relationship between the evaluated Nusselt number and Reynolds number. With the smooth tube as a point of reference, it is easier to determine how coil insertion has affected thermal performance. The Nusselt number increased as the Reynolds number increased, according to the graph. The highest increment of Nusselt number for experimental T25 and T30 is 194 % and 197 % at  $Re=4000$  while the least is 46 % and 48 % at  $Re=16000$ . This result significantly higher compared to Kasturi et al. (2017) study; the investigation used different parameter of ratio pitch and diameter. The Nusselt number increment of wire coils were 3.75 % to 14.54 % (Kasturi et al., 2017).

### 4.2.3 Friction factor



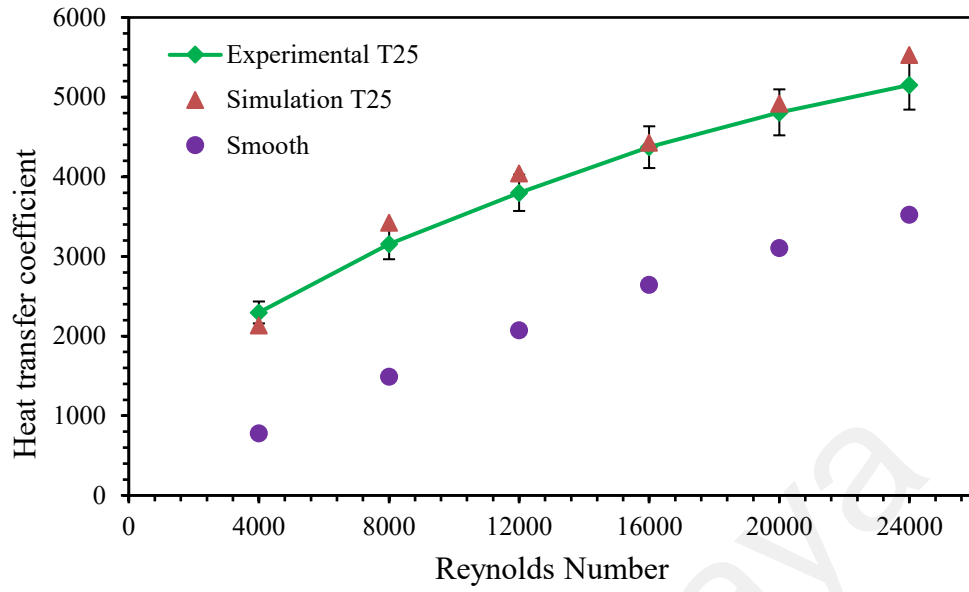
(a)



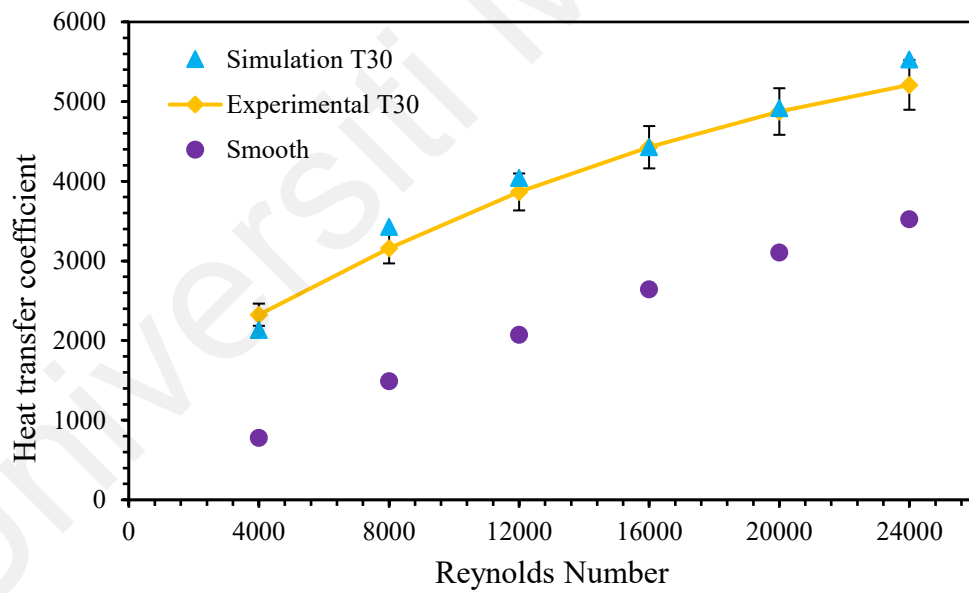
(b)

**Figure 4.23: Friction factor with different Reynolds number of 1 mm wire coil insert tube and smooth tube at (a) bulk temperature 25 °C and (b) bulk temperature 30 °C**

The friction factor represents the number of frictional losses along the pipe length. It is a necessary characteristic for investigating the enhancement of fluid flow. In order to create a durable and effective heat exchanger, the friction factor is taken into account to ensure minimal energy loss during the heat exchanger's operation. In this experiment, a wire coil insert tube with a 1 mm diameter and bulk temperatures of 25 °C and 30 °C were used. According to Figure 4.23, as the Reynolds number increases, the friction factor decreases and follows a decreasing trend. At the lowest Reynolds number, the coefficient of friction is the highest at 0.085, while at the highest Reynolds number, it is the lowest at 0.054. Referred to Biswas and Salam (2013) finding, the friction factor of this study is validated. Biswas and Salam (2013) mentioned the friction factor of wire coil insert decreases with increasing Reynolds number and offers a threefold improvement over smooth tube. While this study showed 1.9 to 2.1 times enhancement compared to smooth tube.



(a)



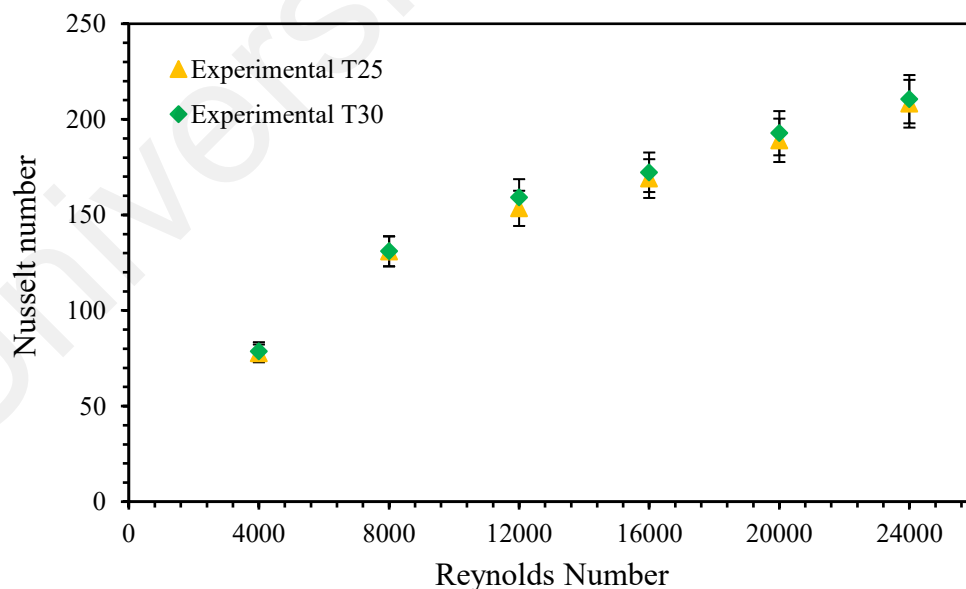
(b)

**Figure 4.24: Heat transfer coefficient with different Reynolds number of 1 mm wire coil insert tube and smooth tube at (a) bulk temperature 25 °C and (b) bulk temperature 30 °C**

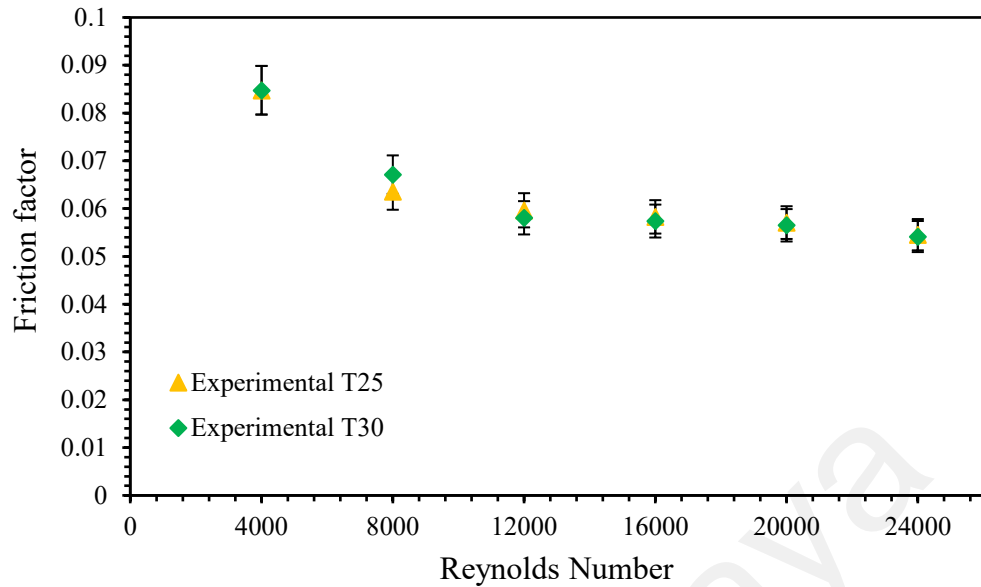
The 1 mm wire coil insert tube exhibits the greatest improvement in heat transfer coefficient compared to the smooth tube, as shown in Figure 4.24. This comparison demonstrated the reliability of the analysis and the successful evaluation of heat transfer in wire coil insertion. The highest increment result of heat transfer coefficient of wire coil insert tube for both bulk temperatures, 25 °C and 30 °C is 2.94 and 2.97 times than smooth tube at Re=4000. The least value is 1.46 and 1.48 times than smooth tube for experimental T25 and T30 at Re=24000. Rathod and Valmiki (2017) reported that copper insert increased the heat transfer coefficient by 1.43 times, validating this study results.

#### 4.2.4 Comparison heat transfer performance for different bulk temperature

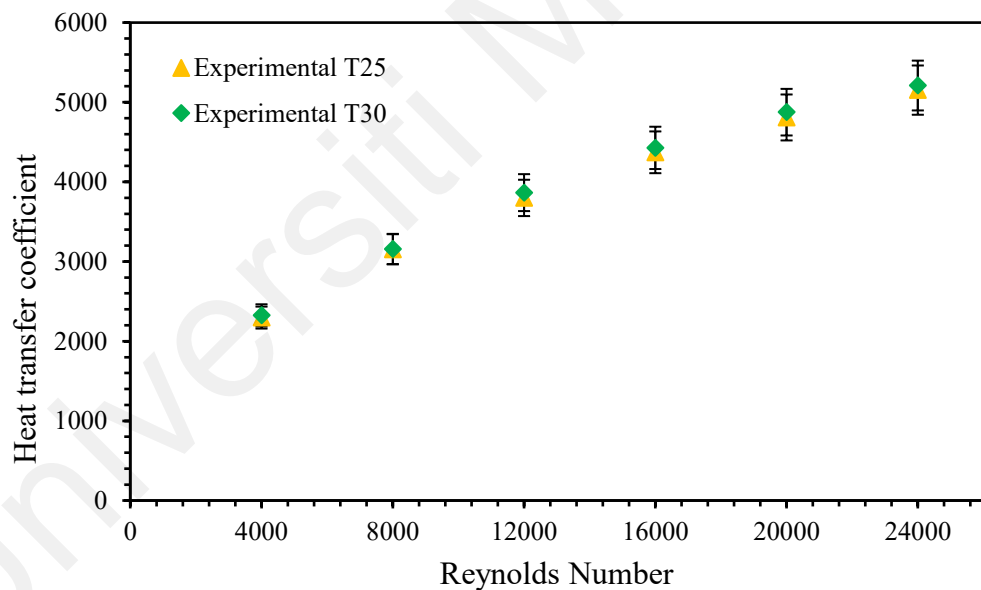
In this subsection, the comparison of Nusselt number, friction factor, and heat transfer coefficient of 1 mm wire coil insert tube at bulk temperatures of 25 °C and 30 °C is represented in Figure 4.25 to Figure 4.27.



**Figure 4.25: Nusselt number with Reynolds number for 1 mm wire coil insert experimental at bulk temperatures 25 °C and 30 °C**



**Figure 4.26: Friction factor with Reynolds number for 1 mm wire coil insert experimental at bulk temperatures 25 °C and 30 °C**



**Figure 4.27: Heat transfer coefficient with Reynolds number for 1 mm wire coil insert experimental at bulk temperatures 25 °C and 30 °C**

Based on Figure 4.25 and Figure 4.26, the experimental data of Nusselt number and friction factor at two different bulk temperatures did not show much difference in values. While the range of difference for heat transfer coefficient is about 5 %, experimental at bulk temperature of 30 °C shows a higher increment.

## CHAPTER 5: CONCLUSION

Numerical and experimental analyses of heat transfer for treated surface copper tubes with varying Reynolds number were performed. Fluent Ansys™ V20 and experimental analysis were used to examine the smooth and proposed treated (circular grooved and wire coil insertion) profiles at bulk temperatures of 25 °C and 30 °C. Under a constant heat flux condition, all tubes were tested for flows with a Reynolds number ranging from 4,000 to 24,000. The simulation results indicated that the 1 mm circular groove tubes and 0.5 mm wire coil insert tubes demonstrated the best performance for the flow conditions and heat transfer enhancement. In simulation, the Nusselt number of a wire coil insert tube with a diameter of 0.5 mm increased by 114 % at a Reynolds number of 8000 and by 31 % at a Reynolds number of 4000 at a bulk temperature of 30 °C. A 1 mm circular groove increased the Nusselt number by 136 % and 19 %, respectively, at Reynolds numbers of 20000 and 24000, when compared to a smooth tube. Also, 1 mm of circular groove tube increased the heat transfer coefficient from Reynolds number 12,000 to 24,000 by 45 % to 192 %. In the experiment analysis of a 1 mm wire coil insert tube, it was determined that the Nusselt number increased from 46 % to 197 % while the friction factor decreased. When compared to the smooth tube, the heat transfer coefficient increased by 2.94 and 2.97 times. In conclusion, the groove tube with a larger diameter and the wire coil insert tube with a smaller cross section have better heat transfer enhancement as a flow generator. Therefore, more studies can be conducted in the future, such as the experimentation on groove tube of 0.5 mm would make this study more comprehensive. The experimental results will be compared to the simulation results in order to further validate the obtained results. Also, the thermal performance of different dimensions of groove tubes and wire coil insertion tubes in combination can be investigated in the future.

## REFERENCES

- Acharya, S., Giri, V. R., Siwakoti, M., Bhattarai, B., Bajracharya, T. R., & Adhikari, N. (2021). Study on effect of grooves on tube heat exchangers *International Journal for Creative Research Thoughts (IJCRT)*, 9(2).
- Al-Gburi, H., Mohammed, A. A., & Al-Abbas, A. H. (2023). Experimental study of the thermal performance of corrugated helically coiled tube-in-tube heat exchanger. *Frontiers in Heat and Mass Transfer (FHMT)*, 20(17).
- Ali, R. K., Sharafeldeen, M. A., Berbish, N. S., & Moawed, M. A. (2015). Convective heat transfer enhancement inside tubes using inserted helical coils. *Thermal Engineering*, 63(1), 42-50.
- Allan Harry Richard, T. L., & Agilan, H. (2015). Experimental Analysis of Heat Transfer Enhancement Using Fins in Pin Fin Apparatus. *International Journal of Core Engineering & Management (IJCEM)*, 2(1).
- Aly, W. I. A., Elbalshouny, M. A., Abd El-Hameed, H. M., & Fatouh, M. (2017). Thermal performance evaluation of a helically-micro-grooved heat pipe working with water and aqueous Al<sub>2</sub>O<sub>3</sub> nanofluid at different inclination angle and filling ratio. *Applied Thermal Engineering*, 110, 1294-1304. <https://www.sciencedirect.com/science/article/pii/S1359431116314909>
- Apet, V., & Borse, S. L. (2015). Heat transfer enhancement in dimpled tube. *International Journal for Scientific Research and Development*, 3(3), 3192-3195.
- Aroonrat, K., Jumpholkul, C., Leelaprachakul, R., Dalkilic, A. S., Mahian, O., & Wongwises, S. (2013). Heat transfer and single phase flow internally grooved tubes. International communications in heat and mass transfer. *International Communications in Heat and Mass Transfer*, 42, 62-68.
- Aubin, J., Fletcher, D. F., & Xuereb, C. (2004). Modeling turbulent flow in stirred tanks with CFD: the influence of the modeling approach, turbulence model and numerical scheme. *Experimental Thermal and Fluid Science*, 28(5), 431-445.

- Azmi, W. H., Abdul Hamid, K., Ramadhan, A. I., & Shaiful, A. I. M. (2021). Thermal hydraulic performance for hybrid composition ratio of TiO<sub>2</sub>–SiO<sub>2</sub> nanofluids in a tube with wire coil inserts. *Case Studies in Thermal Engineering*, 25. <https://doi.org/10.1016/j.csite.2021.100899>
- Bergles, A. E. (1999). Enhanced heat transfer: endless frontier, or mature and routine? *Journal of Enhanced Heat Transfer*, 6(2-4).
- Bergman, T. L., Incropera, F. P., DeWitt, D. P., & Lavine, A. S. (2011). *Fundamentals of Heat and Mass Transfer* (7th ed.). John Wiley & Sons.
- Bilen, K., Cetin, M., Gul, H., & Balta, T. (2009). The investigation of groove geometry effect on heat transfer for internally grooved tubes. *Applied Thermal Engineering*, 29(4), 753-761.
- Biswas, S., & Salam, B. (2013). Experimental investigation of tube side heat transfer enhancement using wire coil insert. *Mechanical Engineering Resources Journal* 9, 18-23.
- Blasius, H. (1913). Das aehnlichkeitsgesetz bei reibungsvorgängen in flüssigkeiten. In *Mitteilungen über Forschungsarbeiten auf dem Gebiete des Ingenieurwesens* (pp. 1-41). Springer.
- Chaudhari, R., Deshmukh, P. W., Bhalla, V., & Lahane, S. V. (2021). International Conference Material Science and Engineering 1185. <https://doi.org/10.1088/1757-899X/1185/1/012007>
- Chompookham, T., Chingtuaythong, W., & Chokphoemphun, S. (2022). Influence of a novel serrated wire coil insert on thermal characteristics and air flow behavior in a tubular heat exchanger. *International Journal of Thermal Sciences*, 171. <https://doi.org/10.1016/j.ijthermalsci.2021.107184>
- Dang, W., & Wang, L.-B. (2021). Convective heat transfer enhancement mechanisms in circular tube inserted with a type of twined coil. *International Journal of Heat and Mass Transfer*, 169. <https://doi.org/10.1016/j.ijheatmasstransfer.2021.120960>



- Dewan, A., Mahanta, P., Sumithra Raju, K., & Suresh Kumar, P. (2004). Review of passive heat transfer augmentation techniques. *Proceedings of the Institution of Mechanical Engineers*, 218.
- Dincer, L., & Erdemir, D. (2021). Chapter 4 - System Analysis. In L. Dincer & D. Erdemir (Eds.), *Heat Storage Systems for Buildings* (pp. 115-178). Elsevier. <https://doi.org/https://doi.org/10.1016/B978-0-12-823572-0.00003-5>
- Eid, M. M. A. A., Zubir, M. N. M., Muhamad, M. R. B., & Newaz, K. M. S. (2021). Computer aided investigation on the effect of internal surface micro grooving for enhanced thermal management of heat exchanger. *AIP Conference Proceedings*, 2403(1), 040004. <https://aip.scitation.org/doi/abs/10.1063/5.0070873>
- Feng, Z., Luo, X., Guo, F., Li, H., & Zhang, J. (2017). Numerical investigation on laminar flow and heat transfer in rectangular microchannel heat sink with wire coil inserts. *Applied Thermal Engineering*, 116, 597-609. <https://doi.org/10.1016/j.applthermaleng.2017.01.091>
- Garcia, A., Solano, J. P., Vicente, P. G., & Viedma, A. (2007). Enhancement of laminar and transitional flow heat transfer in tubes by means of wire coil inserts. *International Journal of Heat and Mass Transfer*, 50(15-16), 3176-3189.
- Gaudiani, A. A. (2008). Numerical methods for engineers . Steven Chapra and Raymond Canale. Mc Graw Hill, 2005. *Journal of Computer Science and Technology*, 8(02), 127-128.
- Ghajar, Y. A. Ç. A. J. (2020). Heat and Mass Transfer: Fundamentals and Applications. 6. (Mcgraw-Hill Education)
- Giram, D. R., & Patil, A. M. (2013). Experimental & Theoretical Analysis of Heat Transfer Augmentation From Dimpled Surface. *International Journal of Engineering Research and Application*, 3(5), 19-23.

- Göksu, T. T., & Yilmaz, F. (2021). Numerical comparison study on heat transfer enhancement of different cross section wire coils insert with varying pitches in a duct. *Journal of Thermal Engineering*, 7(77), 1683-1693. <https://doi.org/https://doi.org/10.18186/thermal.1025930>
- Gunes, S., Ozceyhan, V., & Buyukalaca, O. (2010). The experimental investigation of heat transfer and pressure drop in a tube with coiled wire inserts placed separately from the tube wall. *Applied Thermal Engineering*, 30(13), 1719-1725.
- Haidong, W., & Zhiqiang (John), Z. (2012). Analyzing grid independency and numerical viscosity of computational fluid dynamics for indoor environment applications. *Building and Environment*, 52, 107-118.
- Hasgul, C., & Cakmak, G. (2022). Heat transfer analysis of double tube heat exchanger with wavy inner tube. *Heat Transfer Analysis of Double Tube Heat Exchanger*, 26(4B), 3455-3462.
- Heng, L., Kim, Y. J., & Mun, S. D. (2017). Review of Superfinishing by the Magnetic Abrasive Finishing Process. *High Speed Machining*, 3(1), 42-55.
- Jafari Nasr, M. R., Habibi Khalaj, A., & Mozaffari, S. H. (2010). Modeling of heat transfer enhancement by wire coil inserts using artificial neural network analysis. *Applied Thermal Engineering*, 30(2-3), 143-151.
- Jha, S., & Jain, V. K. (2006). Nanofinishing Techniques. In *Micromanufacturing and Nanotechnology* (pp. 171-195). Springer Berlin Heidelberg.
- Kadhun, A. H., Hamad, Y. M., & Naif, N. K. M. (2015). The Effect of Magnetic Abrasive Finishing on the Flat Surface for Ferromagnetic and non-Ferromagnetic materials. *Al-Nahrain University, College of Engineering Journal (NUCEJ)*, 18(1), 66-75.
- Kadir, B., Murat, C., Hasan, G., & Tuba, B. (2009). The investigation of groove geometry effect on heat transfer for internally grooved tubes. *Applied Thermal Engineering*, 29(4), 753-761.

- Kaji, R., Yoshioka, S., & Fujino, H. (2012). The Effect of Inner Grooved Tubes on the Heat Transfer Performace of Air-Cooled Heat Exchangers of Co2 Heat Pump System. *International Refrigeration and Air Conditioning Conference*.
- Kareem, Z. S., Mohd Jaafar, M. N., Lazim, T. M., Abdullah, S., & Abdulwahid, A. F. (2015). Passive heat transfer enhancement review in corrugation. *Experimental Thermal and Fluid Science*, 68, 22-38.
- Kasturi, M. L., Junaid, M., Awate, Y. S., & Acharya, A. R. (2017). Effect of wire coil turbulators on pressure drop and heat transfer augmentation in a circular tube. *International Conference on Innovations in information Embedded and Communication Systems (ICIIECS)*.
- Keklikcioglu, O., & Ozceyhan, V. (2016). Experimental investigation on heat transfer enhancement of a tube with coiled-wire inserts installed with a separation from the tube wall. *International Communications in Heat and Mass Transfer*, 78, 88-94.
- Keklikcioglu, O., & Ozceyhan, V. (2018). Experimental investigation on heat transfer enhancement in a circular tube with equilateral triangle cross sectioned coiled-wire inserts. *Applied Thermal Engineering*, 131, 686-695. <https://doi.org/10.1016/j.applthermaleng.2017.12.051>
- Kiran, K., Asalammaraja, M., & Umesh, C. (2014). A review on effect of various types of tube inserts on performance parameters of heat exchanger. *International Journal of Research in Advent Technology*, 2(6), 2321-9637.
- Kline, S. J., & McClintock, F. A. (1953). Describing uncertainties in single sample experiments. *Mechanical engineering* 75(1), 3-8.
- Kumar, H., Singh, S., & Kumar, P. (2013). Magnetic Abrasive Finishing- A Review. *International Journal of Engineering Research & Technology*, 2(3).
- Lambrechts, A., Liebenberg, L., Bergles, A. E., & Meyer, J. P. (2006). Heat transfer performance during condensation inside horizontal smooth, micro-fin and herringbone tubes. *Journal of Heat Transfer* 128(7).

- Léal, L., Miscevic, M., Lavieille, P., Amokrane, M., Pigache, F., Topin, F., Nogaredo, B., & Tadriss, L. (2013, June). An overview of heat transfer enhancement methods and new perspectives: Focus on active methods using electroactive materials. *International Journal of Heat and Mass Transfer*, *61*(1), 505-524.
- Lee, M., Park, G., Park, C., & Kim, C. (2020). Improvement of Grid Independence Test for Computational Fluid Dynamics Model of Building Based on Grid Resolution. *Advances in Civil Engineering*, 2020, 8827936. <https://doi.org/10.1155/2020/8827936>
- Li, W., Chen, X., Chen, J., Zhichuan, S., & Simon, T. W. (2017). Shell-Side Flow Condensation of R410A on Horizontal Tubes at Low-Mass Fluxes. *Journal of Heat Transfer* *139*(1).
- Lienhard IV, J. H., & Lienhard V, J. H. (2001). *A Heat Transfer Textbook* (3rd ed.).
- Liu, S., & Sakr, M. (2013). A comprehensive review on passive heat transfer enhancements in pipe exchangers. *Renewable and Sustainable Energy Reviews*, *19*, 64-81.
- Matani, A. G., & Dahake, S. A. (2013). Experimental Study On Heat Transfer Enhancement In A Tube Using Counter/Co-Swirl Generation. *International Journal of Application or Innovation in Engineering & Management (IJAIEM)*, *2*(3), 100-105.
- Miyara, A., Otsubo, Y., Ohtsuka, S., & Mizuta, Y. (2003). Effects of fin shape on condensation in herringbone microfin tubes. *International Journal of Refrigeration*, *26*(4), 417-424.
- Mohite, P. P., Kadam, K. D., & Acharya, A. R. (2018). Enhancement in Heat Transfer by Using Wire Coil Inserts in Tubular Heat Exchanger. *International Journal for Research in Applied Science & Engineering Technology (IJRASET)*, *6*(IV).

- Muhamad, M. R. B., Rony, M. H., Mohd Zubir, M. N., Ibrahim, F. A., & Halim, M. M. A. (2021). *Pipe Internal Grooving Using Closed Magnetic Field System: A Novel Method*.
- Mukherjee, R. (1998). Effective design of shell and tube exchanger. *American Institute of Chemical Engineering*.
- Muñoz Esparza, D., & Sanmiguel Rojas, E. (2011). Numerical simulations of the laminar flow in pipes with wire coil inserts. *Computers & Fluids*, 44, 169-177.
- Nitheesh Krishnan, M. C., & Surresh Kumar, B. (2016). An Over View on Shell and Tube Heat Exchanger. *International Journal of Engineering Science and Computing*, 6(10), 2632-2636.
- Omur, C., Uygur, A. B., & Horuz, I. (2017). The effect of manufacturing limitations on groove design and its implementation to an algorithm for determining heat transport capability of heat pipes. *Journal of Thermal Science and Technology*.
- Padmanabhan, S., Yuvatesjeswar Reddy, O., Venkata Ajith Kumar Yadav, K., Bupesh Raja, V. K., & Palanikumar, K. (2021). Heat transfer analysis of double tube heat exchanger with helical inserts. *Materials Today: Proceedings*, 46, 3588-3595.
- Pandey, M. (2015). Critical Assessment of Literature In The Field of Enhanced Heat Transfer Techniques. *International Journal of Mechanical Engineering and Robotics Research*, 4(2).
- Patil, M. G., Chandra, K., & Misra, P. S. (2012). Study of mechanically alloyed magnetic abrasives in magnetic abrasive finishing. *International Journal of Scientific & Engineering Research*, 3.
- Promvongse, P. (2008). Thermal augmentation in circular tube with twisted tape and wire coil turbulators. *Energy Conversion and Management*, 49(11), 2949-2955.

- Ramadhan, A. A., Anii, Y. T. A., & Shareef, A. J. (2013). Groove geometry effects on turbulent heat transfer and fluid flow. *Heat Mass Transfer*, 49, 185-195.
- Rathod, P., & Valmiki, S. (2017). Heat transfer enhancement in pipe flow using wire coil inserts in forced convection. *International Journal of Engineering Research & Technology*, 6(08).
- Ray, P., & Kumar Jhinge, P. (2014). A Review Paper on Heat Transfer Rate Enhancements by Wire Coil Inserts in the Tube. *International Journal of Engineering Sciences & Research Technology*, 3(6).
- Ridha, M. M., Yanhua, Z., & Hitoshi, S. (2015). Development of a New Internal Finishing of Tube by Magnetic Abrasive Finishing Process Combined with Electrochemical Machining. *International Journal of Mechanical Engineering and Applications*, 3, 22-29.
- Sanvicente, E., Giroux-Julien, S., Ménézo, C., & Bouia, H. (2013). Transitional natural convection flow and heat transfer in an open channel. *International Journal of Thermal Sciences*, 63, 87-104.
- Shinmura, T., & Yamaguchi, H. (1995). Study on a new internal finishing process by the application of magnetic abrasive machining (internal finishing of stainless steel tube and clean gas bomb). *Japan Society of Mechanical Engineers International Journal*, 38(4), 798-804.
- Sonawane, T., Patil, P., Chavhan, A., & Dusane, B. M. (2016). A Review On Heat Transfer Enhancement By Passive Methods. *International Research Journal of Engineering and Technology (IRJET)*, 3(9), 1567-1574.
- Sreenivisalu Reddy, N., Rajagopal, K., & Veena, P. H. (2017). Experimental Investigation of Heat Transfer Enhancement of a Double Pipe Heat Exchanger with Helical Fins in the Annulus Side. *International Journal of Dynamics of Fluids*, 13(2), 285-293.
- Syam Sundar, L., Bhramara, P., Ravi Kumar, N. T., Singh, M. K., & Sousa, A. C. M. (2017). Experimental heat transfer, friction factor and effectiveness analysis of

Fe<sub>3</sub>O<sub>4</sub> nanofluid flow in a horizontal plain tube with return bend and wire coil inserts. *International Journal of Heat and Mass Transfer*, 109, 440-453. <https://doi.org/10.1016/j.ijheatmasstransfer.2017.02.022>

T.Ebisu, Fujino, H., & Torikoshi, K. (1998). Heat transfer characteristics and heat exchanger performances for R407C using herringbone heat transfer tube. *International Refrigeration and Air Conditioning Conference*, 343-348.

Taylor, J. R., & Thompson, W. (1998). An introduction to error analysis: the study of uncertainties in physical measurements. *Measurement Science and Technology*, 9(6), 1015.

Tu, J., Liu, C., & Yeoh, G. H. (2019). *Computational Fluid Dynamics: A Practical Approach* (Third ed.). Butterworth-Heinemann.

Vennila, A., Shivpuje, K. M., Fevija Dhas, A. M., & Gokulanaath, S. (2017). Parametric study of a shell and tube heat exchanger using CDF. *International Journal of Engineering Research & Technology (IJERT)*, 6(8).

Wang, L., & Sunden, B. (2002). Performance comparison of some tube inserts. *International Communications in Heat and Mass Transfer*, 29, 45-56.

Webb, R. L. (1994). *Principles of enhanced heat transfer*. Wiley.

Yadav, D. S., Dixit, V. K., Vikramaditya, Kumar Gond, N., & Paul, B. (2022). Numerical analysis of heat transfer augmentation using wire coil insert in tube. *International Journal for Creative Research Thoughts (IJCRT)*, 10(1).

Young, H. D. (2012). *Sears & Zemansky's College Physics* (N. Whilton, Ed. 9 ed.). Jim Smith.

Yu, C., Zhang, H., Wang, Y., Zeng, M., & Gao, B. (2020). Numerical study on turbulent heat transfer performance of twisted oval tube with different cross sectioned wire

Yusof, S. N. A., Muhammad, N. M. A., Aziz Japar, W. M. A., Asako, Y., Hong, C., Tan, L. K., & Che Sidik, N. A. (2022). Validity of performance factors used in recent studie on heat transfer enhancement by surface modification or insert devices. *International Journal of Heat and Mass Transfer*, 186.  
<https://doi.org/https://doi.org/10.1016/j.ijheatmasstransfer.2021.122431>

Zidan, E., Halim, M. A., Omara, M. A., & Badawy, A. E. (2018). Experimental investigation of heat transfer and pressure drop inside elliptic tube with inserted helical coils. *Mansoura Engineering Journal (MEJ)*, 43(3).

Zimparov, V. (2002). Energy conservation through heat transfer enhancement techniques. *International Journal of Energy Research*, 26(7), 675-696.

Zohir, A. E., Habib, M. A., & Nemitallah, M. A. (2015). Heat transfer characteristics in a double pipe heat exchanger equipped with coiled circular wires. *Experimental Heat Transfer*, 28, 531-545.